

DISSERTATION

DIFFERENTIAL GENE EXPRESSION IN *Escherichia coli* FOLLOWING EXPOSURE
TO NON-THERMAL ATMOSPHERIC-PRESSURE PLASMA

Submitted by

Ashish Sharma

Department of Electrical and Computer Engineering

In partial fulfillment of the requirements

For the Degree of Doctor of Philosophy

Colorado State University

Fort Collins, Colorado

Fall 2008

UMI Number: 3346484

INFORMATION TO USERS

The quality of this reproduction is dependent upon the quality of the copy submitted. Broken or indistinct print, colored or poor quality illustrations and photographs, print bleed-through, substandard margins, and improper alignment can adversely affect reproduction.

In the unlikely event that the author did not send a complete manuscript and there are missing pages, these will be noted. Also, if unauthorized copyright material had to be removed, a note will indicate the deletion.

UMI[®]

UMI Microform 3346484

Copyright 2009 by ProQuest LLC.

All rights reserved. This microform edition is protected against unauthorized copying under Title 17, United States Code.

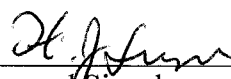
ProQuest LLC
789 E. Eisenhower Parkway
PO Box 1346
Ann Arbor, MI 48106-1346

COLORADO STATE UNIVERSITY

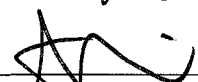
July 1, 2008

WE HEREBY RECOMMEND THAT THE DISSERTATION PREPARED UNDER OUR SUPERVISION BY ASHISH SHARMA ENTITLED DIFFERENTIAL GENE EXPRESSION IN *Escherichia coli* FOLLOWING EXPOSURE TO NON-THERMAL ATMOSPHERIC-PRESSURE PLASMA BE ACCEPTED AS FULFILLING IN PART REQUIREMENTS FOR THE DEGREE OF DOCTOR OF PHILOSOPHY.

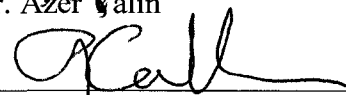
Committee on Graduate Work



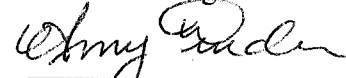
Dr. Howard Siegel



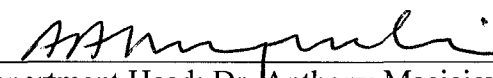
Dr. Azer Valin



Adviser: Dr. George Collins



Co-Adviser: Dr. Amy Pruden



Department Head: Dr. Anthony Maciejewski

ABSTRACT OF DISSERTATION

DIFFERENTIAL GENE EXPRESSION IN *Escherichia coli* FOLLOWING EXPOSURE TO NON-THERMAL ATMOSPHERIC-PRESSURE PLASMA

Plasma decontamination provides a low temperature and non-toxic means of treating objects where heating and exposure to poisonous compounds is not acceptable especially in applications relating to medical devices and food packaging. The effects of various plasma constituents (UV photons, reactive species, charged particles etc.) acting independently and/or synergistically on bacteria at the biomolecular level is not well understood.

High-density oligonucleotide microarrays were used to explore the differential gene expression of the entire genome of *E. coli* following plasma treatment. The results indicate a significant induction of genes involved in DNA repair and recombination suggesting that plasma exposure caused substantial DNA damage in the cell. There was also evidence of oxidative stress and suppression of genes involved in housekeeping functions of energy metabolism and ion transport. Experiments were also carried out to optimize plasma operating parameters to achieve a higher rate of inactivation of microbes. Overall, the results of this study will help to further optimize non-thermal plasma applications for bacterial inactivation.

Ashish Sharma
Electrical and Computer Engineering Department
Colorado State University
Fort Collins, CO 80523
Fall 2008

TABLE OF CONTENTS

Chapter 1: Introduction	1
Chapter 2: Plasma Fundamentals	6
2.1 Introduction.....	6
2.2 Debye Length and Plasma Sheath	6
2.3 Local Thermal Equilibrium in Plasmas.....	8
2.4 Atmospheric Pressure Glow Discharge Plasma	11
2.5 Paschen Curve and Gas Breakdown Voltage.....	11
Chapter 3: Hollow Slot Atmospheric-Pressure Plasma	16
3.1 Introduction.....	16
3.2 Literature Review	16
3.3 Hollow Slot Plasma-Configuration.....	17
3.4 Experimental Setup	18
Chapter 4: Microarrays: Fabrication and Data Analysis.....	21
4.1 Introduction.....	21
4.2 GeneChip Array Fabrication.....	22
4.3 GeneChip <i>E. coli</i> Genome 2.0 Array-Technical Details	24
4.4 Data Analysis-dChip Software	24
4.5 Normalization.....	25
4.5.1 Invariant Set Method.....	25
4.6 Model Based Expression Index.....	26
4.7 Outlier Detection Algorithm	27
Chapter 5: Functional Description of Genes.....	29

5.1	SOS Genes.....	29
5.2	Oxidative Damage.....	39
5.3	Other Stress Related Genes.....	40
5.4	Regulatory Genes.....	41
5.5	Metabolism.....	43
5.6	Transport Genes.....	48
5.7	Predicted and Pseudo Genes.....	49
5.8	Other Genes-Phantom, Cell Division, Protein Binding and Folding.....	52
Chapter 6: DNA Damage Repair and Processes.....		54
6.1	Introduction.....	54
6.1	UV Radiation Damage.....	54
6.2	Oxidative Damage.....	56
6.3	Nucleotide Excision Repair system.....	56
6.4	Recombination Repair.....	57
6.5	SOS Response.....	58
6.6	Translesion Synthesis.....	59
Chapter 7: Microarray Analysis of Differential Gene Expression.....		60
7.1	Introduction.....	60
7.2	Materials and Methods.....	61
7.2.1	Bacterial Strain, Growth Conditions and Plasma Treatment.....	61
7.2.2	RNA Isolation and Microarray Procedures.....	62
7.2.3	Data Analysis.....	63
7.3	Results and Discussion.....	64

7.3.1	Global Gene Expression Profile.....	64
7.3.2	SOS Response.....	68
7.3.3	Oxidative Damage Repair.....	69
7.3.4	Other Stress Response Genes.....	71
7.3.5	Regulation.....	72
7.3.6	Metabolism and Transport.....	72
7.3.7	Predicted and Pseudo Genes.....	74
Chapter 8: Varied Plasma Parameters for Bacterial Inactivation Optimization.....		78
8.1	Experimental Setup.....	78
8.2	<i>E. coli</i> Strain Information and Sample Preparation.....	79
8.3	Varied Conditions.....	80
8.3.1	Gas ON Plasma OFF.....	81
8.3.2	Distance from the Electrode.....	81
8.3.3	Frequency.....	81
8.3.4	Oxygen.....	81
8.3.5	UV Effect.....	82
8.3.6	Gas Composition and Flow rate.....	82
8.3.7	Power.....	83
8.4	Results and Discussion.....	83
8.4.1	Gas ON Plasma OFF.....	84
8.4.2	Distance from the Electrode.....	84
8.4.3	Frequency.....	84
8.4.4	Oxygen.....	85

8.4.5	UV Effect.....	87
8.4.6	Gas Composition and Flow	88
8.4.7	Power Variation	89
8.5	Conclusion	90
Chapter 9: Conclusions and Future Work		91
References		93
Appendix A		120
Appendix B		133

Chapter 1

Introduction

The elimination of disease causing agents from various surfaces is an absolutely necessary requirement in many fields that can sometimes be challenging to fulfill without using toxic chemicals or high temperatures and/or pressures. Historically many different approaches have been used to inactivate pathogens. Two widely used inactivation methods, especially in the medical field, are autoclaving and exposure to gases such as ethylene oxide (EtO). Although effective at eliminating pathogens, both methods suffer from drawbacks such as exposure to extremely high temperatures ($>100\text{ }^{\circ}\text{C}$), in the case of autoclaves, and toxic chemical exposure, in the case of EtO. Another concern with the use of these methods is the long treatment times, which can vary from about half an hour to almost 30 hours [Steelman1992].

In the past decade there has been a great interest in investigating the suitability of non-thermal atmospheric-pressure plasma as a potential agent for bacterial inactivation. Low temperature plasmas operating at atmospheric pressure are particularly well suited for treatment of sensitive materials such as medical instrumentation, food packaging, biological materials, etc. [Laroussi2005; Moisan2001].

The goals of this research were two-fold. First, to investigate the biochemical response of a bacterium to plasma exposure, so as to understand the mechanism of

plasma inactivation. Second, to vary plasma parameters such as feed gas composition and flow rate, RF power and frequency, etc. to optimize bacterial inactivation.

High-density oligonucleotide microarrays were employed to characterize differential gene expression in *E. coli* in response to plasma exposure. Plasma exposure was found to significantly induce the SOS mechanism (named after the universal distress signal), consisting of about 20 genes. Other genes involved in regulating response to oxidative stress were also observed to be up-regulated. Conversely, the expression of several genes responsible for housekeeping functions, ion transport and metabolism, was observed to be down-regulated.

The results of microarray data analysis suggest that plasma constituents cause substantial DNA damage in *E. coli* leading to an incomplete damage repair response.

Since the work carried out as part of this inter-disciplinary dissertation encompasses many diverse fields, ranging from plasma physics to biochemistry, an effort has been made in this report to elucidate some of the fundamental concepts needed for understanding the broad spectrum of topics covered in Chapters 3, 6 & 7. The dissertation is organized as follows-

Chapter 2: Plasma Fundamentals

Fundamental plasma concepts as they relate to the working of a non-thermal atmospheric pressure plasma used in this dissertation are discussed here. Some of the key topics covered in Chapter 2 are Debye length, plasma sheath, local thermal equilibrium, Paschen curve and gas breakdown voltage.

Chapter 3: Hollow Slot Atmospheric Pressure Plasma

The electrode geometry and configuration, electrical parameters such as current and power densities, and other operating conditions of the hollow slot plasma device used for the experiments presented in this dissertation are described in detail in Chapter 3.

Chapter 4: Microarrays: Fabrication and Data Analysis

A high-density oligonucleotide array is an ideal candidate for investigating differential gene expression on a genome wide scale. The working principle of a DNA microarray is hybridization of complementary nucleic acid strands. The fabrication process of GeneChip microarrays (Affymetrix, CA) and technical details of the *E. coli* Genome-2 array that was used for experiments are briefly explained in Chapter 4.

Data analysis is an important and integral part of microarray experiments. Salient features of the DNA Chip Analyzer (dChip) software including normalization and Model Based Expression Index (MBEI) calculation are explained in Chapter 4.

Chapter 5: Functional Descriptions of Genes

Since the breadth of differentially expressed genes obtained through microarray experiments spanned many functional categories, a detailed listing of these genes and their functional roles are presented in Chapter 5.

Chapter 6: DNA Damage and Repair Mechanisms

Gene expression data indicates that DNA damage plays a major role in bacterial inactivation and therefore a thorough understanding of the topic is essential to investigate the mechanism of plasma inactivation of bacteria. The nature and sources of DNA damage are discussed in Chapter 6. Also, some of the relevant general and specific DNA repair processes are described.

Chapter 7: Microarray Analysis of Differential Gene Expression

The analysis of differential gene expression in *E. coli*, following exposure to plasma, utilizing GeneChip high-density oligonucleotide arrays (Affymetrix, CA) is presented in Chapter 7. The chapter also contains information on the materials and methods used for plasma exposure, sample preparation for microarray analysis, and data analysis. The various results obtained from microarray data analysis are also discussed in this chapter.

Chapter 8: Varied Plasma Parameters for Bacterial Inactivation Optimization

Besides investigating the genetic response of the bacterium to the plasma species, another set of experiments was conducted to explore the optimization of bacterial inactivation by varying plasma parameters such as feed gas composition and flow rate, RF power and frequency, etc. The experimental setup and results of these experiments are presented in Chapter 8.

Chapter 9: Conclusions and Future Work

Finally, the significance and impact of this dissertation on the biomedical applications of non-thermal atmospheric-pressure plasma are discussed in Chapter 9. There is also a brief discussion about future areas of research.

Appendix A: Normalization Plots and CEL Images

Microarrays can have variation in the intensity signals based on experimental variation and therefore it is necessary to normalize arrays with respect to a baseline array. The results of normalization are presented in Appendix A

Appendix B: RNA Isolation and Microarray Sample Preparation

RNA was isolated from *E. coli* cells using an RNeasy Mini kit (Qiagen, Valencia, CA) and subsequent sample preparation for microarray hybridization was conducted according to Affymetric prokaryotic sample preparation protocol. These procedures are presented in Appendix B.

Chapter 2

Plasma Fundamentals

2.1 Introduction

Plasma is a collection of partially or completely ionized gas. Also known as the fourth state of matter, the term *plasma* was coined by Irving Langmuir in 1928 [Brown1978; Tonk1929], comparing the electron and ion oscillations in a gas to the blood plasma. Plasmas are abundantly available making up most of the matter in the universe [Chen1974; Kamenetskii1978] including the sun, stars, interstellar space, etc. Research in plasmas really took off in the latter half of the 20th century and is broadly classified into gas discharge physics (<1000 K), and solar and thermonuclear plasma physics (>1000 K) [Boyd2003; Rosenbluth1983]. Although occurrence in a gaseous state is more common, plasmas can also occur in a liquid or a solid state [Kunhardt2000]. This dissertation only deals with plasmas in the gaseous state.

2.2 Debye Length and Plasma Sheath

Plasmas are characterized by their quasi-neutral and collective behavior. Quasi-neutrality implies that the net charge density in the plasma is zero, although at any given time the charge balance may deviate by a small amount at a given point within the plasma. Collective nature implies that long range coulomb forces that the charged

particles are subjected to do not diminish as a function of $1/r^2$ (r : average distance between an electron and an ion) [Chen1974]. On the contrary, potential Φ decreases according to the following relation

$$\Phi \sim \Phi_0 \exp(-|r|/\lambda_d)$$

where λ_d is Debye length

$$\lambda_d = \left(\frac{KT_e}{4\pi m_e e^2} \right)^{1/2} \quad (2.1)$$

where, K is the Boltzmann's constant, e is the charge of an electron, n_e is the electron density (also known as plasma density) and T_e is the electron temperature (T_i is the ion temperature and it is much lower than T_e).

The potential distribution next to a metal strip immersed in plasma is depicted in Figure 2.1.

Since electrons are much lighter and smaller in size than ions they have higher kinetic energy and collide with the metal strip more often and as a result charge the strip negatively. This build up of negative charge around the strip leads to a potential barrier as electrons are now repelled and positive space charges and ions accumulate next to the strip. The layers of positive space charges around the strip screen the negative charge and at a distance equal to the Debye length its effect is completely screened. This region is known as the sheath.

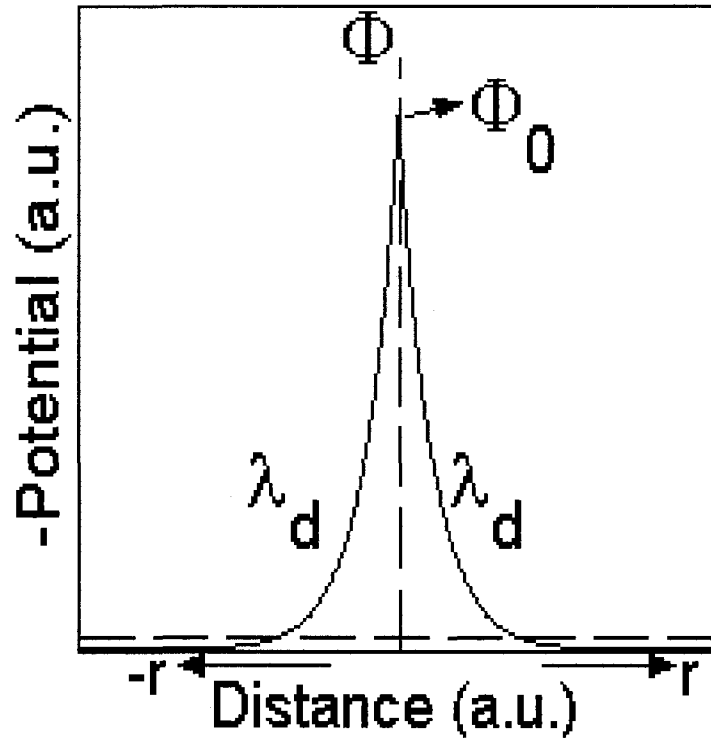


Figure 2.1: Potential distribution next to a metal strip ($r=0$) immersed in plasma due to ion accumulation. The base of the vertical axis is the plasma potential and the dashed horizontal line represents zero potential. λ_d : Debye length, marking the spatial decay constant at which potential approaches the plasma potential [Chen1974]

2.3 Local Thermal Equilibrium in Plasmas

Plasmas can be divided into two categories based on the ratio of gas temperature to electron temperature: low temperature plasmas and high temperature plasmas. In low temperature plasma, the ion temperature and the gas temperature are much lower than the electron temperature and therefore the temperature of the plasma constituents are not at equilibrium and thus the plasma is referred to as cold or non-local thermal equilibrium (non-LTE) plasma. In high temperature plasma, temperatures of all constituents are in local thermal equilibrium (LTE) and thus the plasma is referred to as thermal or LTE

plasma. High temperature plasmas are often used in high temperature applications like welding, plasma cutting and metal melting [Heberlein2002].

In low temperature or non-LTE plasmas, the plasma ion energies and densities can be controlled externally by varying various parameters (current, voltage, gas species, gas pressure etc.) over wide ranges and thus allowing precision work in many applications. In non-LTE plasmas applied electrical energy is mainly delivered to energetic electrons and therefore electron temperature is much higher than gas temperature.

Among the various applications of non-LTE plasmas are material deposition and etching [Babayan1998] in the semiconductor industry, thrusters and plasma contactors [Kirkici1995] in the space industry and as spectral light sources [Arslanbekov1998].

Current-Voltage characteristics of DC plasma are presented in Figure 2.2. There are three main operating regions for typical low pressure DC plasma [Raizer1997].

As seen in Figure 2.2, the left region works under the Townsend regime where a corona discharge exists, the conditions for which require a high voltage applied to sharp edge or tip. In a corona discharge the presence of the charged particles does not distort the applied electric field and the discharge is unipolar. Corona charges are used extensively for ozone generation [Raizer1997]. The right region works under an arc regime where the plasma is under local thermal equilibrium and is characterized by thermionic emission and low cathode fall voltage.

The middle region is where the plasma is in the form of a glow discharge and exists in non-LTE conditions. Many industrial applications depend on the operation of the plasma in this region because of benefits like high plasma uniformity and low gas temperature. The glow discharge exists past gas breakdown at point E and is marked by a

sharp decrease in voltage to point F. From point F to G the current increases without any significant rise in voltage and this region is known as the normal glow. In the normal glow region if the pressure is constant, the current density will remain constant even though the current may vary [Gambling1956; Kunhardt2000] i.e. the area of the glow discharge increases when current increases from point F to point G. Beyond point G, the positive slope in the I - V curve leads to an abnormal glow as the current density is no longer constant. A hysteresis loop is observed in the glow discharge if the current is reduced below the initiation point after the ignition of glow discharge plasmas (F'F).

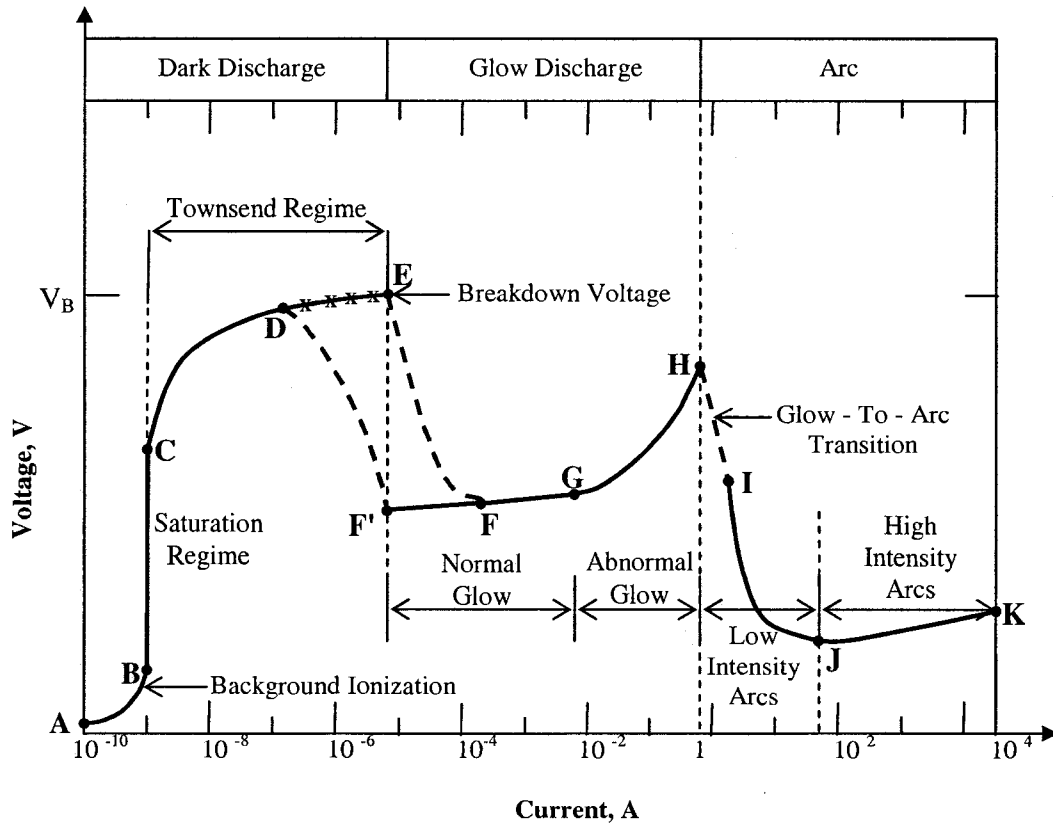


Figure 2.2: Current-Voltage characteristics of DC plasma [Roth2001].

2.4 Atmospheric Pressure Glow Discharge Plasma

Glow discharge plasmas at atmospheric pressure have many benefits over low pressure plasmas. First, an expensive and bulky vacuum apparatus is not needed for the operation of atmospheric pressure plasmas unlike for the operation of low pressure plasmas. Atmospheric pressure plasmas are especially suitable for treating materials with higher vapor pressure like certain chemicals and biological materials [Laroussi1996; Selwyn2001]. However operation at atmospheric pressure also poses certain unique challenges. First, the mean free paths of various energetic species is far less than at lower pressures and therefore more electrical energy or higher frequency might be required for plasma operation without instabilities.

2.5 Paschen Curve and Gas Breakdown Voltage

To get a better understanding of plasma operation at atmospheric pressure an insight into the gas breakdown voltage and Paschen curve is needed. There are two primary gas breakdown mechanisms; the Townsend mechanism and the spark mechanism [Akishev1994].

The Townsend mechanism is characterized by the creation of γ electrons at the cathode and subsequent collision with atoms or molecules in the discharge gap to liberate electrons (α -electrons). These newly created α -electrons can generate even more electrons by colliding with atoms and molecules thus leading to avalanches of electrons in the discharge gap. These avalanches of electrons move from the cathode towards the anode. The condition to create a self-sustaining current in a discharge gap (d) the criterion $(\gamma \exp(\alpha d) - 1) = 1$ needs to be fulfilled [Akishev1994; Fridman2005 and Raizer1997]. In the case of low pressure non-LTE plasma the relationship between

discharge gap, pressure and gas breakdown voltage is defined by the following equation also known as the Paschen law [Fridman2005]:

$$V_b = \frac{Cpd}{\ln(Apd / \ln[1 + (1/\gamma)])} \quad (2.2)$$

where, V_b is the gas breakdown voltage, A and C are constants that are dependent on the gas, p is the pressure, d is the distance of the discharge gap and γ is the secondary electron emission coefficient that is dependent on the cathode material.

The minimum breakdown voltage $(V_b)_{min}$ related to the **pd product** (pressure multiplied by the **distance** between electrodes) is obtained by differentiating equation (2.2) with respect to pd and equating to zero

$$(pd)_{min} = \frac{2.718}{A} \ln\left(1 + \frac{1}{\gamma}\right) \quad (2.3)$$

where, $(pd)_{min}$ is the pd product corresponding to $(V_b)_{min}$.

Paschen curve relates the breakdown voltage to the discharge gap and is obtained by considering the dimensionless variables

$$X = pd / (pd)_{min} \quad (2.4)$$

$$Y = V_b / (V_b)_{min} \quad (2.5)$$

For any arbitrary value of pd , equation (2.2) must be satisfied [Fridman2005] and therefore

$$Y = \frac{X}{1 + \ln X} \quad (2.6)$$

As seen in Figure 2.3 at values of X below 1, the increase in the breakdown potential is due to an insufficient number of neutrals that can be ionized to obtain gas breakdown. At values of X above 1 the gas breakdown voltage increases because

electrons lose energy due to increased number of collisions. The point on the Paschen curve where $pd = pd_{min}$ is called Stoletow's point and at this point the ion-electron pair generation is most efficient in terms of power expenditure [Fridman2005].

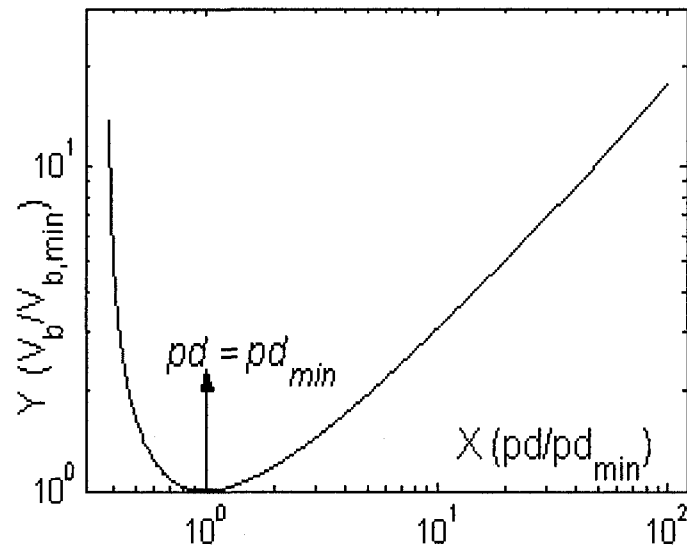


Figure 2.3: Theoretical Paschen curve of normalized breakdown voltage versus normalized pd products [Fridman2005].

As seen in Figure 2.4, the breakdown voltage minima for rare gases are less than what they are for molecular gases and occur at higher pd_{min} values. The curves obtained in the Figures 2.3 and 2.4 use DC excitation and are dependent on γ electrons that are released due to secondary emission. As a result, electron yield is a function of ion bombardment and photoelectric effect and is dependent on the electrode material.

Under low pressure conditions in RF discharges the ions are largely immobile as they cannot follow changes in electric field due to inertia and therefore the breakdown of gases is not caused by ion bombardment of electrodes thus electrode material is not a factor. On the other hand electrons resonate with the frequency of the applied electric field and therefore oscillate back and forth between the electrodes. The electrons ionize the volume of the gas and when the mean free path of ionization is approximately equal

to the discharge gap, the Paschen minimum occurs [Roth2001]. The gas breakdown voltages for RF discharges are observed to be lower than those for DC discharges.

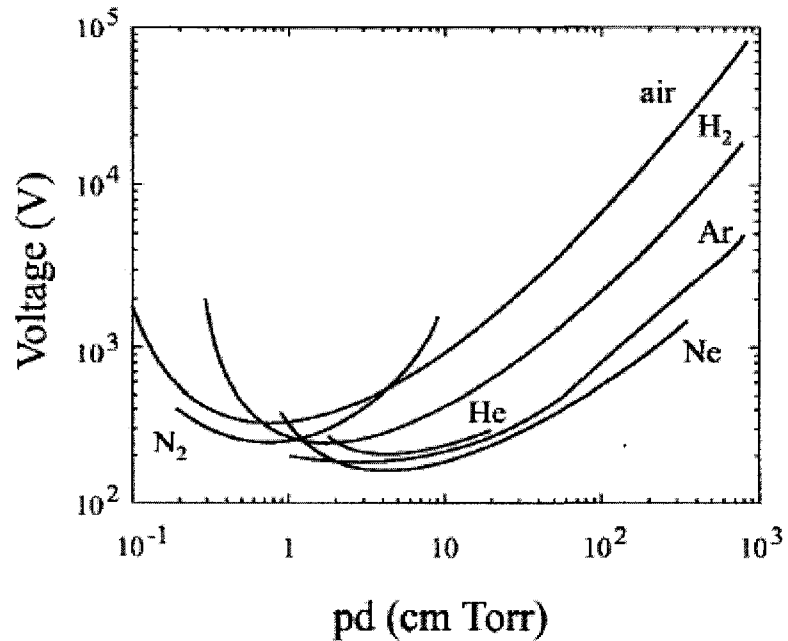


Figure 2.4: Breakdown voltage of various gases as function of the pd product [Schutze1998]

In atmospheric pressure plasma due to higher level of collision frequencies the mean free path is greatly reduced and therefore the discharge is similar to a DC discharge and secondary emission of electrons gains relevance and gas breakdown voltage is higher than what it is at low pressures. The glow discharge operation at atmospheric pressure requires a larger voltage across the discharge gap at higher pd values. Since most of the applied voltage drops across the sheath, the probability of the arc formation is enhanced beyond a certain pd product and the non-thermal glow discharge has the possibility to turn into a plasma with local thermal equilibrium. Generation of uniform APGD plasmas tends to be difficult due to the limitation imposed by the pd product. The breakdown of gas in atmospheric pressure plasmas requires high voltage.

For glow discharge operation of rare gases, the pd product range is ~ 1 -10 Torr-cm [Schutze1998; Smith2003]. These values correspond to a discharge gap d between approximately 10 and 100 μm at atmospheric pressure. If the pd product lies in this range, the gas breakdown is due to primary avalanche in the bulk region and can be explained by the Paschen gas breakdown law [Massines1998].

The spark mechanism of gas breakdown is observed at higher pd values. At these higher pd values, the gas breakdown can also occur due to space charge accumulation anywhere between the electrodes instead of the cathode. As the space charge field becomes comparable to the applied field, highly conducting filamentary channels causes gas breakdown. The non-uniformities that arise in the plasma due to the spark mechanism make these discharges not very useful for material processing.

Chapter 3

Hollow Slot Atmospheric-Pressure Plasma

3.1 Introduction

Atmospheric-pressure plasmas that are not in local thermal equilibrium (non-LTE) have gas temperatures of hundreds of degrees Kelvin, electron temperatures of about 1 eV, and electron number densities on the order of $10^{11-14}/\text{cm}^3$ with metastable densities 1-2 orders of magnitude greater than ion densities. A straightforward means of generating non-LTE atmospheric pressure plasmas is to operate a glow discharge at a current density below the threshold for glow-to-arc transitions. This was first demonstrated in the 1950s [Gambling1953].

3.2 Literature Review

Several research groups have investigated the use of atmospheric plasma technology for inactivation of bacteria [Herrmann2002; Kelly-Wintenberg1999; Koinuma1992; Laroussi2005; Moisan2001]. Many different electrode configurations, feed-gas mixtures, and operating conditions have been tested with varying results [Moisan2001]. Some groups achieve operation near room temperature but the treatment methodology is not suitable for wide area treatment as the plume area is relatively small [Laroussi2005]. Other researchers have created chambers that can be used for treating the

contaminated specimen [Herrmann2002; Kelly-Wintenberg1999]. However a drawback of this approach is that device portability and convenience of use are compromised. Still other research groups have developed needle plasmas [Koinuma1992; Stoffels2002] that work at relatively low voltages but are not suitable for wide area treatment.

3.3 Hollow Slot Plasma-Configuration

The research in this dissertation is focused on radio frequency (RF) driven open-air hollow slot microplasmas that can be tens of cm in length. The active electrodes excite a rare gas mixture and the effluents flow into open air as an afterglow plasma plume at near room temperature. The powered wedge electrode is recessed within a volume behind the grounded slot (See Figure 3.1) as is much of the associated inter-electrode plasma, so that (external) work pieces require no electrical connection or sealed chamber to operate. The two electrodes of extended length are spaced fractions of mm from each other. This close-coupled plasma-electrode design facilitates surface electrode phenomena, such as cold emission of electrons from surfaces crucial to stable plasma operation via photo- and ion-induced secondary emission.

The slot plasma has a unique geometry and operating conditions as compared to prior work [Yalin2003; Yu2003; Rahul2005; Rahman2005]. Some of the salient features of the hollow slot plasma are

- Operation is in open-air with a line source plasma afterglow of high (>900) aspect ratio that is spatially homogenous, even at hundreds of watts of delivered RF power.
- The work piece is not placed on an electrode nor is part of the electrical circuit, but rather is placed in the afterglow plume.

- The work piece can be about one cm away from the active plasma with a clear optical path to surfaces to be treated allowing for high fluxes of plasma species and high energy photons from the active plasma.

It is judged that this electrode geometry is scalable to meter long lengths, allowing for wide-area treatment. Further, there is evidence that at higher RF frequencies, the need for rare gases is much reduced and perhaps may be eliminated.

3.4 Experimental Setup

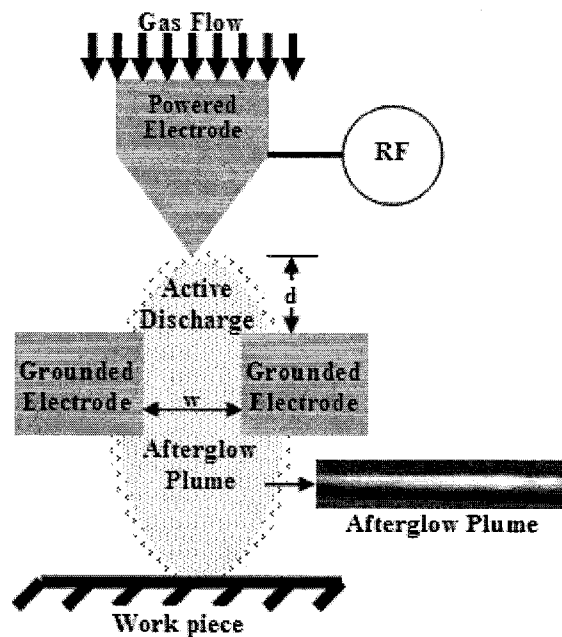


Figure 3.1: Schematic diagram of the device showing critical dimensions w (slot width) and d (inter-electrode spacing). The major regions are *active discharge* and downstream *afterglow plume*. The work piece surface, where bacterial inactivation occurs is 2.5-10 mm away from the active plasma in the afterglow plume. A photo of the plume emerging from the linear slot is presented in the bottom right inset. The length of the linear slot can be extended to 30 cm, depending on electrode design, gas flow, the rare gas employed, and total RF power applied.

Previous publications present the detailed technical aspects of the hollow slot plasma reactor [Yalin2003; Yu2003; Rahul2005; Rahman2005]. The hollow slot electrode configuration consisted of two electrodes as seen in Figure 3.1, which are coming out and into the plane of the paper. Included in this figure inset is a photograph of the actual plasma plume emerging from the slot into open-air. Electrode shape, critical electrode spacing, feed gas flow and applied RF voltage locations are also indicated in Figure 3.1. An external open-slot electrically-grounded hollow electrode opposes an internal RF powered wedge shaped electrode. It is judged that this electrode design allows a corona-initiated ignition and subsequent glow confinement of the linear plasma to the electrode area. This allows for two distinct micro-discharge regions to be formed: a luminous glow of active discharge between electrodes and a downstream afterglow plume. In between is a gas expansion region. The open slot width (w) was fixed at 200 μm for current studies but is variable from 50 to 800 μm . Similarly for the results presented in this dissertation the inter-electrode spacing (d) was fixed at 500 μm , but other values are possible. The length of the electrode used in this study is approximately 75 mm (3"), but it has also been extended to 300 mm for other applications of the device. It must be emphasized that the surfaces are processed in open-air and are neither part of the electrical circuit nor are they placed on electrodes in enclosures, all considerable practical advantages well beyond the present focus on bacterial treatment.

In the inter-electrode region, representative operating conditions are PD \sim 10 Torr-cm, average RMS $E \sim 20\text{kV/cm}$, average RMS $E/N \sim 70\text{ Td}$, current density $\sim 0.7\text{ A/cm}^2$, associated power density ($E J \cos \theta$) $\sim 14\text{ kW/cm}^3$ and energy per volume delivered to the flowing gas $\sim 100\text{-}200\text{ J/L}$. A plasma afterglow plume of linear shape 1-

30 cm long exits the grounded slot and extends 1-8 mm from the slot. Moreover the active plasma is millimeters away and delivers a strong flux of both UV and VUV (Vacuum-UV) photons.

Chapter 4

Microarrays: Fabrication and Data Analysis

4.1 Introduction

Messenger RNA (**mRNA**) is the first-degree product of gene expression. The process of transcription converts information stored in the form of DNA into mRNA, which is the macromolecule responsible for encoding information to manufacture proteins that perform various functions in the cell. The amount of mRNA transcripts from a given gene present in a cell at a certain time is dependent on which functions a cell needs to perform at that time. Therefore by observing the mRNA profile in the cell at a certain time one can get an idea of the various functions a cell intends to perform. These functions vary based on various environmental conditions the cell is exposed to and therefore a differential gene expression profile is obtained by subjecting the cells to different environmental conditions.

A DNA Microarray is a powerful tool that can be used to study differential gene expression in a much higher throughput manner than with other technologies like Northern Blotting, as microarrays allow the analysis of genome-wide gene expression. This high throughput technology has recently come of age since the completion of the full genomic sequences of many organisms is now a reality. Microarrays can be used not only to determine biological functions of individual genes but are also useful in the more

challenging task of discovering highly complex regulatory networks inside living cells which involve genes, proteins and metabolites. The combination of speed, miniaturization, parallelism and automation make microarrays ideal candidates for the above-mentioned explorations [Gupta1999].

An array consists of an ordered set of microscopic elements and the basic working principle of a DNA microarray is the hybridization of complementary nucleic acid strands. The four bases in the DNA chain have the following pairing scheme

- Adenine (**A**) pairs with Thymine (**T**) using two hydrogen bonds.
- Cytosine (**C**) pairs with Guanine (**G**) using three hydrogen bonds.

The samples to be analyzed termed as “**targets**” consist of chains of labeled single stranded cDNA that hybridize to complementary “**probes**”, which are manufactured chains of single stranded DNA.

Although DNA microarrays are fabricated based on many different technologies this dissertation will focus on GeneChip (Affymetrix, CA) microarrays.

4.2 GeneChip Array Fabrication

The fabrication of the GeneChip microarrays consists of the following steps-

- Substrate Preparation: This involves making the glass wafer suitable for synthesis of the probes
- Synthesis: This process uses standard practices similar to those used by semiconductor chip manufacturing industry and involves
 - Chemistry
 - Photolithography
- Packaging: After synthesis the glass chips are packaged in cartridges.

The synthesis of arrays involves building of vertical strands of DNA nucleotides (oligonucleotides) that are 25 bases long. The process is based on photolithography and a general scheme is depicted in Figure 4.1. As seen in Figure 4.1, light shines through a mask onto a wafer that has initial starting strands for oligonucleotide building. All areas that are not hidden by the mask are stripped of the protective groups from the strands. The wafer is then washed with a solution containing the appropriate free nucleotides that attach to the unprotected parts of the wafer (Thymine in the case of Figure 4.1). The above steps are repeated numerous times until each strand is 25 bases long. The whole process occurs through the controlling of the light to hit specific features on the chip.

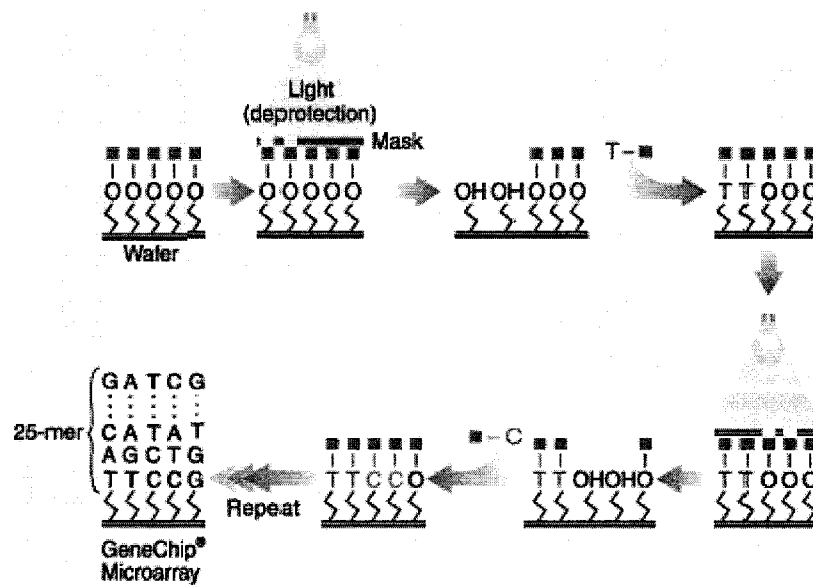


Figure 4.1: GeneChip Fabrication-General Scheme (Image courtesy Affymetrix Inc.)

Depending on the size of the chip either 40 or 400 chips can be manufactured on each wafer. The manufacturing process is scalable and with a feature size of 10 μm , each chip can contain about 1.6 million features, which enables expression monitoring of thousands of transcripts. The chips are 1.28 cm^2 in area.

4.3 GeneChip *E. coli* Genome 2.0 Array-Technical Details

The GeneChip *E. coli* Genome 2.0 array used for this study has a feature size of 11 μm and the detection sensitivity is 1:100,000. There are approximately 10,000 probe sets that map to 20,366 genes and 714 inter-genic regions in the following four strains of *E. coli* with corresponding sequence information.

1. K12 strain (m56 version) -ASAP database-April 2003.
2. O157:H7-EDL933 strain (version 1) -ASAP database-April 2003.
3. O157:H7-Sakai strain-NCBI databases-May 2004.
4. CFT073 strain -NCBI databases-May 2004.

Due to high sequence similarity many of the probe sets on the array are tiled to represent the equivalent ortholog in all four strains. Oligonucleotide probes are synthesized *in-situ* complementary to each corresponding sequence. Eleven probe-pairs: Perfect-Match (PM) and Mis-Match (MM) probes are in each probe-set to measure the transcription level of a sequence represented on the array.

4.4 Data Analysis-dChip Software

The analysis of data obtained from a high density oligonucleotide microarray consisting of gene expression information about thousands of transcripts is a complex task not only because of large data sets involved but also because of many sources of biases introduced in the upstream experiments. Therefore, a software application to analyze gene expression data from microarrays should have capabilities of identifying and handling cross-hybridizing probes, contaminating regions in the arrays and at the same time should be able to translate probe level data from multiple arrays into meaningful information.

In this study the expression data obtained in the form of CEL (Cell intensity) files from the Affymetrix scanner were analyzed using dChip (DNA Chip Analyzer), a Windows based software package that can be used for both probe-level and high-level analysis of gene expression data obtained from Affymetrix microarrays. At the probe-level, dChip was used for displaying and normalizing the CEL files and high-level analysis included comparing *treatment group* and *control group* samples.

4.5 Normalization

The simultaneous analysis of multiple arrays can suffer from biases affecting the overall image intensity of an array. These biases are introduced if the images have been generated at different times and places. Normalization is a process of adjusting the overall chip brightness of the arrays to a similar level before comparing the expression level of genes between arrays.

4.5.1 Invariant Set Method

The method used in dChip to normalize arrays is based on the principle of an *invariant set* that works for a group of arrays, on the basis of identification of a common baseline array (having median overall brightness) and adjustment of the overall chip brightness of all the other arrays relative to the baseline array.

Specifically, the normalizing relation is a curve drawn on the scatter-plot of two arrays with the baseline array on y-axis and the array to be normalized on x-axis. The normalization is based on probes that belong to non-differentially expressed genes. It is not easy to determine which genes are non-differentially expressed, however the intensity ranks of non-differentially expressed genes are expected to be similar (where intensity

ranks on the two arrays are calculated separately). An iterative process is used to obtain a set of points (invariant set) representing presumably non-differentially expressed genes.

In detail, the iterative procedure starts with all PM probes on an array numbering in the thousands. A point is chosen in the new set if its *proportion rank difference* (PRD) in the two arrays divided by the number of all the PM probes is small enough. The threshold of being small is dependent on a point's average rank difference in the two arrays

For,

Large average rank difference in the two arrays: $PRD < 0.007$

Small average rank difference in the two arrays: $PRD < 0.003$

This strategy yields more points at lower intensity range. The above procedure is applied iteratively to the new sets until the number of points in a new set does not decrease anymore. A piecewise linear running median line is calculated and used as the normalization curve.

4.6 Model Based Expression Index

Model Based Expression index is used to calculate the gene expression values based on the low level data obtained from the probe sets on the arrays. There are two options to calculate the expression values using this model; PM (Perfect Match)/MM (Mismatch) difference and PM-only. The PM-only model was used for this study to calculate all positive expression values. The model uses the outlier detection algorithm (described below) to eliminate potential cross-hybridizing probes by absorbing some background signal in the expression values.

Background subtraction is achieved by dividing the whole array into 10 by 10 sectors and the 5th percentile of PM and MM values are calculated as the local background of that sector. Then these values are subtracted from all PM and MM values in that sector. If negative values are obtained they are set to zero (the error introduced by setting the values is compensated by adding a term ε in the multiplicative model as described below).

Applying multiplicative model to the background-adjusted PM values:

$$PM_{ij} = \theta_i * \Phi_j + \varepsilon$$

where θ_i is the model-based expression index (MBEI) of the target gene in array i and Φ_j is the probe sensitivity index (PSI) of probe j in a probe set.

4.7 Outlier Detection Algorithm

The algorithm mentioned below coupled with curve fitting applying the multiplicative model is iterated up to 30 times to either reach a converged set of array, probe and single outliers or one of the cycling outlier sets at round 30.

Image Spikes check: Image spikes are identified using the absolute values of the adjusted PM values. The 80th percentile of the absolute values of the data points in one array multiplied by three is called the array wise value threshold. If the absolute value of a data point exceeds this threshold it is labeled as an image spike. Similar criteria are applied to determine probe spikes.

Single Outlier detection: If the absolute residual of a data point exceeds both the 80th percentile of the absolute residuals of the data points in one array and probe multiplied by 3 then it is labeled as a single outlier. To detect a single outlier there has to be at least six arrays and probes for comparison.

Probe and array outlier detection: If the model-based standard error for a probe is three times larger than the median standard error of all the probes it is labeled as a probe outlier. Similar criteria are applied to determine array outliers.

Model fitting and outlier detection iteration: After the three types of outliers are determined the model is refitted with the remaining probes or arrays. Following this step the expression index for probe or array outliers is computed using local regression and taking into account the probe sensitivity index values of only non-outlier probes or arrays. The outlier detection and model fitting is iterated until the number of outliers does not change or up to 30 times. The final fitted model does not allow the sum square of probe sensitivity index values of non-probe outliers to exceed those that of probe outliers.

The above measures enhance the likelihood of obtaining reliable information on differential gene expression from the scanned arrays.

Chapter 5

Functional Description of Genes

5.1 SOS Genes

- *dinB*

Cell survival during nucleotide starvation conditions is enhanced by *dinB* [Godoy2006]. DNA polymerase IV (DNA pol IV) which is part of the Y family of proteins [Ohmori2001] is encoded by *dinB*. DNA pol IV is actively involved in repairing many different kinds of lesions, for instance DNA template/primer pairs with misalignments [Wagner1999]. Spontaneous mutations are caused due to the activity of DNA pol IV [Kim2001; Tang2000], and is responsible for adaptive mutations [McKenzie2001]. DNA poly IV does not contribute significantly to chromosomal mutation rate under normal growth conditions [Kuban2004]. Proofreading is not exhibited by DinB and DNA pol IV activity is not very processive [Wagner1999].

- *dinD*

Under normal conditions the induction of *dinD* is repressed by LexA [Bagg1981]. The induction of *dinD* is often caused in response to DNA damaging agents like UV and hydrogen peroxide, and its expression fails in *recA* and *lexA* mutants [Kenyon1980]. The expression also reduces upon photoreactivation after UV induction of the SOS response

thereby indicating that cyclobutane pyrimidine dimer as the possible primary inducer of SOS response genes upon UV exposure [Brash1985].

– *dinF*

DinF is a member of the multi drug and toxin extrusion (MATE) family of transporter proteins [Brown1999], and is DNA damage inducible [Kenyon1980]. DinF may function as a proton-driven efflux system, possibly for nucleotides given its potential role in response to DNA damage. Location of the *dinF* gene is downstream of the *lexA* gene.

– *dinI*

DNA damage inducible protein-I is a small protein with 80 amino acids and is encoded by *dinI* [Yasuda1996]. The *dinI* gene is a chromosomal locus containing a high affinity operator for the LexA repressor [Lewis1994]. Induction of *dinI* is controlled by the LexA-RecA regulatory system [Voloshin2001].

Function of DinI is dependent on its concentration. If the concentrations of DinI are stoichiometric with those of RecA, DinI acts mainly as a positive modulator of RecA function as it stabilizes the RecA filament, reducing or preventing disassembly which does not affect RecA-mediated ATP hydrolysis and LexA co-protease activities [Lusetti2004]. DinI and RecX (a negative modulator of RecA, which blocks RecA filament extension and leads to net filament disassembly) constitute a regulatory network of RecA [Lusetti2004]. However if the concentrations of DinI are very high relative to those of RecA, it has contradictory effects on RecA. Over-expression of *dinI* in *E. coli* mutants causes increased UV sensitivity [Yasuda1998]. DinI inhibits the ability of RecA to induce cleavage of UmuD and its recombinase activity [Yasuda1998]. DinI binds to

active RecA filament and inhibits its coprotease activity, but not its ATPase activity [Yasuda2001]. DinI tightly binds to the central region of RecA (between the N- and C-terminal domains) and this interaction is enhanced upon the oligomerisation of RecA [Yoshimasu2003].

– *lexA*

This is a vital regulatory gene responsible for controlling the expression of genes in the SOS response regulon [Madan2003]. An autocatalytic cleavage mechanism mediated by RecA is responsible for the cleavage of LexA. As a result of the cleavage, the transcriptional repressor nature of LexA over the SOS genes is reduced and therefore induces an up regulation of those genes. The gene *lexA* itself is under the influence of the LexA binding. The SOS response is usually triggered in the event of DNA damage [Cole1983].

– *polB*

DNA polymerase II (Pol II) is encoded by *polB* gene and it is a combined polymerase and 3' to 5' exonuclease that enables the restart of replication following UV exposure [Rangarajan2002]. It also takes part in translesion synthesis and nucleotide excision repair that fixes DNA crosslinks [Berardini1999]. In addition, Pol II also plays a role in surviving thymine dimers and avoiding the effects of mutagenic agents [Escarcelle1994; Sedliakova2001].

Compared to other DNA polymerases, in replication of AT-rich sequences by Pol II is more error prone [Wang2002]. Pol II is also known for bypassing certain DNA lesions during the process of replication. Certain conditions dictate the presence of Pol II for bypassing of abasic lesions [PazElizur1996; Tessman1994]. Bypassing of abasic

increases when Pol II exonuclease activity is disabled [PazElizur1996]. Pol II can also bypass 3,N(4)-ethenocytosine lesions and carries out mutagenic bypass of 2-acetylaminofluorene-induced lesions, the latter causes -2 frameshifts [Al2005; Napolitano2000]. Pol II and Pol V seem to compete directly to bypass AAF lesion sites [Becherel2001]. Pol II has also been linked to bypassing of crosslinking lesions [Kanuri2005].

– *recA*

RecA performs multiple biochemical functions. It is a regulatory protein that acts on LexA repressor to induce the SOS response and furthermore is required for mutagenic bypass of DNA lesions during SOS response [Courcelle2003]. It also functions as a catalyst in DNA strand exchange reactions in the homologous recombination process.

RecA plays a pivotal role in SOS response. When activated, RecA forms nucleoprotein filaments on DNA. Free LexA protein binds within the deep helical groove of the RecA nucleoprotein filament [Yu1993] thus leading to an efficient autocatalytic cleavage of the transcriptional repressor LexA. As a result, the amount of LexA that can bind to the specific sites (20 base pair) in the promoter/operator region of the LexA regulated genes decreases dramatically and therefore many of these genes are released from negative transcription.

Activated RecA also promotes the autocatalytic cleavage of the lambda phage repressor and UmuD protein. Cleavage of the lambda phage repressor plays no role in DNA repair, but stimulates prophage induction. Cleavage of the UmuD protein creates UmuD', which combines with UmuC to form UmuD'C, also known as polymerase V that plays a role in catalyzing translesion DNA synthesis. This is an alternative to repair

which inserts random bases opposite some non-coding lesions. This strategy can lead to point mutations due the error-prone synthesis and is a measure of last resort in cases of massive DNA damage [Kuzminov1999]. The genes *lexA* and *recA* are also derepressed in the SOS response.

DNA damage can affect either one or both strands of the double helix and RecA helps in the repair of both kinds of damages. In the case of double stranded breaks the RecA pathway facilitates homologous recombination with a separate intact homologous region of DNA. RecA pathway can exist in two forms. In both forms RecA uses RecBCD for homologous recombination. On the other hand, one form utilizes resolvase enzyme, RuvABC, while the other form utilizes RecG helicase [Meddows2004]. RecA also binds to single-stranded DNA in regions of stalled replication and thus serves a structural as well as a regulatory role. By binding to the single-stranded DNA it protects it from degradation by exonucleases while awaiting repair [Courcelle2003].

— *recN*

RecN is another protein whose production is controlled by the LexA transcriptional repressor and therefore is damage inducible and plays an important role in various repair mechanisms especially involving double strand breaks [Meddows2005]. RecN usually is not activated until there are double strand breaks at two or more locations in the chromosome. RecN utilizes the help of DksA in repairing these breaks. It has been known that *recN* mutations can lead to increased susceptibility of the cell to ionizing radiation and UV induced damage. In fact experiments have shown that *recN* mutants are 90% deficient in repairing X-ray induced double strand breaks

[Sargentini1986]. RecN is also involved in post-replication repair of daughter strand gaps and bleomycin lesion repair [Kosa2004; Wang1988].

– *recX*

An inhibitor of RecA, RecX interferes with ATP hydrolysis, coprotease and DNA strand exchange activities of RecA [Stohl2003]. However, RecX does not appear to regulate transcription of *recA* and levels of RecX are about 500 times less abundant than RecA [Pages2003]. Overproduction of RecX can cause UV sensitivity and defects in DNA damage induction of transcription and proteolysis of LexA and UmuD [Stohl2003]. RecX induction is caused by DNA damage and its induction is part of the SOS response.

– *ruvB*

This gene produces a product that is involved in the enzymatic reaction that causes DNA to combine with exogenous DNA to form a recombination junction. This enzymatic reaction comprises of two other proteins, RuvA and RuvC.

The RuvABC enzymatic complex functions in recombination pathways by binding to recombinational junctions and catalyzing strand cleavage and branch migration. Although both *ruvA* and *ruvB* are part of the SOS inducible operon, *ruvC* is not part of that operon [Kuzminov1999]. The RuvABC resolvase as the enzymatic complex is known, helps RecA in the repair of double strand breaks.

Double strand breaks unlike single strand breaks cannot be repaired by excision repair pathways as they lack an intact strand to be used as a template and therefore RecA pathway provides the separate, intact and homologous region of DNA. To complete the process of recombinational repair, DNA junctions formed during the RecA filament strand exchange must be resolved and the RecA filament removed. This is achieved using

two independent enzymatic systems: the RecG helicase and the RuvABC resolvase [Kuzminov1999]. RuvA, a junction-specific binding protein, forms a hexameric ring in conjunction with RuvB under in-vitro conditions. The two enzymes then interact to catalyze branch migration of three and four arms (Holliday) junctions [Courcelle2003, Parsons92]. RuvC interacts with RuvA and RuvB as an endonuclease which cuts symmetrically at the points of crossover and thus resolves joint molecule junctions [Courcelle2003, Shah1994].

— *sbmC*

This protein inhibits gyrase mediated DNA supercoiling and thus protects the cell from toxins that act via DNA damage caused by DNA-bound gyrase [Chatterji2002; Nakanishi1998]. Also, SbmC prevents damage from alkylating agents that disrupt gyrase function [Chatterji2002].

SOS induction of the *sbmC* gene is governed by the RpoS protein and the binding of the H-NS protein to the promoter region [Oh2001].

— *ssb*

The highly stable single-stranded DNA binding protein SSB is the product of *ssb* gene. It is involved in replication, recombination and repair in the DNA metabolism of *E. coli*.

One of the major functions of SSB is protection of DNA as SSB interferes with binding of a number of proteins to DNA including exo- and endo-nucleases. SSB is also involved in the assembly of the DNA polymerase III complex onto DNA [Meyer1990]. SSB is required for DNA replication as it is involved in stabilization of DNA replication origins and primosome formation. SSB interacts with helicases in the unwinding of DNA

by stabilizing the single-stranded DNA and inhibiting reannealing. SSB may also be involved in promoting binding of polymerases to DNA. The ability of SSB to prevent secondary structure in DNA results in improved processivity of DNA polymerases. SSB also acts to increase the rigidity of ssDNA resulting in increased ability of polymerases to recognize mistakes. This leads to decreased mutagenesis [Meyer1990].

SSB is required for methyl-directed mismatch repair in unwinding, excision, and re-synthesis of DNA. SSB is also involved in the SOS response as it acts by providing ssDNA as a cofactor for RecA to promote the deactivation of the LexA repressor. SSB also protects DNA from excessive degradation [Meyer1990].

SSB seems to be involved in nucleoprotein filament formation during RecA-mediated recombination. SSB is also involved in the RecBCD pathway of homologous recombination in the capacity of stabilization of the ssDNA upon excision at Chi sites [Meyer1990].

— *sulA*

This gene is induced by the SOS response and inhibits cell division through interaction with FtsZ [Higashitani1997].

— *umuDC (umuC and umuD)*

UmuC and UmuD, both take part in the formation of DNA polymerase V (Pol V) that is responsible for the highly mutagenic bypass of DNA lesions that are not acted upon through the normal replication process using DNA Polymerase III [MaorShosha2000].

Pol V is involved in a number of repair processes and repairs involving catalysis of bypass synthesis account for about one fifth of all DNA damage repairs

[Berdichevs2002]. Notable contributions of DNA Pol V have been documented at many error sites, namely-

- Thymine dimers, guanine oxidation products and abasic lesions [Neeley2007; Tang2000]
- Replication restart following UV irradiation [Rangarajan2002]
- Repair of MMS-induced lesions [MaorShosha2000]

UmuC is required for some spontaneous base-pair substitutions [Bhamre2001]. Loss of *umuC* results in UV sensitivity and difficulty repairing daughter strand gaps. UmuD is proteolytically processed into UmuD' in a cleavage reaction that depends on activated RecA. The sequences of *lexA* and *umuD* are similar and therefore both are cleaved in a RecA mediated manner. RecA does not directly cleave UmuD instead it promotes cleavage of one member of an UmuD pair by its dimerization partner [Nohmi1988]. This cleavage to form UmuD' is an important step to form Pol V protein complex where UmuD' combines with its functional partner UmuC. Sometimes following SOS induction, the amount of UmuD can be about twelve times as abundant as its partner protein UmuC [Woodgate1991].

UmuC and UmuD act together to delay replication restart. This UmuDC-mediated replication block causes a lag for the conversion of UmuD to UmuD', which allows the formation of Pol V. This lag may allow time for other repair mechanisms to act before error-prone synthesis catalyzed by Pol V begins [Opperman1999].

If, however the other repair mechanisms fail to rectify the extensive DNA damage the UmuD'₂C complex is formed as described above to initiate the error prone translesion synthesis repair (TLS) process [Snyder2007]. In the TLS process, DNA polymerase III

the normal replicating holoenzyme gets stalled at the location of the DNA damage in a replicating fork. However DnaB enzyme continues to separate the strands ahead of the replicating polymerase. This separated single stranded DNA ahead of the stalled replication point then attracts RecA to form nucleoprotein filaments [Snyder2007]. Since the UmuD'₂C complex binds well with RecA, it is attracted to the stalled site and it randomly inserts deoxynucleotides opposite the damaged sites. Since the inserted bases by the UmuD'₂C complex are random they can cause mutagenesis and therefore TLS is restricted to about five bases after which normal replication restarts by reloading DNA polymerase III [Snyder2007].

– ***uvrA and uvrB***

UvrA and UvrB are subunits of the UvrABC nucleotide excision repair (NER) generalized DNA repair process and are produced when the cell is under stress and the SOS response is activated. UvrA forms homodimers in presence of ATP [Sancar1988], and associates with UvrB at physiological concentrations to form an UvrA₂B complex in an ATP-dependent interaction [Orren1989].

Nucleotide excision repair is a major repair pathway and can act on a variety of DNA lesions including

- UV-induced photoproducts- cyclobutane dimers, 6-4 photoproducts, thymine glycol.
- Bulky adducts, apurinic/aprimidinic (AP) sites and cross-links.

This pathway consists of the following steps

1. Recognition of the damaged area.
2. Incision 3' and 5' to the damaged area.

3. Excision of the damage containing oligonucleotide.
4. Re-synthesis of the excised strand and ligation to form a repaired duplex.

The main constituents of the pathway are the products of the genes *uvrA*, *uvrB* and *uvrC* [Lin1989]. It must be noted that unlike *uvrA* and *uvrB*, *uvrC* is not induced as part of the SOS response.

– *yebG*

This is another gene under the influence of the SOS regulon and therefore its expression is regulated by LexA [Lomba1997]. It encodes a conserved protein.

5.2 Oxidative Damage

– *katG*

KatG is an enzyme that is a bifunctional hydroperoxidase I, and therefore acts both as a catalase and peroxidase [Claiborne1979]. Involved in the removal of the superoxide radical, the catalase uses two-electron transfer in the dismutation of H₂O₂ to oxygen and water, while the peroxidase uses a one-electron transfer to a hydroperoxide acceptor [Loewen1990].

– *oxyS*

A regulatory-RNA, OxyS plays a regulatory role in oxidative stress response [Altuvia1997]. Present in high abundance, it is involved in the regulation of *flhA*, *rpoS* and other genes. It binds to FhlA mRNA and inhibits translation by interfering with the binding of the mRNA by the ribosome [Altuvia1998]. The binding of OxyS mRNA to other mRNA species like RpoS mRNA is influenced by the Hfq protein [Zhang2002]. OxyS also has an antimutator effect [Altuvia1997].

– ***sodA and sodB***

The two superoxide dismutases, SodA and SodB, contain manganese and iron respectively. While *sodB* is expressed in both aerobic and anaerobic conditions, *sodA* is only expressed in aerobic conditions [Touati1988]. It is believed that SodA is more effective than SodB in preventing damage to DNA, while SodB is more effective in protecting a cytoplasmic superoxide-sensitive enzyme [Touati1988].

– ***soxS***

This regulator acts in response to superoxide radicals as part of the oxidative stress response. It activates the transcription of the following genes/operons- *acrAB*, *fldA-fur*, *fpr*, *fumC*, *fur*, *inaA*, *marRAB*, *nfo*, *sodA*, and *zwf* by facilitating the binding of RNA polymerases to the promoter sites. Transcription can be induced by biofilm formation [Ren2004]. SoxS is an unstable molecule due to proteolytic degradation. This instability enables it to rapidly curtail its transcriptional response once inducing conditions have disappeared [Griffith2004].

5.3 Other Stress Related Genes

– ***cspC***

A cold shock protein, CspC is not actually induced by cold condition unlike CspA. CspC is able to bind to RNA or single-stranded DNA sequences, specifically AT/AU-rich regions [Phadtare2006].

– ***frmB***

A protein involved in detoxification, FrmB is a serine hydrolase that associates highly with the substrate S-formylglutathione [Gonzalez2006]. It is encoded in an operon

with FrmR and FrmA, proteins that take part in oxidation of formaldehyde [Gonzalez2006].

— *mntH*

A member of the NRAMP (natural resistance-associated macrophage proteins) family, MntH is a metal ion transporter protein [Haemig2004]. It is involved in the uptake of Metal²⁺ as a permease. Uptake of Mn²⁺ is mediated by a high affinity proton support reaction. The permease also transports Fe²⁺ at a lower affinity [Haemig2004].

— *otsB*

Expressed under osmotic stress, OtsB is a haloacid dehalogenase (HAD)-like hydrolase. It is induced by transition to stationary phase and at low temperatures [Kandror2002].

— *smpA*

A lipoprotein, SmpA is found in the outer membrane of the cell and it is a member of the σ^E regulon and its expression is controlled by the stress response sigma factor σ^E [Rezuchova2003]. Its expression is upregulated in the presence of autoinducer 2 [DeLisa2001]

5.4 Regulatory Genes

— *abgR*

Located in the cytoplasm, AbgR may transcriptionally regulate the *abg* operon [Hussein1998]

– ***cobB***

The CobB protein belongs to the sirtuins, a family of NAD⁺-dependent protein deacetylases that are broadly conserved. The protein also has weak ADP ribosyltransferase activity [Landry2000].

– ***lsrR***

The LsrR protein is a transcriptional regulator whose activity is inhibited by autoinducer-2 binding [Hardie2003].

– ***malI***

MalI is a transcriptional repressor involved in the transport of maltose-glucose and is auto-regulated negatively and coordinately represses the transcription of the *malXY*-divergent operon [Reid1991].

– ***paaX***

PaaX is a protein that is regulatory in a negative manner and it participates in controlling transcriptional regulation of divergent *paa* catabolic operons that are involved in phenylacetic acid degradation in *E. coli*, as *paaZ* and *paaABCDEFGHIJK* operons [Ferrandez2000]. PaaX binding is inhibited by phenylacetyl-CoA [Ferrandez2000].

– ***ryhB***

RyhB acts in reducing iron consumption under low-iron conditions [Masse2002]. It is an antisense RNA that down-regulates *sdhCDAB* RNA abundance [Masse2002]. RyhB is protected by Hfq protein from getting degraded by RNaseE. It also regulates *acnA*, *fumA*, *fnrA*, *bfr*, and *sodB* using the protein Fur which in turn represses *ryhB* [Masse2002].

5.5 Metabolism

– *acpS*

The protein AcpS encoded by the *acpS* gene is located in the cytoplasm and is involved in the metabolic pathway of biosynthesis of fatty acids and phosphatidic acids. It transfers 4-phosphopantetheine moiety of CoA to the apo-ACP to form holo-ACP, the active form of the carrier in lipid synthesis [Lambalot1995].

– *astB*

The protein succinylarginine dihydrolase is encoded by the gene *astB* is involved in the arginine degradation II pathway. It catalyzes the second reaction in the ammonia-producing arginine catabolic pathway. In this reaction the guanidino group of succinylarginine is completely degraded. [Schneider1998]

– *deoB*

The enzyme phosphopentomutase is encoded by the gene *deoB* and it is involved in the degradation of pyrimidine deoxyribonucleosides and purine deoxyribonucleosides. The enzyme catalyzes the reversible transfer of a phosphate group between the C1 and the C5 carbon atoms of ribose and deoxyribose, respectively [Leer1975].

– *fadH*

The gene *fadH* encodes the enzyme 2,4-dienoyl-CoA reductase. The enzyme takes part in the reductive removal of double bonds that extend from even-numbered carbon atoms in polyunsaturated and unsaturated fatty acids. The reductase is also involved in the catalytic reduction of 2-*trans*, 4-*cis* and 2-*trans*,4-*trans* isomers almost the same efficiency [Liang2000].

– *fdoG, fdoH & fdoI*

The α , β & γ subunits of formate dehydrogenase-O, are encoded by the *fdoG*, *fdoH* and *fdoI* genes respectively. Formate dehydrogenase-O is part of a system in which *E. coli* uses alternative terminal electron acceptors to generate proton motive force (PMF) that is responsible for the synthesis of the energy carrier ATP [Abaibou1995].

– *frdA, frdB & frdC*

The proteins FrdA, FrdB & FrdC are subunits of fumarate reductase with FrdD forming the last membrane subunit.

– FrdA = fumarate reductase flavoprotein

– FrdB = fumarate reductase iron-sulfur protein

– FrdC = fumarate reductase membrane protein

– FrdD = fumarate reductase membrane protein

Fumarate reductase acting as a catalyst allows the acceptance of a terminal electron by fumarate when *E. coli* is growing under anaerobic conditions [Cole1985].

– *glf*

UDP-D-galactopyranose mutase catalyzes the reversible inter-conversion of UDP-galactopyranose (the product encoded by the gene *glf*) and UDP-galactofuranose [Nassau1996]. This is part of a metabolic process involved in the biosynthesis of O antigen [Stevenson1994].

– *gnd*

The gene *gnd* encodes the protein 6-phosphogluconate dehydrogenase (decarboxylating) that is involved in both oxidative and non-oxidative branches of the pentose pathway [Westwood1974].

– ***hisA, hisC and hisF***

The genes *hisA*, *hisC* and *hisF* are involved in the histidine biosynthesis I pathway. N-(5'-phospho-L-ribosyl-formimino)-5-amino-1-(5'-phosphoribosyl)-4-imidazolecarboxamide isomerase (HisA) is involved in the fourth step of histidine biosynthesis. HisA catalyzes an internal redox reaction known as an Amadori rearrangement [HennSax2002]. Histidinol-phosphate aminotransferase (HisC) catalyzes the seventh step in histidine biosynthesis. HisC catalyzes the conversion of imidazole acetol-phosphate to histidinol-phosphate [Grisolia1985]. Imidazole glycerol phosphate synthase (HisFH) is a heterodimer that takes part in the fifth step in histidine biosynthesis. It also helps in generating aminoimidazole carboxamide ribonucleotide, an intermediate in purine nucleotide biosynthesis [Klem1993].

– ***hyaC and hyaF***

Both HyaC and HyaF are part of the Hydrogenase 1 proteins. *hyaC* encodes the b-type cytochrome subunit and *hyaF* encodes the operon subunit of Hydrogenase 1. Hydrogenase 1 mediates hydrogen uptake in the presence of high-potential acceptors such as ferricyanide and phenazine methosulfate [Laurinavic2001].

– ***hybA***

The *hybA* encoded protein might take part in the periplasmic electron-transferring activity of hydrogenase 2 during catalytic turnover [Sargent1998].

– ***nagK***

NagK is the only known cytoplasmic GlcNAc (N-acetyl-D-glucosamine) kinase in *E. coli* [Uehara2004] and it is released in the cytoplasm during murein recycling.

– ***nrdA***

NrdA is a subunit of ribonucleoside-diphosphate reductase (multifunctional) that catalyzes the conversion of nucleotides to deoxynucleotides, a necessary step in DNA synthesis [Brown1969].

– ***oppB, oppC, oppD and oppF***

Part of the OppABCDF ATP-dependent oligopeptide transporter, which is a member of the ATP-Binding Cassette (ABC) super family of transporter proteins. OppB and OppC are the membrane components of the ABC transporter, and OppD and OppF are the ATP-binding components of the ABC transporter.

– ***paaK***

PaaK is a phenylacetate-CoA ligase which is involved in the first step in an aerobic pathway of phenylacetate degradation [Ferrandez1998].

– ***poxB***

Pyruvate oxidase is encoded by the *poxB* gene and it is a peripheral membrane enzyme that catalyzes the oxidative decarboxylation of pyruvate to form acetate and CO₂ [Blake1982].

– ***rfbB and rfbD***

RfbB forms the subunit of dTDP-glucose 4,6-dehydratase and RfbD also known as dTDP-4-dehydrothamnose reductase take part in the dTDP-L-rhamnose biosynthesis I pathway [Yao1994].

– ***rfc***

Rfc is an O-antigen polymerase that is part of the lipopolysaccharide in the outer membrane of *E. coli* [Yao1994].

– *ribC*

Riboflavin synthase catalyzes the final step in riboflavin biosynthesis. Since there is no homolog of this enzyme in humans it is an attractive target for antimicrobial agents against microbes that are dependent on endogenous synthesis of riboflavin [Fischer2005].

– *sseB*

Sensitivity to serine is a result of overexpression of *sseB* [Hama1994]. On the other hand, mutation of *sseB* causes increased fimbrial production in *E. coli* [Huisman1996].

– *sucC*

The protein encoded by the *sucC* gene is a subunit of succinyl-CoA synthetase. It exists in form of a tetramer and is part of the TCA cycle [Neidhardt1996].

– *trxC*

The gene *trxC* encodes both an oxidized and reduced version of the compound thioredoxin 2 and takes an important part in a number of cellular functions as categorized below [Butland2005] -

Biological Processes: electron transport, glycerol ether metabolic process, glutaredoxin biosynthetic process and cell redox homeostasis.

Molecular Function: protein binding, zinc ion binding, electron carrier activity, protein disulfide oxidoreductase activity, oxidoreductase activity, metal ion binding and protein-disulfide reductase activity.

– *ubiE*

C-methyltransferase is a gene product of *ubiE* and catalyzes reactions in both menaquinone (MK) and ubiquinone (Q) biosynthesis [Lee1997]. In MK biosynthesis,

UbiE catalyzes the conversion of demethylmenaquinone to menaquinone [Lee1997]. In Q biosynthesis, UbiE catalyzes the conversion of 2-octaprenyl-6-methoxy-1,4-benzoquinone to 2-octaprenyl-3-methyl-6-methoxy-1,4-benzoquinone [Lee1997].

– *uxaC*

The gene *uxaC* encodes D-glucuronate isomerase / D-galacturonate isomerase that take part in the glucuronate and galacturonate degradation pathways [Portalier1974].

– *uxuA*

Mannonate dehydratase is encoded by the gene *uxuA* and it catalyzes the final reaction of the glucuronate branch that is part of the hexuronate pathway. The enzyme gets induced by glucuronate and fructuronate. [RobertBaud1982]

– *wbbI*

β -1,6-galactofuranosyltransferase is encoded by the gene *wbbI* and it takes part in the lipopolysaccharide biosynthetic process [Wing2006].

– *ynjE*

Sequence similarity suggests that YnjE is a predicted protein, 3-mercaptopyruvate sulfurtransferase that is part of the sulfur metabolic process [Reed2003].

5.6 Transport Genes

– *argT*

ArgT is a periplasmic binding protein that is a subunit of the lysine/arginine/ornithine ABC transporter [Nonet1987].

– *fhuA*

FhuA is an outer membrane protein receptor for ferrichrome and part of the ferrichrome uptake system. It builds a monomeric channel that consists of a 22-strand,

antiparallel β -barrel which is obstructed by a plug formed by residues 19-159 [Locher1998].

– *ftnA*

ftnA encodes an iron-storage protein called ferritin which forms a multi subunit of 24 individual ferritin proteins that can hold up to 200 iron atoms [Hudson1993].

– *glnH*

Part of the glutamine ABC transporter, the polypeptide GlnH is the periplasmic glutamine-binding protein [Masters1981].

– *gsiD*

Part of the glutathione ABC transporter, the polypeptide GsiD is the predicted inner membrane component [Suzuki2005].

– *lsrD*

LsrD is a membrane component of a predicted ATP-dependent sugar transporter located in the inner membrane [Serina2004].

– *proX*

The periplasmic protein ProX binds glycine betaine with a high affinity and is part of the proline ABC transporter system [Barron1987].

– *putP*

PutP is a member of the SSS family of sodium/proline transporter proteins that is responsible for the uptake of proline [Mogi1986].

5.7 Predicted and pseudo genes

Pseudo genes are regions of DNA that have sequence similarity to functional genes, however pseudogenes are nonfunctional because of sequence changes that prevent

their transcription or translation due to disruption of its promoter or introduction of a premature stop codon.

Interrupted genes: form a category of pseudogenes that is nonfunctional because the genes in this category contain an interruption such as a premature stop codon or a prophage insert.

- *gapC_1* and *gapC_2*

Both these genes encode a polypeptide, split glyceraldehyde 3-phosphate dehydrogenase C which is in an interrupted state and therefore has no functionality.

- *lsrK*

This is a putative kinase.

- *rmuC*

Induced under the influence of LexA, RmuC is a putative alpha-chain helix polypeptide [Van2001a].

- *spr*

The gene *spr* is believed to encode a lipoprotein [Brokx2004].

- *wbbJ*

The protein WbbJ is a predicted acyl transferase.

- *wbbL_1*

This is an interrupted gene and encodes the N-ter fragment of lipopolysaccharide biosynthesis protein. Since the gene is interrupted, it does not have a functional purpose.

- *yafN*

YafN is a conserved hypothetical protein with a possible role in spontaneous mutagenesis and is part of the *dinB* operon [McKenzie2003].

– *ybiJ*

This gene encodes a protein with no known function.

– *yciL*

This gene encodes a predicted enzyme with no known function.

– *ycjX*

This gene encodes a conserved protein with no known function.

– *ydeH*

This gene encodes a conserved protein with no known function.

– *ydhR*

This gene encodes a predicted mono-oxygenase that belongs to the α/β barrel superfamily of proteins. It might take part in the oxygenation of polyaromatic ring compounds [Revington2005].

– *yeeA*

YeeA is a protein located in the inner membrane which has six predicted transmembrane domains and the C terminus is located in the cytoplasm [Daley2005].

– *yebF*

A protein of unknown function, YebF is located in the extracellular space and is known to be damage inducible indicating a possible role for the protein in DNA repair [Van2001b].

– *yebW*

This gene encodes a predicted protein with no known function.

– *yecE*

This gene encodes a conserved protein.

– *yedE*

YedE is a protein in the inner membrane and has ten predicted transmembrane domains. The C terminus of the protein is located in the cytoplasm [Daley2005].

– *yhaK*

This gene encodes a predicted pirin-related protein with no known function

– *yjdN*

This gene encodes a conserved protein.

– *ylaC*

YlaC is a protein in the inner membrane and has two predicted transmembrane domains. The C terminus of the protein is located in the cytoplasm [Daley2005].

– *yobF*

This gene encodes a predicted protein. The protein has been predicted to be a target of RNA OxyS and therefore overexpression of OxyS decreases the expression of *yobF* [Tjaden2006].

– *yqhD*

In the crystallized form YqhD is an asymmetric dimer of dimers and has a zinc atom at the active site. It also exhibits NADP-dependent alcohol dehydrogenase activity [Sulzenbach2004].

5.8 Other Genes-Phantom, Cell Division, Protein Binding and Folding

– *def*

The gene *def* encodes an enzyme called peptide deformylase which releases the formyl group from the amino terminal methionine residue of most newly synthesized proteins [Neidhardt1996].

– *fhuF*

The protein FhuF takes part in iron reduction during utilization of a ferrioxamine B iron source [Muller1998]. The gene expression of *fhuF* is regulated by iron [Niehaus1991].

– *minC* and *minD*

These genes form the MinC MinD complex that inhibits septum formation at any site within the cell. It also interferes with the FtsZ ring assembly [Pichoff1995]. MinC expression ensures correct placement of the septum during cell division. MinD exhibits ATPase activity that is required for MinC mediated inhibition pathway [deBoer1992].

– *ycdF*

This is a phantom gene and therefore does not have any known function.

Chapter 6

DNA Damage Repair and Processes

6.1 Introduction

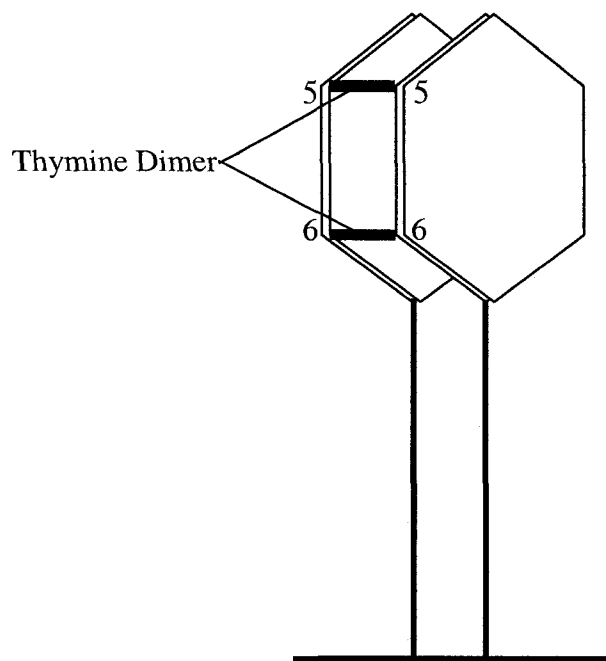
The stability of DNA is an essential condition for species to reproduce in a stable manner and since DNA is a chemical, it is prone to constant damage due to various environmental factors and this often leads to mutagenesis. As a result organisms have evolved many sophisticated ways of recognizing and repairing lesions: chemical damage in DNA. The repair mechanisms can be categorized as either specific repair pathways consisting of repair of deamination of bases, alkylation and pyrimidine dimers, or general repair pathways consisting of the methyl directed mismatch repair system, nucleotide excision repair and SOS inducible repair mechanism.

Although as mentioned above there a multitude of mutagenic agents and repair processes, for brevity only mechanisms relevant to this dissertation are discussed below.

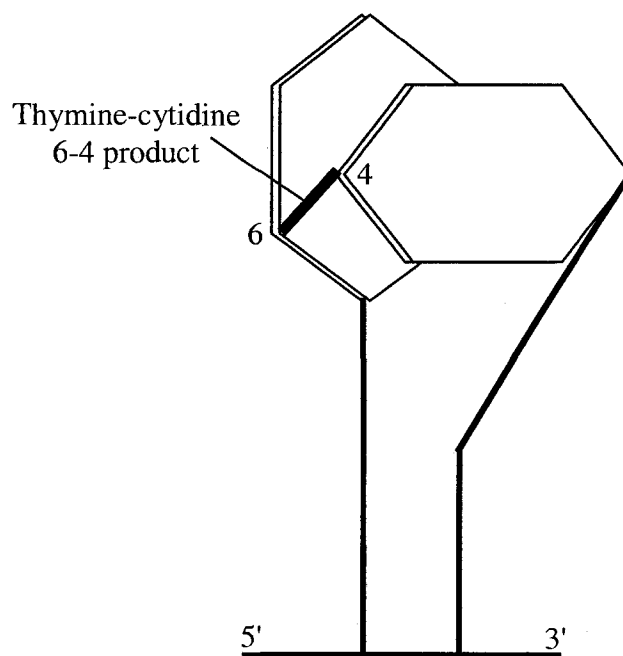
6.1 UV Radiation Damage

Ultra-violet radiation has been a primary natural cause of DNA damage in many organisms as sunlight is a major UV source. The DNA bases have a conjugated ring structure and therefore absorb light energy in the UV range efficiently. The photons cause the double bonds in bases to react with neighboring atoms to form additional chemical

bonds [Snyder2007]. This causes abnormal bonds between bases and sugars of the nucleotides.



(a)



(b)

Figure 6.1 (a & b): Two different forms of cyclobutane pyrimidine dimer

A common type of abnormal bond formation due to UV damage is the cyclobutane pyrimidine dimer and this happens when two adjacent pyrimidine bases fuse together. It exists in two forms as seen in Figure 6.1. In the first form (Figure 6.1a) two adjacent thymine bases get linked through 5- and 6- carbon atoms of their rings to make a cyclobutane ring. In the second form (Figure 6.1b) 6-carbon atom of a cytosine base joins with the 4-carbon atom of an adjacent thymine base thus creating a 6-4 lesion [Snyder2007]. The Photoreactivation repair process separates the fused bases of the cyclobutane pyrimidine dimer with the aid of visible light [Snyder2007].

6.2 Oxidative Damage

Oxygen in its molecular form is not generally harmful to bio macromolecules but when it is present in a reactive state (hydroxyl radical, hydrogen peroxide, superoxide radicals etc.) it can cause deleterious DNA changes [Snyder2007].

A mutagenic lesion commonly caused by reactive oxygen is the oxidized base **7,8- dihydro-8-oxoguanine** also referred to as **8-oxoG** or **GO**, which forms instead of the normal guanine base. This leads to confusion in the replication process as the polymerase Pol III mistakenly pairs 8-oxoG with the base adenine instead of the correct base cytosine [Snyder2007].

The products of *mut* genes: MutM, MutY and MutT are specifically involved in fixing problems caused by the mutagenic lesion 8-oxoG.

6.3 Nucleotide Excision Repair system

An important general repair system of major DNA damage in *E. coli*, nucleotide excision repair system consists of cutting off entirely, damaged nucleotides and replacing them [Snyder2007]. It is non specific and repairs different types of damage based on

recognition of distortion in the DNA helix including 6-4 cyclobutane pyrimidine dimers and base-sugar cross-links [Snyder2007].

Some of the genes involved in the nucleotide excision repair system are

- *uvrA*: DNA binding protein.
- *uvrB*: UvrA loads UvrB to form a DNA complex that cuts DNA 3' end of lesion.
- *uvrC*: It binds to the UvrB-DNA complex and cuts the DNA 5' end of lesion.
- *uvrD*: This is a helicase that helps remove damage containing oligonucleotide.
- *polA*: This gene encodes polymerase I that fills in single strand gap.
- *lig*: This is a ligase that seals the single strand cut.

The mechanism of repair involves the UvrABC endonuclease [Snyder2007]. Specifically, one copy of UvrB binds to two copies of UvrA and this protein complex attaches to a random site on DNA and then travels along the helix to find a damaged nucleotide. At the damaged site UvrA is replaced by UvrC which leads to the excision of 4 nucleotides 3' of the damage by UvrB and 7 nucleotides 5' of the damage are cleaved by UvrC. After the excision, UvrD helicase removes the damaged oligonucleotide and PolA creates a new strand using the complementary strand as a template [Snyder2007].

The induction of some of the nucleotide excision repair genes like *uvrA*, *uvrB* & *uvrD* is triggered by DNA damage and some of the above-mentioned genes are also part of the SOS regulon [Snyder2007].

6.4 Recombination Repair

After DNA damage has already occurred, the cell takes certain DNA damage tolerance measures to limit the extent of negative consequences especially to the

replication machinery. Many of these measures fall under the recombination repair process. Although not fully understood still, the recombination process is a primary mechanism by which replication forks are reset following derailment or collapse of the forks caused by DNA damage [Snyder2007].

6.5 SOS Response

Named after the universal distress signal, SOS response is one of the most well understood regulatory systems in *E. coli* that is activated in response to DNA damage. Some of the early research conducted in this area investigated the survival of UV irradiated bacteriophage λ [Weigle1953]. It was observed that irradiated phage survived better if they were placed in irradiated *E. coli* cells. This was attributed to the induction of a repair mechanism in irradiated *E. coli* cells that also worked on inserted phage DNA.

Later it was discovered that a LexA-RecA regulated process was responsible for the control of many genes induced in response to DNA damage [Radman1975]. Many of these genes are repressed under normal conditions by the binding of the protein LexA to a sequence upstream of the gene called the SOS box. The SOS box is close to the promoter region of the gene and therefore prevents transcription of that gene. Extensive DNA damage causes autocleavage of the LexA repressor and is mediated by the protein RecA. The autocleavage of LexA allows the transcription of the genes that were previously repressed by the SOS box binding.

The autocleavage of LexA is a well understood process and its mechanism is as follows. The LexA polypeptide exists as a dimer and has two distinct domains, one of which called the DNA binding domain binds to the SOS box and the other domain called the dimerization domain participates in the dimerization complex. The DNA binding

domain is effective only when LexA is in a dimer state. The autocleavage separates the dimerization domain from the DNA binding and therefore rendering it ineffective.

The autocleavage happens after DNA damage because there is an increase in the amount of single stranded DNA because of the blockage of the replication forks owing to DNA damage. This single stranded DNA forms a nucleoprotein complex with the protein RecA. These nucleoprotein filaments bind to LexA causing its autocleavage.

Many of the SOS genes that are regulated by the LexA-RecA regulator perform a number of important functions to rectify the damage caused to DNA. Their detailed functioning is explained in Chapter 5

6.6 Translesion Synthesis

This is an error-prone DNA repair process and it allows the replication forks to proceed over damaged DNA so that the cell might survive because of some replication of the molecule despite the damage. This repair mechanism comes into play when the damage is so extensive that other less mistake prone repair mechanisms will not work. The two proteins that play a key role in translesion synthesis are UmuC and UmuD, and they are described in detail in Chapter 5.

Chapter 7

Microarray Analysis of Differential Gene Expression

7.1 Introduction

Although a significant body of literature exists describing extensively various electrode configurations, plasma operating regimes and possible bacterial inactivation mechanisms [Laroussi2005; Moisan2001], the relative effectiveness of various plasma species (charged particles, reactive species, UV, etc.) and their potential synergistic impacts at the bio-molecular level are still not well understood. A deeper understanding of the complex mechanisms in play when various plasma species interact with microbes is needed to enable the optimization of plasma devices for efficient bacterial inactivation. A high density synthetic oligonucleotide array is ideally suited to quickly survey a whole genome for differential gene expression following plasma exposure.

There has been a prolific rise in the use of microarrays in the last few years to study global gene expression profiles in bacteria when exposed to various germicidal agents such as UV and hydrogen peroxide [Qiu2005; Zheng2001]. In this part of the dissertation global gene expression in *E. coli* was observed after plasma treatment. The bacterium *E. coli* was chosen as it is a problematic pathogen and its genome is

particularly well annotated and various complex regulatory networks are well understood. To my knowledge this is the first time microarrays were applied to characterize the genetic response of a living organism to plasmas.

7.2 Materials and Methods

Microarray analysis was conducted in triplicate for plasma exposed and unexposed controls. Additionally, the experiment itself was replicated twice. This experimental design resulted in one control and one treatment sample in the first experimental run and two controls and two treatment samples in the second experimental run. Thus, both biological and technical replication was ensured.

7.2.1 Bacterial Strain, Growth Conditions and Plasma Treatment

E. coli strain K-12 MG1655 (ATCC® Number: 700926™) from glycerol freezer stocks stored at -80 °C was grown in Bacto tryptic soy broth (TSB) (Becton, Dickinson & Co, Sparks, MD) in two stages. In the first stage, 1 ml of bacterial culture was suspended in 100 ml TSB and grown for 12 hours. A 0.5 ml aliquot was taken from this solution, suspended in 250 ml soy broth and grown for an additional five hours until the cells reached exponential log phase. In both cases the cultures were maintained at 37 °C on a rotary shaker at 250 rpm for constant aeration. Exponential log phase cells (10 ml) were harvested and transferred from the broth under sterile conditions to a phosphate buffer solution (PBS) (90 ml, pH 7.0) and then nine milliliters of the log phase cells were transferred to a sterile petri dish and exposed to the afterglow plasma plume emitted from the grounded hollow-slot electrode. The plasma electrode was swept over the Petri dish for 120 s utilizing a motor for constant translational motion as seen in Figure 7.1. The distance between the plasma electrode and PBS in the Petri dish was maintained at 5 mm.

Details of the plasma electrode configuration and operating parameters have been described in Chapter 3. In brief, the plasma device was powered by a 13.56 MHz power supply (Advanced Energy, Fort Collins, CO) and an in-house constructed matching network was used to optimize power delivery to the load, which consisted of the hollow slot electrode. The plasma device employed argon as the feed gas at a flow rate of 15 L/min and the power output from the RF power supply was 125 W. Control samples were not exposed to the plasma.

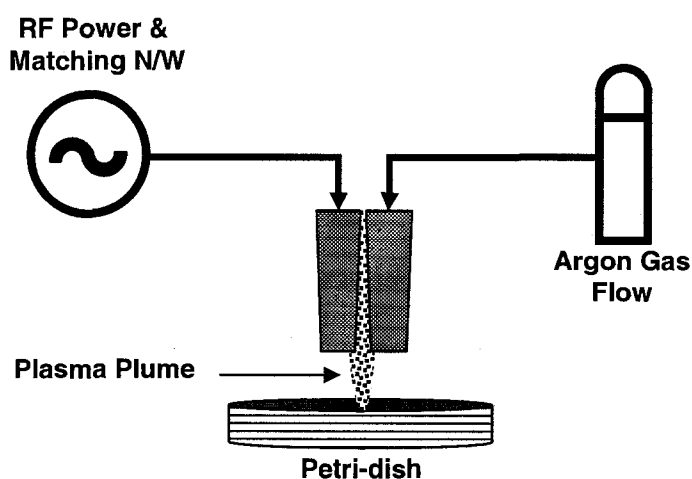


Figure 7.1: Schematic: Bacterial treatment using non-thermal atmospheric-pressure plasma device.

7.2.2 RNA Isolation and Microarray Procedures

RNA isolation was performed immediately after the cells were subjected to plasma treatment. An RNeasy[®] Mini kit (Qiagen, Valencia, CA) with associated protocol for isolation of total RNA from bacteria [see Appendix B] was used and following the isolation procedure the quantity and quality of RNA was determined by measuring absorbance at 260 nm and 280 nm by photospectrometry (Nanodrop, Wilmington, DE). RNA was stored at -80 °C until microarray processing. Affymetrix GeneChip[®] *E. coli*

Genome 2.0 arrays and procedures as part of the prokaryotic target preparation protocol were implemented to perform the microarray analysis [see Appendix B]. In brief, the extracted DNA was converted to cDNA using random hexamer primers. cDNA was fragmented into smaller fragment of 50-200 bp size using DNase I enzyme and then labeled with biotin at the 3' end. The resulting product was then hybridized to the arrays and scanned to obtain expression data.

7.2.3 Data Analysis

DNA analysis was carried out using the DNA-Chip Analyzer (dChip) software version 2-9-2008, available at <http://www.dchip.org/> [Li2001a; Li2001b]. The array with the median file cell intensity values out of the six arrays (three-treatment, three-control) was chosen as the baseline array and the other arrays were normalized according to the invariant set method. Model-based expression values with background subtraction option set to PM only (5th percentile of region) were calculated. Transcript expression values among the control and treatment arrays were compared according to the following criteria,

$$\left. \begin{array}{l} \mathbf{E/B \text{ or } B/E > 1.2, 90\% \text{ confidence bound of fold change} \\ \mathbf{or} \\ \mathbf{E-B \text{ or } B-E > 100} \\ \mathbf{where,} \\ \mathbf{B: \text{intensity value of a transcript in the control arrays}} \\ \mathbf{E: \text{intensity value of a transcript in the treatment arrays}} \end{array} \right\}$$

The transcripts meeting the above criteria were subjected to gene ontology and functional classification analysis using the EcoCycTM annotation tool available at

<http://ecocyc.org/> [Karp2007]. A few transcripts mapped to other strains or represented intergenic regions on the chromosome and therefore were excluded from functional classification.

7.3 Results and Discussion

7.3.1 Global Gene Expression Profile

Results of the microarray data analysis yielded 109 differentially expressed transcripts. Out of these, 53 transcripts were up-regulated, while 56 transcripts were down-regulated. The distribution of the transcripts across various cellular functions is presented in the pie chart; Figure 7.2 and a detailed listing of the genes is provided in Table 7.1.

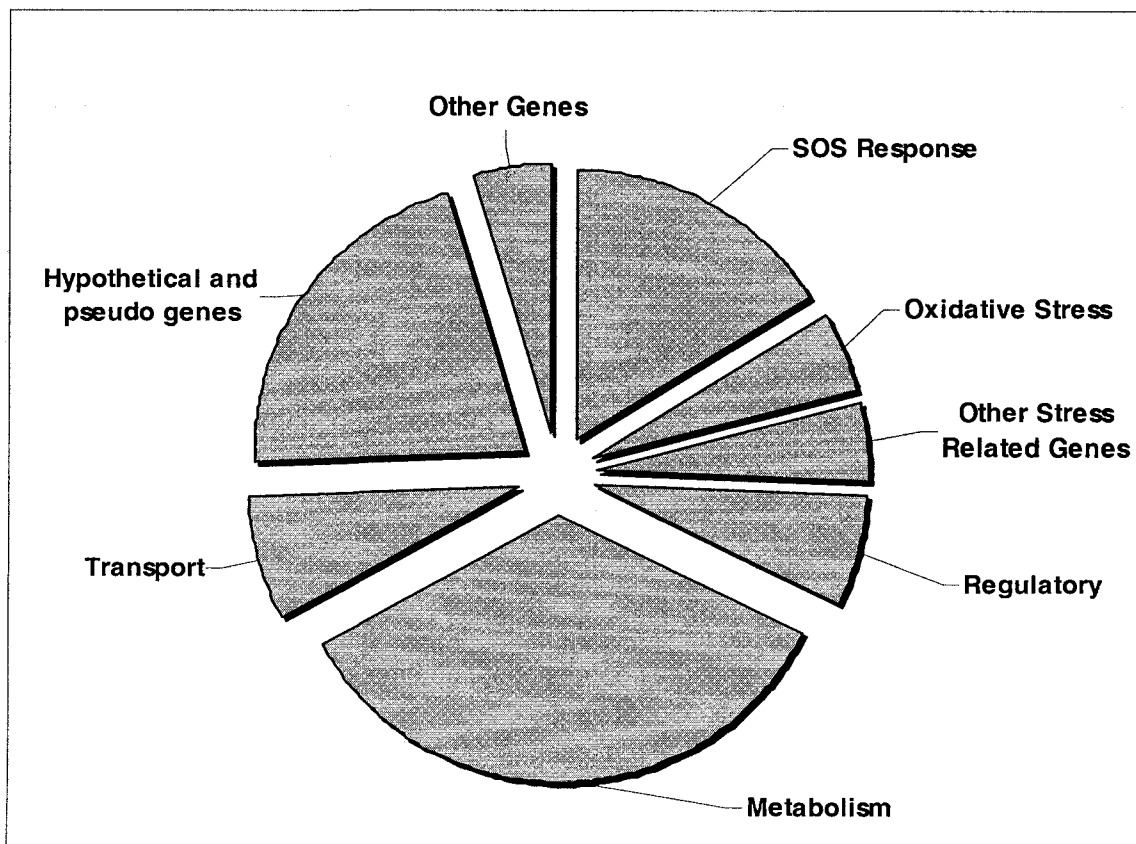


Figure 7.2: Categories of differentially expressed genes (up and down regulated) determined by functional classification based on gene ontology information.

Table 7.1: List of differentially expressed genes

Gene	Functional Description
SOS Genes	
<i>umuD</i>	DNA polymerase V, subunit D
<i>recN</i>	DNA recombination and repair
<i>sulA</i>	SOS cell division inhibitor
<i>dinI</i>	DNA-damage-inducible protein
<i>yebG</i>	Conserved protein regulated by LexA
<i>dinB</i>	DNA repair - DNA polymerase IV
<i>recA</i>	DNA recombination and repair
<i>recX</i>	Inhibitor of RecA
<i>sbmC</i>	DNA gyrase inhibitor
<i>polB</i>	Replication Restart
<i>umuC</i>	DNA polymerase V, subunit C /// DNA polymerase IV
<i>dinD</i>	DNA-damage-inducible protein
<i>uvrA</i>	Part of NER excinuclease UvrABC
<i>uvrB</i>	Part of NER excinuclease UvrABC
<i>lexA</i>	Subunit of LexA transcriptional repressor
<i>dinF</i>	DNA repair-LexA repressed
<i>ruvB</i>	DNA recombination and repair
<i>ssb</i>	ssDNA-binding protein
Oxidative Damage	
<i>oxyS</i>	Regulatory-RNAs-oxidative stress response
<i>katG</i>	Removal of superoxide radicals-protection-detoxification
<i>soda</i>	Removal of superoxide radicals (Mn)-protection-detoxification
<i>soxS</i>	Transcriptional dual regulator-response to oxidative stress
<i>sodB</i>	Removal of superoxide radicals (Fe)-protection-detoxification
Other Stress Related Genes	
<i>ompA</i>	Subunit of Outer Membrane Protein Assembly Complex-stress related protein
<i>mntH</i>	Manganese ion NRAMP transporter-protection-detoxification
<i>otsB</i>	Increased under osmotic stress
<i>frmB</i>	S-formylglutathione hydrolase-protection-detoxification
<i>cspC</i>	Cold shock protein
Regulatory Genes	
<i>ryhB</i>	Reduces iron consumption under low-iron conditions
<i>lsrR</i>	<i>lsr</i> operon transcriptional repressor
<i>cobB</i>	Protein deacetylase
<i>paaX</i>	Transcriptional repressor
<i>abgR</i>	Putative transcriptional regulator LYSR-type
<i>mall</i>	MallI transcriptional repressor
<i>putA</i>	Transcriptional repressor

Continued Table 7.1

Gene	Functional Description
Metabolism	
<i>trxC</i>	Reduced thioredoxin 2 , oxidized thioredoxin 2
<i>poxB</i>	Pyruvate oxidase monomer
<i>fdoG</i>	Formate dehydrogenase-O, alpha subunit
<i>uxaC</i>	D-galacturonate degradation
<i>fdoH</i>	Formate dehydrogenase-O, beta subunit
<i>uxuA</i>	β -D-glucuronide degradation
<i>fdoI</i>	Formate dehydrogenase-O, gamma subunit
<i>deoB</i>	Nucleotide and nucleoside conversion
<i>ubiE</i>	Menaquinone biosynthesis , ubiquinone-8 biosynthesis
<i>sucC</i>	Succinyl-CoA synthetase, β subunit
<i>ribC</i>	Subunit of riboflavin synthase
<i>hisC</i>	Histidine biosynthesis I
<i>nagK</i>	Chitobiose degradation
<i>sseB</i>	Overproduction causes enhanced serine sensitivity
<i>acpS</i>	Subunit of holo-[acyl-carrier-protein] synthase
<i>hyaC</i>	Hydrogenase 1, b-type cytochrome subunit
<i>fadH</i>	2,4-dienoyl-CoA reductase
<i>astB</i>	Succinylarginine dihydrolase
<i>nrdA</i>	Purine nucleotides de novo biosynthesis I
<i>rfdD</i>	dTDP-L-rhamnose biosynthesis I
<i>oppC</i>	Oligopeptide transporter subunit
<i>oppB</i>	Oligopeptide transporter subunit
<i>hisF</i>	Histidine biosynthesis I
<i>hyaF</i>	Hydrogenase-1 operon protein
<i>hisA</i>	Histidine biosynthesis I
<i>paaK</i>	Phenylacetate degradation I
<i>hybA</i>	Subunit of hydrogenase 2
<i>oppD</i>	Oligopeptide transporter subunit
<i>rfdC</i>	dTDP-L-rhamnose biosynthesis I
<i>ynjE</i>	Predicted thiosulfate sulfur transferase
<i>glf</i>	UDP-galactopyranose mutase
<i>frdA</i>	Subunit of fumarate reductase, flavoprotein
<i>wbbI</i>	β -1,6-galactofuranosyltransferase
<i>frdC</i>	Subunit of fumarate reductase, membrane protein
<i>oppF</i>	Oligopeptide transporter subunit
<i>gnd</i>	Subunit of 6-phosphogluconate dehydrogenase
<i>rfc</i>	O-antigen polymerase
<i>frdB</i>	Subunit of fumarate reductase, iron-sulfur protein

Continued Table 7.1

Gene	Functional Description
Transport	
<i>fhuA</i>	Outer membrane protein receptor
<i>lsrD</i>	LsrA/LsrC/LsrD/LsrB ABC transporter
<i>gsiD</i>	Subunit of gsiABCD glutathione ABC transporter
<i>argT</i>	Subunit of lysine/arginine/ornithine ABC Transporter
<i>glnH</i>	Subunit of glutamine ABC transporter
<i>proX</i>	Subunit of proline ABC transporter
<i>ftnA</i>	Cytoplasmic ferritin, subunit of iron-storage complex
<i>putP</i>	Proline SSS transporter
Predicted and pseudo genes	
<i>ybiJ</i>	Predicted protein
<i>yeeA</i>	Conserved inner membrane protein
<i>yebF</i>	Predicted protein
<i>yhaK</i>	Predicted pirin-related protein
<i>rmuC</i>	Induction requires LexA
<i>yafN</i>	Hypothetical protein possible role in spontaneous mutagenesis
<i>yqhD</i>	NADP-dependent alcohol dehydrogenase
<i>gapC_2</i>	Glyceraldehyde 3-phosphate dehydrogenase C- Pseudo-Genes - Interrupted-Genes
<i>yjdN</i>	Conserved protein
<i>gapC_1</i>	Glyceraldehyde 3-phosphate dehydrogenase C- Pseudo-Genes - Interrupted-Genes
<i>yebW</i>	Predicted protein
<i>ylaC</i>	Predicted inner membrane protein
<i>ydhR</i>	Subunit of predicted mono-oxygenase
<i>yobF</i>	Predicted protein
<i>lsrK</i>	Putative kinase
<i>ycjX</i>	Conserved protein
<i>ydeH</i>	Conserved protein
<i>yecE</i>	Predicted protein
<i>spr</i>	Outer membrane lipoprotein
<i>ycil</i>	Predicted enzyme
<i>wbbL_1</i>	Lipopolysaccharide biosynthesis protein- Pseudo-Genes - Interrupted-Genes
<i>yedE</i>	Predicted inner membrane protein
<i>wbbJ</i>	Predicted acyl transferase
Other Genes-Phantom, Cell Division, Protein Binding and Folding	
<i>fhuF</i>	Reduction of ferrioxamine B iron
<i>ycdF</i>	Phantom-Genes
<i>def</i>	Post-translational modification
<i>minC</i>	Cell division inhibitor of the MinC-MinD-MinE
<i>minD</i>	Membrane ATPase of the MinC-MinD-MinE system

7.3.2 SOS Response

The SOS regulon, named after the universal distress signal, consists of many genes involved in DNA repair, cell division, etc. that are cooperatively expressed following DNA damage [Snyder2007]. These genes are controlled by a complex regulatory network comprised of two proteins; RecA and LexA. Under normal conditions SOS genes are inhibited by the LexA repressor but in the case of severe DNA damage, a higher accumulation of DNA-RecA nucleoprotein filaments triggers autocleavage of LexA [Koch1998]. Another feature of the SOS response is its quantitative response capability. This is achieved through the relative binding affinity of LexA for each gene's binding site and therefore minimal damage leads to the activation of relatively few repair processes that are error free while extensive damage leads to the expression of *umuC* and *umuD* that are responsible for error prone translesion synthesis of damaged DNA [Koch1998]. Translesion synthesis is one of the last resort mechanisms whereby the cell attempts to correct unrepaired DNA lesions by replacing nucleotide bases randomly [Wang2001]. If unrepaired DNA lesions persist then a *sulA*-dependent filamentation is induced and this allows a prophage to escape a potentially inviable cell by entering into a lytic growth cycle [Koch1998]. The SOS response regulon was observed to have been significantly up-regulated as presented in Figure 7.3.

The SOS response is one of the best characterized regulatory networks in *E. coli* and has been extensively reviewed [Friedberg1995]. In much of the reviewed work on the SOS response, the main agent responsible for DNA damage is UV light and its role has been well characterized previously by the use of microarrays [Qiu2005].

Previous bacterial inactivation studies using our plasma device, also suggested that UV light was the primary plasma constituent driving inactivation [Sharma2005]. The significant induction of genes that are part of the SOS regulon (7.3) further supports the conclusion that the primary cause of the DNA damage to the cells was UV light.

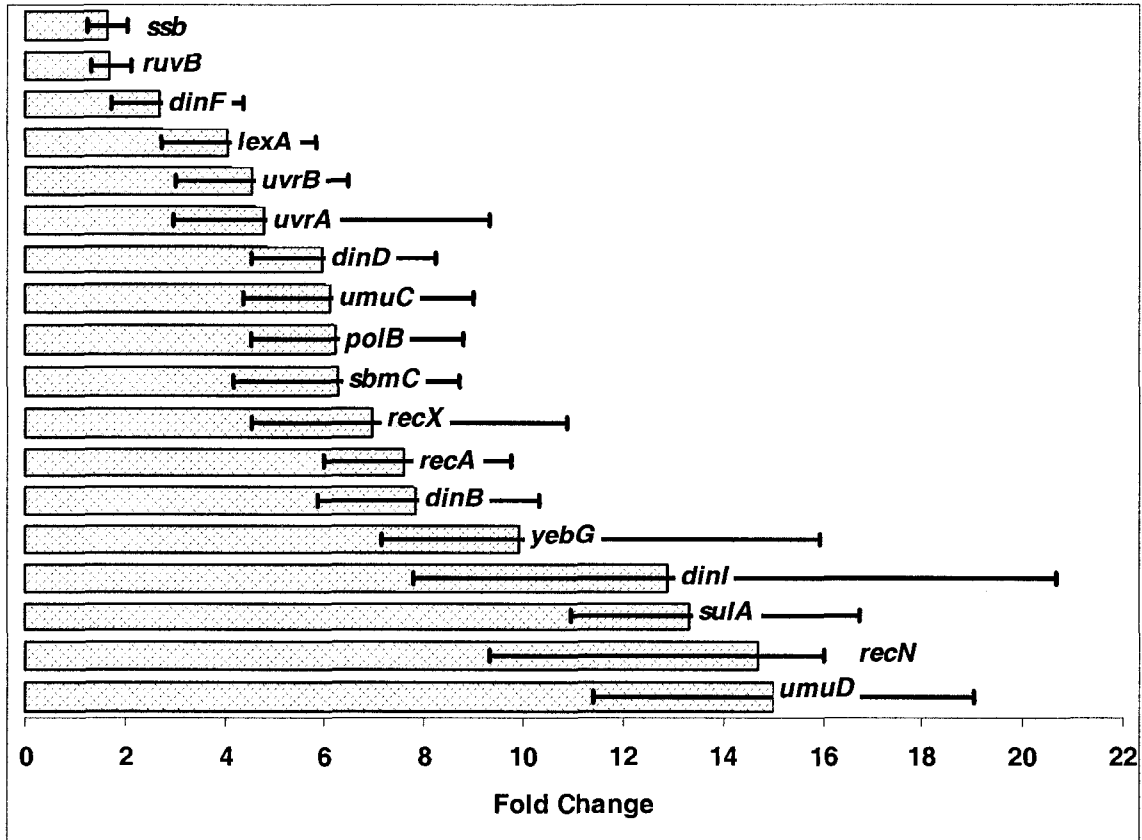


Figure 7.3: Expression profile of genes involved in SOS response.

7.3.3 Oxidative Damage Repair

The differentially expressed genes involved in oxidative stress response are presented in 7.4. *oxyS* encodes a small non-coding RNA involved in riboregulation. It is induced in response to oxidative damage and activates genes that detoxify oxidative damage. It is an example of trans-acting small RNA that regulates multiple targets [Altuvia1997]. The *oxyS* gene was noted to have the highest level of induction-43 fold. A gene involved in the removal of superoxide radicals, *katG* was noted to have a 10-fold

increase in expression. This gene encodes an enzyme called bifunctional hydroperoxidase 1 that acts both as a catalase and peroxidase [Claiborne1979]. There was also a minor increase in the expression of *soxS* gene, which is a transcriptional regulator that acts in response to superoxide radicals [Griffith2004].

The high induction of *oxyS*, 43 fold in this study (Figure 7.4), was most probably caused exclusively by oxidative damage. Previous studies have shown negligible to no induction of this gene under other stress conditions such as heat shock, cold shock and acid shock [Altuvia1997]. This suggests that oxidative species produced by the plasma may work synergistically to enhance bacterial inactivation.

Interestingly, despite the high induction of *oxyS*, none of the genes that are regulated by *oxyS* were differentially expressed (down-regulation of *yobF* was an exception). This may be a result of the highly temporal nature of this regulon, since RNA was isolated from cells immediately following exposure to the plasma plume

The two superoxide dismutases, SodA and SodB, contain manganese and iron respectively [Touati1988]. While there was an increase in the expression of *sodA*, the expression of *sodB* declined. *sodB* is expressed in both aerobic and anaerobic conditions, whereas *sodA* is only expressed in aerobic conditions [Touati1988]. It is believed that *sodA* (upregulated) is more effective than *sodB* (downregulated) in preventing damage to DNA, while *sodB* is more effective in protecting a cytoplasmic superoxide-sensitive enzyme [Touati1988]. The increase in expression of the small regulator RNA RyhB might have had an inhibitory effect on the expression of *sodB*.

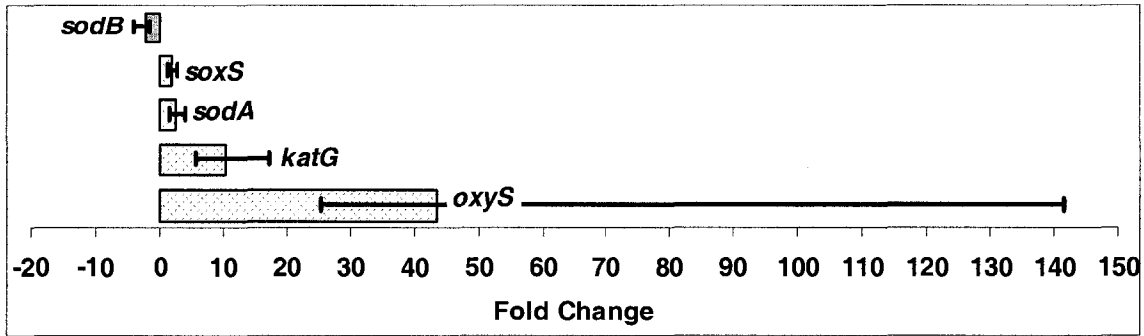


Figure 7.4: Expression profile of genes involved in response to oxidative stress.

7.3.4 Other Stress Response Genes

Differential expression of certain other genes induced as a response to various stress conditions was also observed (Figure 7.5). There was a minor increase in the expression of the protein FrmB, which is a serine hydrolase and takes part in the oxidation of formaldehyde [Gonzalez2006]. There was also a 3-fold increase in the induction of the *mntH* gene that encodes a manganese ion transporter protein that is part of the NRAMP (natural resistance-associated macrophage proteins) family [Haemig2004]. The gene *otsB*, which acts in response to stress caused by osmotic pressure [Kandror2002] was also observed to have a modest increase in expression. Conversely, the *cspC* gene, which acts in response to cold shock [Phadtare2006], was observed to have a modest decrease in expression.

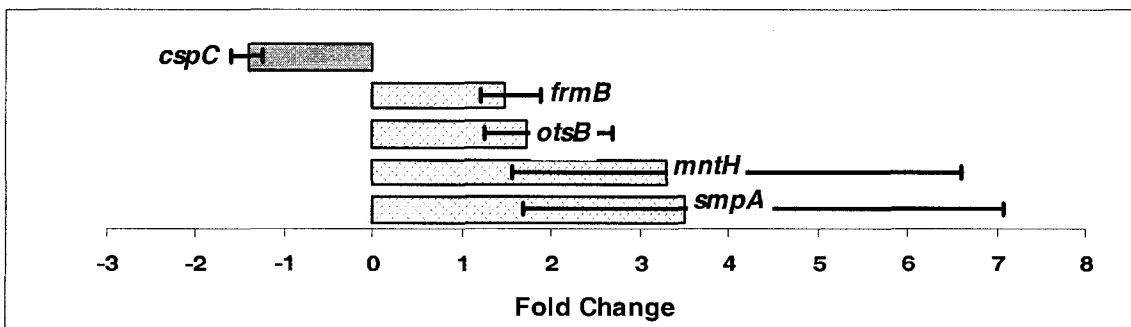


Figure 7.5: Expression profile of genes involved in other stress response measures.

7.3.5 Regulation

The expression profile of genes involved in gene regulation is presented in Figure 7.6. Except for the small regulatory RNA RyhB all the other regulatory genes were observed to be down-regulated.

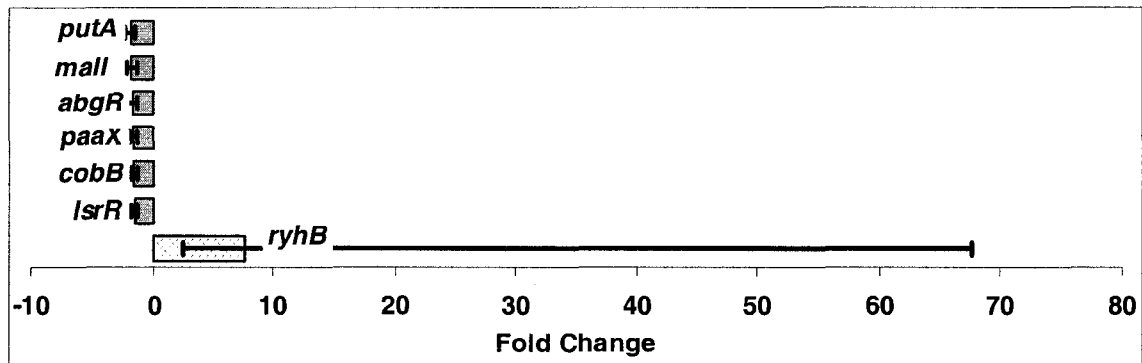


Figure 7.6: Expression profile of regulatory genes.

7.3.6 Metabolism and Transport

The vast majority of genes involved in energy metabolism and transport processes were observed to be down-regulated (Figures 7.7 and 7.8). The notable exceptions were genes in the Formate dehydrogenase-O family of genes, *fdoG*, *fdoH* and *fdoI*. Also, *trxC*, which encodes the compound thioredoxin 2, and *fhuA*, which takes part in the uptake of ferrichrome, were observed to be up-regulated.

The vast majority of energy metabolism and transport related genes were down-regulated (Figures 7.7 & 7.8) indicating that the cells were minimizing housekeeping functions in order to refocus all available resources into damage repair mechanisms.

The vast majority of energy metabolism and transport related genes were down-regulated (Figures 7.7 & 7.8) indicating that the cells were minimizing housekeeping functions in order to refocus all available resources into damage repair mechanisms.

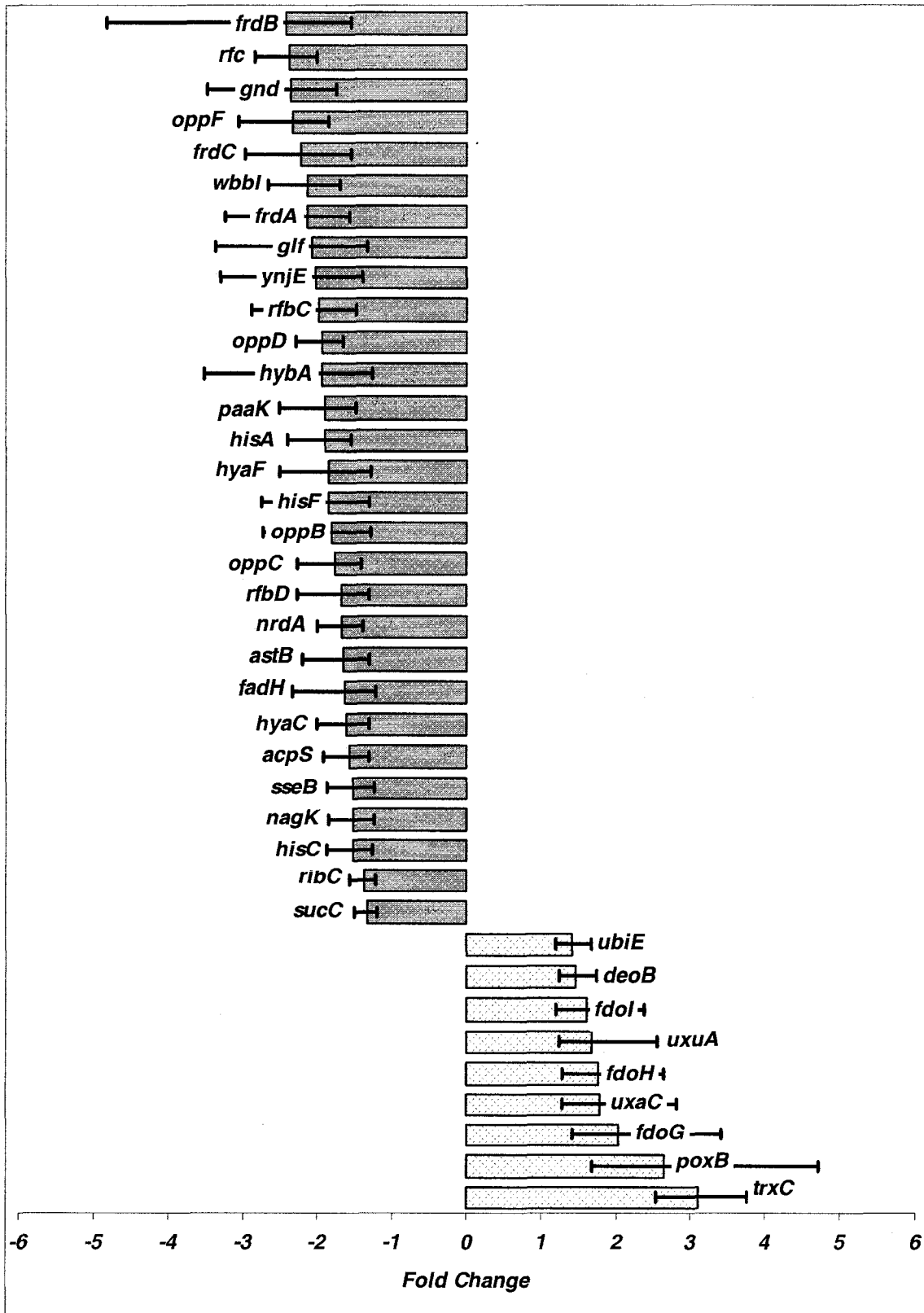


Figure 7.7: Expression profile of genes involved in metabolic processes in the cell.

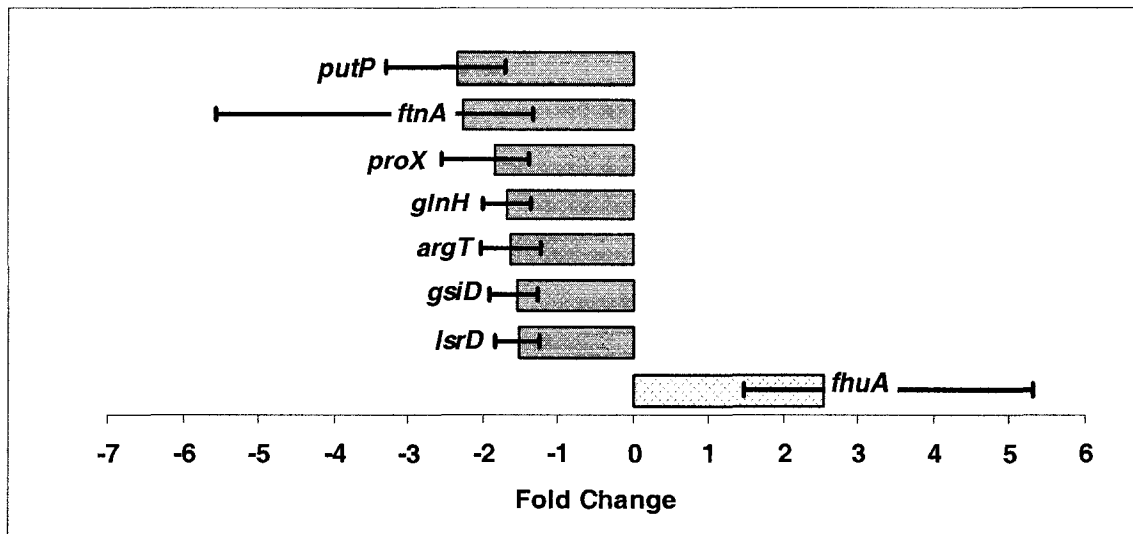


Figure 7.8: Expression profile of genes involved in transport processes in the cell.

7.3.7 Predicted and Pseudo Genes

A number of differentially expressed transcripts were observed that code for open reading frames for which functions have not yet been determined (Figure 7.9). Among them *yafN* is known to be damage inducible and may possibly play a role in spontaneous mutagenesis. *yafN* is also a part of the *dinB* operon [McKenzie2003] and therefore could be associated with the SOS mechanism. Another transcript that is damage inducible and putatively involved in DNA damage repair, *yebF*, was observed to be up-regulated 6 fold [Van Dyk2001]. *rmuC* is believed to be regulated under the influence of the LexA repressor and was observed to be up-regulated 3 fold [Van Dyk2001]. The *yobF* gene is known to be repressed when levels of the regulatory RNA OxyS rise [Tjaden2006] and as seen in Figure 7.6 a modest decrease in the level of *yobF* expression was observed. There were modest increases in the expression of *GapC_1* and *GapC_2*, which are considered to be pseudogenes. Pseudogenes are regions of DNA that have sequence similarity with functional genes; however they are nonfunctional because of sequence mutations that prevent their transcription or translation due to disruption of their promoter or

introduction of a premature stop codon. Conversely, the expression of *wbbL_1*, another pseudogene, was repressed.

The differential expression of a relatively large number of transcripts with unknown functions (Figure 7.9) seems to suggest that they might play a role in response to plasma induced cellular damage, especially in the case of transcripts, *rmuC*, *yafN*, and *yebF* that are known to be damage inducible. Further studies would be needed to ascertain the exact roles of these transcripts.

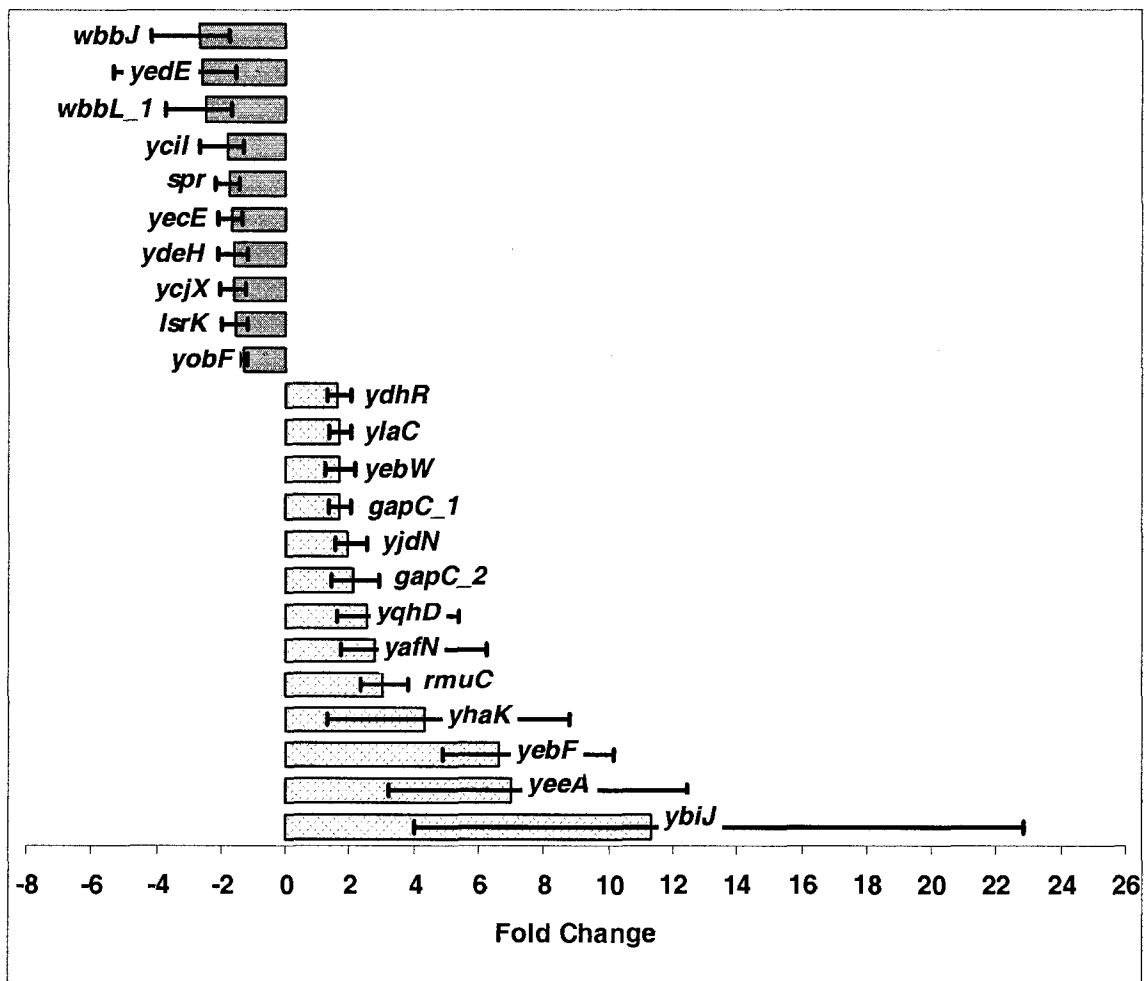


Figure 7.9: Expression profile of hypothetical and pseudo genes, consisting of various predicted and conserved proteins.

7.3.8 Other Genes

There were a handful of other genes with modest changes in expression (Figure 7.10). There was a two fold decrease in the expression of *minC* and *minD* that are involved in the inhibition of septum formation at any site within the cell [Pichoff1995]. There was a five fold increase in the expression of *fhuF*, a gene involved in protein folding [Muller1998] and a modest increase in the expression level of *def*, a gene involved in post-translational modification [Neidhardt1996].

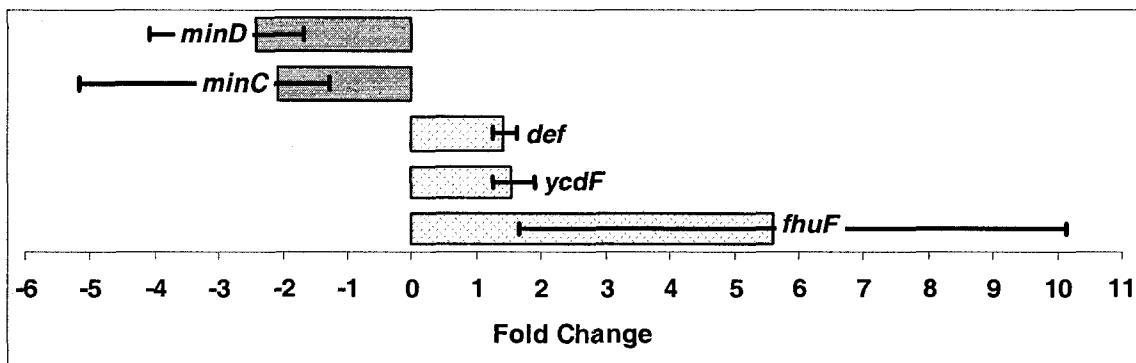


Figure 7.10: Expression profile of genes involved in various miscellaneous processes; cell division, protein binding and folding (*ycdF* is a phantom gene and has no known function).

The results indicate an incomplete induction of certain DNA damage repair mechanisms like the nucleotide excision repair (NER) system. For instance, in the NER system one copy of UvrB binds to two copies of UvrA, and this protein complex attaches to a random site on DNA and then travels along the helix to find a damaged nucleotide [Snyder2007]. At the damaged site, UvrA is replaced by UvrC, which leads to the excision of 4 nucleotides upstream (towards the 3' end) of the damage by UvrB and 7 nucleotides downstream (towards the 5' end) of the damage are cleaved by UvrC [Snyder2007]. After the excision, UvrD helicase II removes the damaged oligonucleotide

and PolA creates a new strand using the complementary strand as a template [Snyder2007]. Although plasma treatment led to the induction of *uvrA* and *uvrB* thus enabling the cell to recognize damaged nucleotides, the absence of *uvrC*, *uvrD* and *polA* would probably lead to a nonfunctional NER process.

A minor increase in temperature of the medium exposed to the plasma plume has been demonstrated previously [Sharma2006] which may also play a role in inactivating the cells. The expression of some heat shock proteins can be enhanced if there is an increase in temperature (e.g., 30 to 42 °C) of the cells [Yura2000]. However none of the proteins involved in the heat shock response were found to be up-regulated suggesting that heat did not play a significant role in cellular damage.

In conclusion the data obtained suggest that UV and oxygen radicals were the primary agents responsible for cellular damage and evidence of the induction of the error-prone translesion synthesis process and incomplete induction of other repair processes indicates massive amount of DNA damage therefore plasma treatment could be used as an effective strategy to control the growth of harmful microbes. The experimental results presented here should be treated as a baseline for the bacterial genetic response to plasmas and further studies would be required to elucidate the nature of a temporal response by the bacterium to the plasma and also how changing different plasma parameters (e.g. ratio of UV to oxygen radicals) can cause variation in the gene expression profile.

Chapter 8

Varied Plasma Parameters for Bacterial Inactivation Optimization

8.1 Experimental Setup

Different experimental conditions were examined to optimize bacterial inactivation and estimate the underlying inactivation pathways. All experiments were conducted in open air and without windows at atmospheric pressure. External gas flow was applied through the electrode regions using a mixture of rare gas (argon or helium) and oxygen flowing at rates of 5-20 liters/minute (l/m) and 6-20 standard cubic centimeters/minute (sccm) respectively. The reactor was provided power using 13.56 MHz and 60 MHz RF power supplies (Advanced Energy, Fort Collins, CO) and a matching network was connected between the power supply and the plasma reactor to optimize power transmission. Power delivered to the reactor was varied from 50 W to 150 W.

The samples to be exposed were kept at a fixed position, varying from 2.5 mm to 1 cm below the open reactor slot. A motor drive was used to achieve translational motion of the afterglow plasma plume in order to uniformly sweep the entire surface area of the target sample with the afterglow plasma, creating a “push-broom” source of photons,

radicals, and ions, all of which may play an active role in bacterial inactivation. Varying exposure times were achieved by passing the plasma slot over the sample at various rates and varying the number of passes using a motor to move the plasma slot. For instance a single pass lasting 2.5 min. resulted in an effective exposure of about 0.6 s per unit area.

8.2 *E. coli* Strain Information and Sample Preparation

E. coli (ATCC 9637, Biosafety level 1) was used in the plasma experiments. The strain was obtained from Invitrogen (Carlsbad, CA) with the following genotype: F-*mcrA* Δ (*mrr-hsdRMS-mcrBC*) ϕ 80*lacZ* Δ M15 Δ *lacX74* *deoR* *recA1* *araD139* Δ (*ara-leu*)7697 *galU* *galK* *rpsL* (*StrR*) *endA1* *nupG*.

E. coli cultures were grown overnight in a petri-dish containing LB agar (Difco, Sparks, MD) at 37 °C and then a single colony was transferred into 250 ml of Bacto™ tryptic soy broth (Becton, Dickinson and Company, Sparks, MD) that was maintained for 8 hours at 37 °C. This allowed the cells to reach exponential log phase. 10 ml of exponential log phase cells were harvested and transferred from the broth under sterile conditions to 90 ml of phosphate buffer solution (PBS, pH 7.0). The solution was serially diluted further to the required concentration range. Five milliliters of the diluted solutions were filtered in triplicate for each dilution onto pre-sterilized filter membranes (0.45 μ m mixed cellulose esters, 47 mm dia. (Millipore)).

Following filtration, the membranes were placed on sterile 10 ml petri-dishes containing 9 ml LB agar. The petri-dishes with the filter membranes in place on the LB agar were exposed to the afterglow plume emitted from the grounded hollow slot electrode for the required time. After the plasma treatment, the petri dishes were

incubated at 37°C for one day prior to determining the resulting number of colony forming units (CFU).

The experimental process is depicted in Figure 8.1

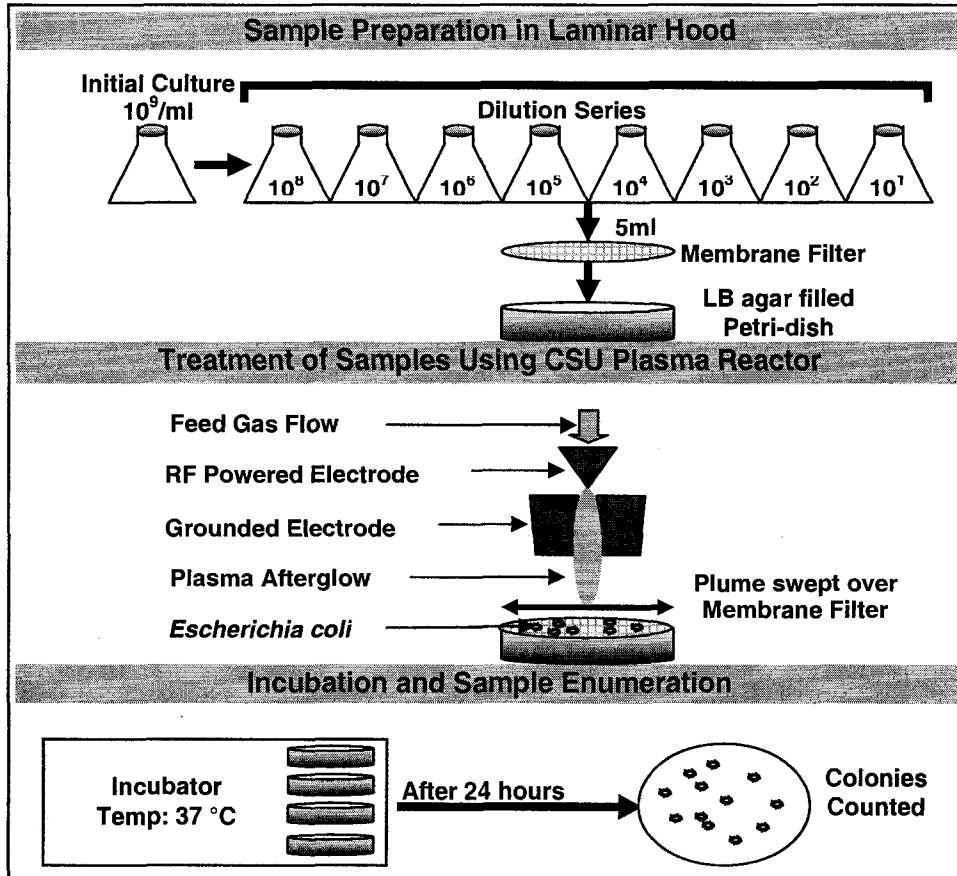


Figure 8.1: Schematic of inactivation methodology.

8.3 Varied Conditions

To better understand the underlying mechanism of inactivation by investigating the roles played by different plasma constituents and also to optimize bacterial inactivation, a variety of experiments were performed utilizing multiple experimental conditions.

8.3.1 Gas ON Plasma OFF

To ensure that the bacteria were being inactivated by the actual plasma (radical and photon species) and not merely being blown off the surface by the gas flow, a control experiment was performed in which the bacteria laden filter membranes were exposed only to gas flowing through the electrodes with the power turned off.

8.3.2 Distance from the Electrode

As the plume exits from the electrodes into open air, the conditions downstream are expected to vary with distance from the electrode. To study the impact of sample distance from the electrode on inactivation, an experiment was performed in which the distance of the samples was varied from 0.25-1.00 cm. The temperatures that the samples were exposed to were measured using temperature strips (± 1 °C, Omega, Stamford, CT).

8.3.3 Frequency

The plasma characteristics can change dramatically with change in the frequency of RF power supplied to the powered electrode. To determine the exact nature of this change on the inactivation levels, a comparison of inactivation was done by powering the device at two different frequencies: 13.56 MHz and 60 MHz. For this range of frequencies rare gas flow was required.

8.3.4 Oxygen

For the baseline experiments, the main gas fed to the device was argon, supplemented with a fixed and minute amount of oxygen. To determine the effect of oxygen on inactivation, an experiment was conducted where varying amounts of oxygen were mixed with the main argon gas feed. This was done in order to explore the possibility of enhancing the formation of oxygen radicals, powerful species with the potential to destroy bacterial cells.

8.3.5 UV Effect

A significant amount of ultraviolet (UV) radiation is known to be produced by the plasma reactor. UV is well-known for its ability to inactivate microbes and thus is used widely in the drinking water industry as a final disinfectant. Two different approaches were used to estimate the role of UV in bacterial inactivation by the plasma plume. First, a magnesium fluoride (MgF_2) window was placed between the device and the samples. Magnesium fluoride allows UV light above 100 nm while blocking particles, such as radicals and ions. This provided a means to isolate the effect of UV. A variation of the above experiment was also conducted by covering the sample with the polystyrene lid of the petri-dish that blocked both particles and UV below 300 nm.

Second, spectroscopic analysis of the plasma plume was performed in order to qualitatively determine the nature of UV flux emitted. The optical spectra, $I(\lambda)$, were obtained using a 0.2m McPherson VM 502 scanning monochromator, with a grating of 1200 Gmm^{-1} blazed at 120 nm. Light was detected using an Acton 781 photomultiplier tube. The optical emission was measured by placing the linear slot plasma in close proximity, and parallel, to the entrance slit of the spectrometer. The spectral resolution of the detection system (FWHM of slit function) was about 0.7 nm. An optical window (MgF_2) and a mask were employed to define the emitting area. The output spectra correspond to light emitted from a 4 mm length slot (defined by the mask).

8.3.6 Gas Composition and Flow rate

Discharge characteristics are known to vary with the type of feed-gas used. To determine the role of gas composition and flow in inactivation, argon was compared with helium as the primary feed gas at different flow rates.

8.3.7 Power

Finally, different levels of power were transmitted through the electrodes to estimate the amount of energy needed to achieve the desired level of inactivation.

8.4 Results and Discussion

Exposure of *E. coli* to the downstream plasma plume generated by the RF powered hollow slot device was observed to cause a total inactivation of well over five logs in less than two seconds (per unit area). A survival curve for the baseline condition of argon gas at a flow rate of 20 l/m powered by a 60 MHz device is presented in Figure 8.2 This demonstrated that the 60 MHz plasma was capable of microbial inactivation, as was observed previously for 13.56 MHz [Sharma2005] and defined the baseline for subsequent experiments. In the following sections the effect of changing various operational parameters are presented and insight with respect to the inactivation pathways is discussed.

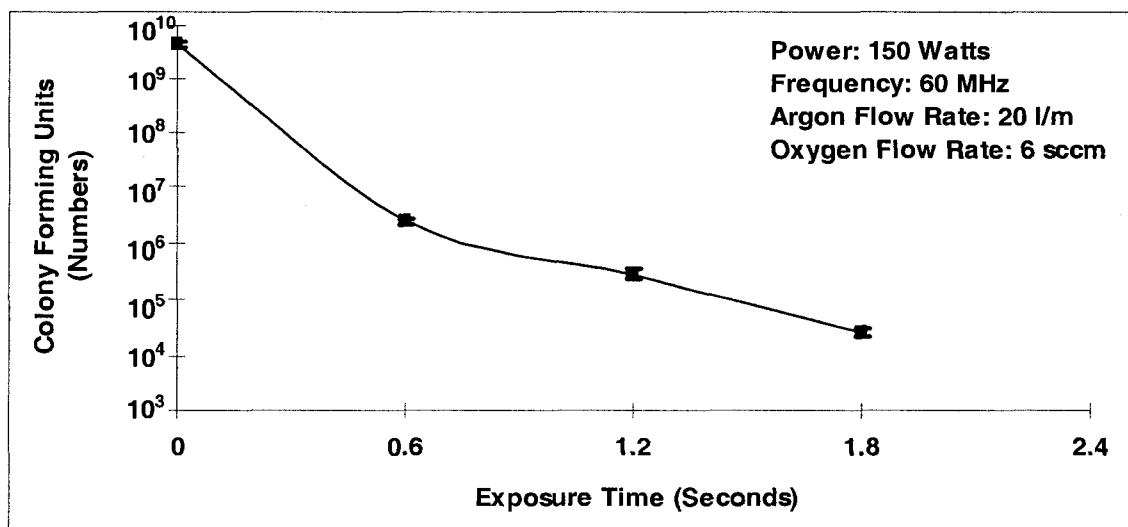


Figure 8.2: Survival curve of *E. coli* when exposed at 0.5 cm from the electrode (baseline experiment).

8.4.1 Gas ON Plasma OFF

Gas flow in and of itself was not observed to have an effect on bacterial inactivation (Figure 8.3). This confirmed that the plasma plume, containing radicals and photons, was the driving force in bacterial inactivation.

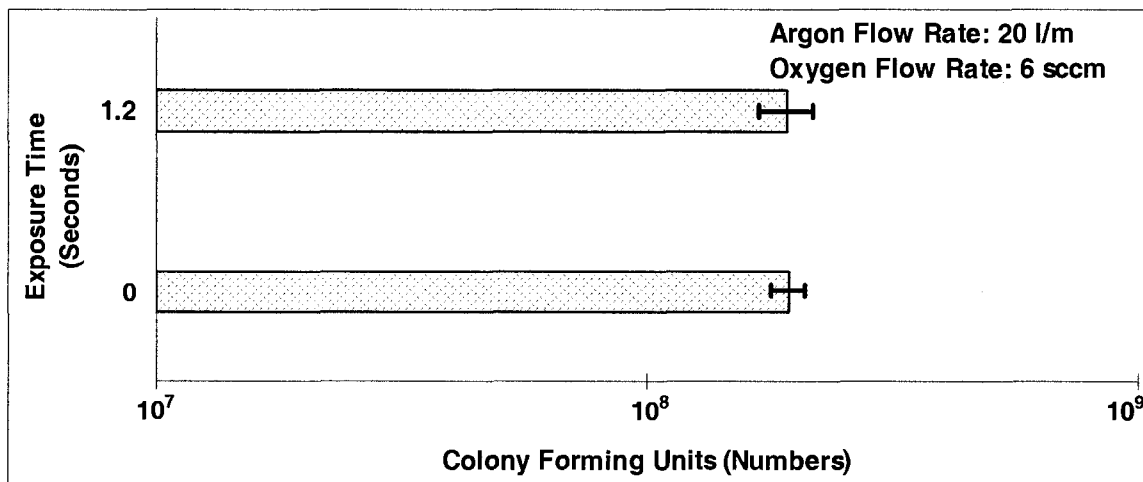


Figure 8.3: Effect of gas flow (instrument off) on inactivation of *E. coli*.

8.4.2 Distance from the Electrode

As presented in Figure 8.4, as the distance of the sample was varied from 0.25 cm to 1 cm away from the electrode, there was no significant change in the relative inactivation of *E. coli*. This was despite the gradient in temperature observed between 40 °C and 70 °C. This indicates that heat does not play a significant role in inactivation, considering that the temperature was less than 40 °C at 1 cm away from the electrode.

8.4.3 Frequency

A comparison of inactivation while powering the device with two different power supplies, one operating at 13.56 MHz and the other at 60 MHz, is presented in Figure 8.5. It can be deduced that the higher fluxes produced by the 60 MHz resulted in a higher

level of inactivation. It is judged that this is due to the different radical and photon distributions measured for the two different RF frequencies.

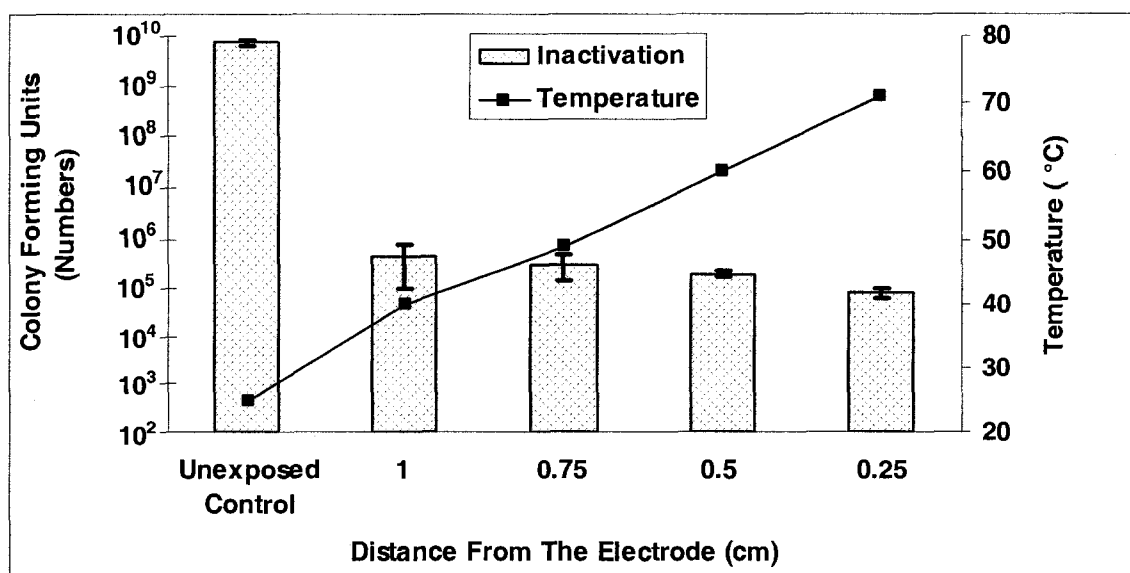


Figure 8.4: Effect of distance from electrode on inactivation of *E. coli*. All the samples were exposed for about 0.6 s per unit area. Power delivered and gas flow rates for argon and oxygen were 100 W, 5 l/m, and 6 sccm, respectively.

8.4.4 Oxygen

Oxygen can play an important role in the inactivation process as its decomposition into atomic oxygen, which is a powerful oxidant. Also, radicals such as OH• may form from atmospheric water vapor dissociation, which may physically attack the cells. To test this, minute quantities of oxygen were added to the main feed-gas of argon. However, because the device operates in open-air, there is always some atmospheric oxygen present. As seen from Figure 8.6, the inactivation rate was not significantly affected by oxygen addition. In fact, the average inactivation rate was slightly lower when the highest amount of oxygen was added to the feed. A reason for

this might be that the addition of oxygen made the discharge slightly unstable and hence had a net negative influence on the flux of active species.

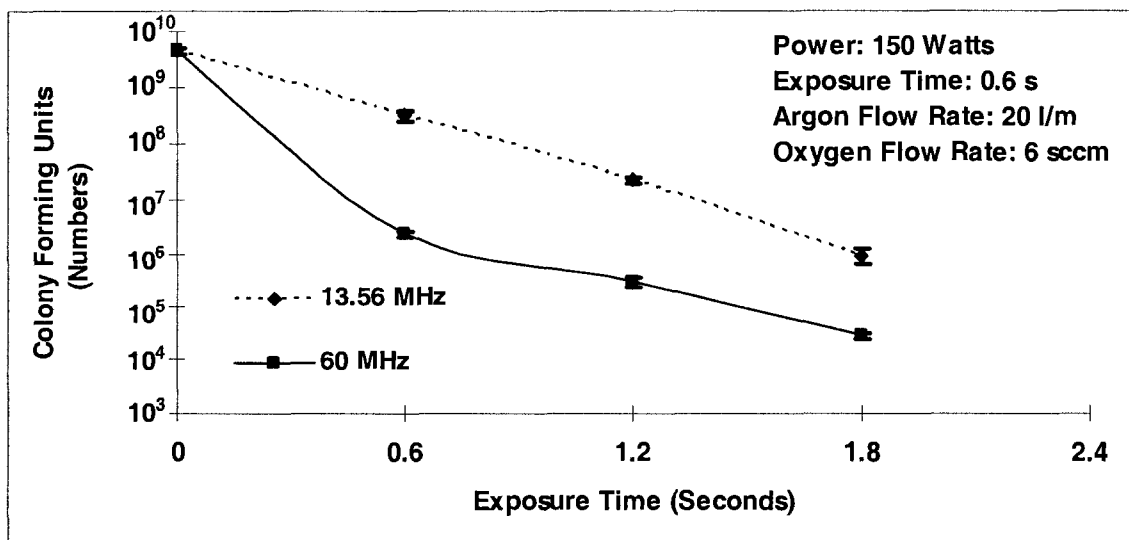


Figure 8.5: Comparison of inactivation of *E. coli* by 60 MHz and 13.56 MHz powered devices.

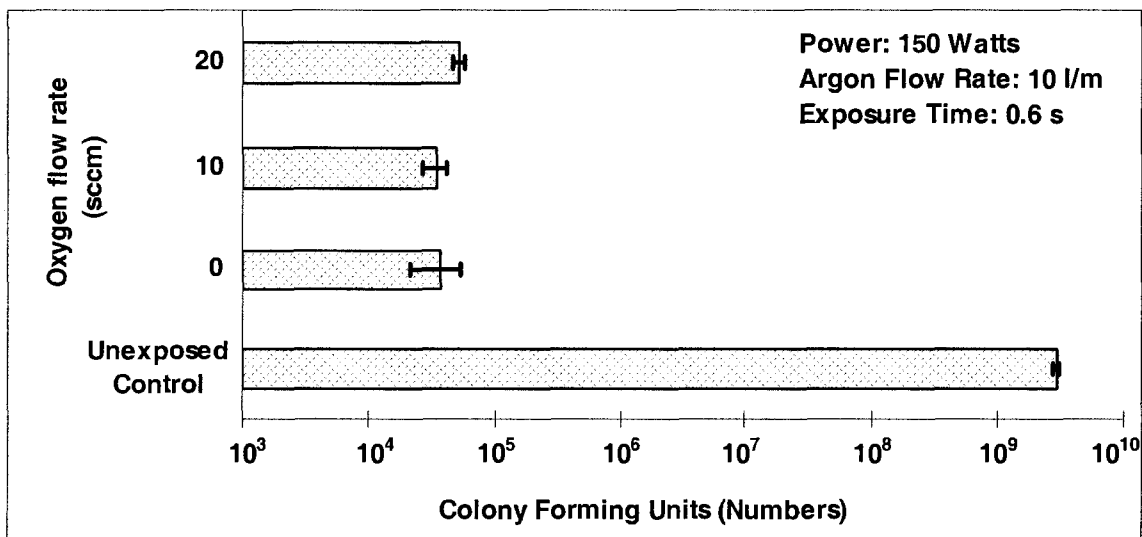


Figure 8.6: The effect of oxygen flow-rate on inactivation. The control was unexposed to the plasma.

8.4.5 UV Effect

The germicidal effects of UV light are well-known. UV light inactivates organisms by absorption of the photons which causes a photochemical reaction that alters molecular components essential to cell function. As UV rays penetrate the cell wall of the microorganism, the energy reacts with nucleic acids and other vital cell components, resulting in injury or death of the exposed cells [USEPA1999]. As can be seen from Figure 8.7, the inactivation in the sample covered with the $MgFl_2$ was much higher than in the sample covered with the polystyrene lid. This suggests that UV played a major role in the inactivation. Also, as polystyrene is known to filter out light below 300 nm, the results further emphasize the role of UV in the range of 100-300 nm.

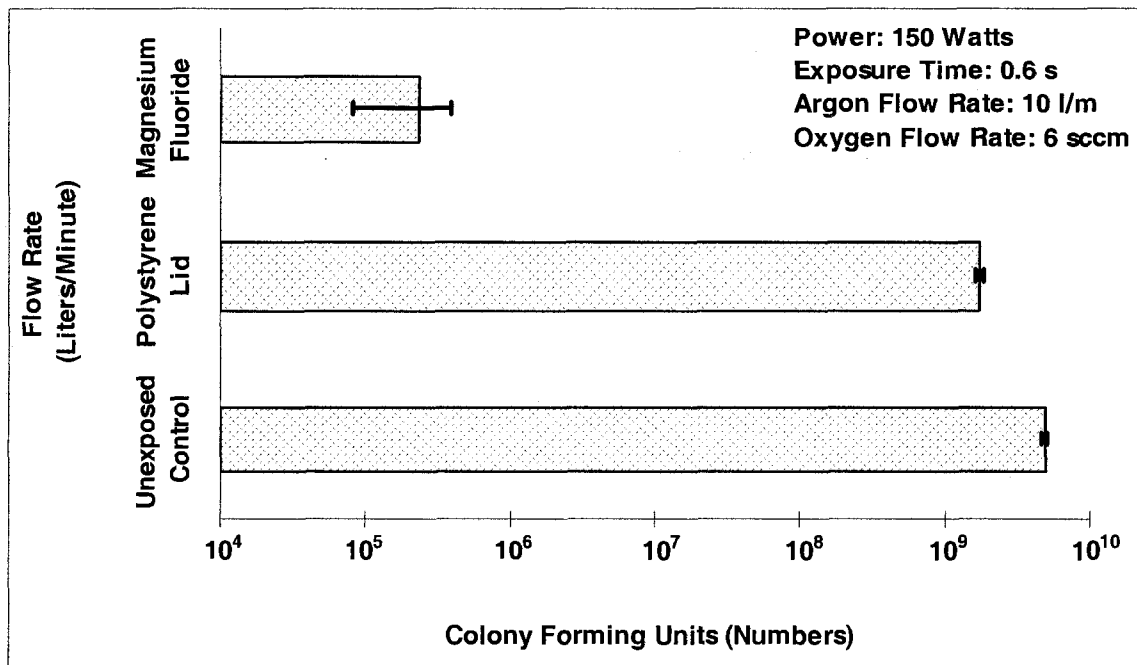


Figure 8.7: Survival of *E. coli* when sample covered with a polystyrene lid or MgF_2 window.

UV in the range from about 180 nm to about 280 nm can be very destructive to microbes for a variety of reasons. There is a sizeable amount of production of lethal

ozone at about 185 nm. Ozone, like UV, is commonly used as a disinfectant in drinking water treatment. Also 240-280nm is known as the “germicidal range” where the microbial DNA absorbs the most energy with 265nm being the peak germicidal wavelength. The spectroscopic analysis of the device is presented in Figure 8.8 and indicates that the transitions observed are within the ozone production range as well as the germicidal range.

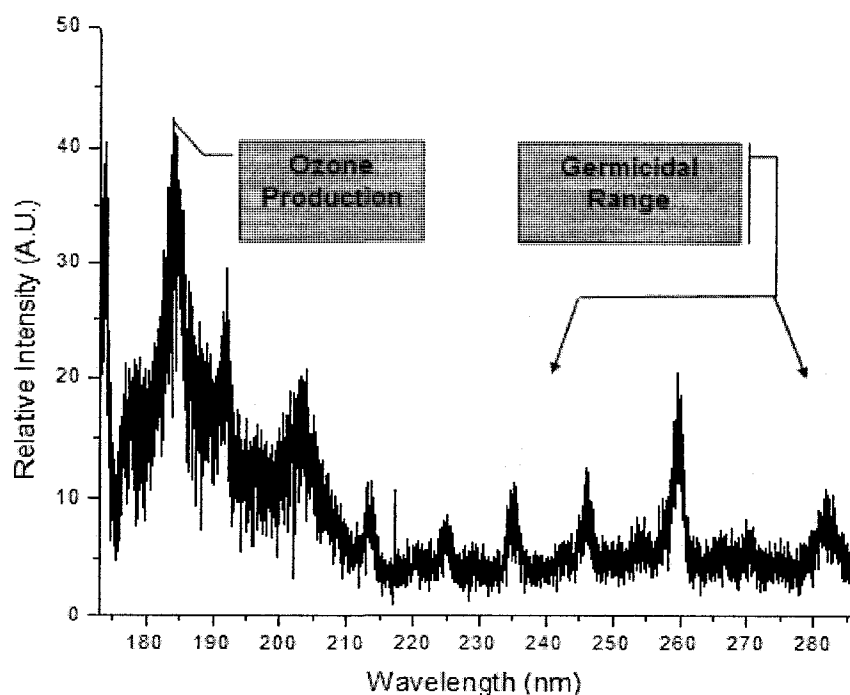


Figure 8.8: Spectroscopic analysis of the hollow slot device using a 0.2m McPherson VM 502 scanning monochromator. Power delivered and gas flow rates for argon and oxygen were 150 W, 10 l/m and 6 sccm respectively.

8.4.6 Gas Composition and Flow

The results of the experiments comparing argon and helium at different flow rates are presented in Figure 8.9. The results indicate that helium was not as effective as argon in inactivating the bacteria. A possible reason could be because of lack of UV generation in the germicidal range. With respect to flow rates, it was observed that in the case of

argon the inactivation rate was higher for lower flow rates. This could be attributed to the fact that the plasma constituents remain in the vicinity at lower flow rates. Conversely, average inactivation levels actually increased with increased helium flow, however only slightly. This could be due to the minor role that temperature plays in inactivation as observed in Figure 8.4.

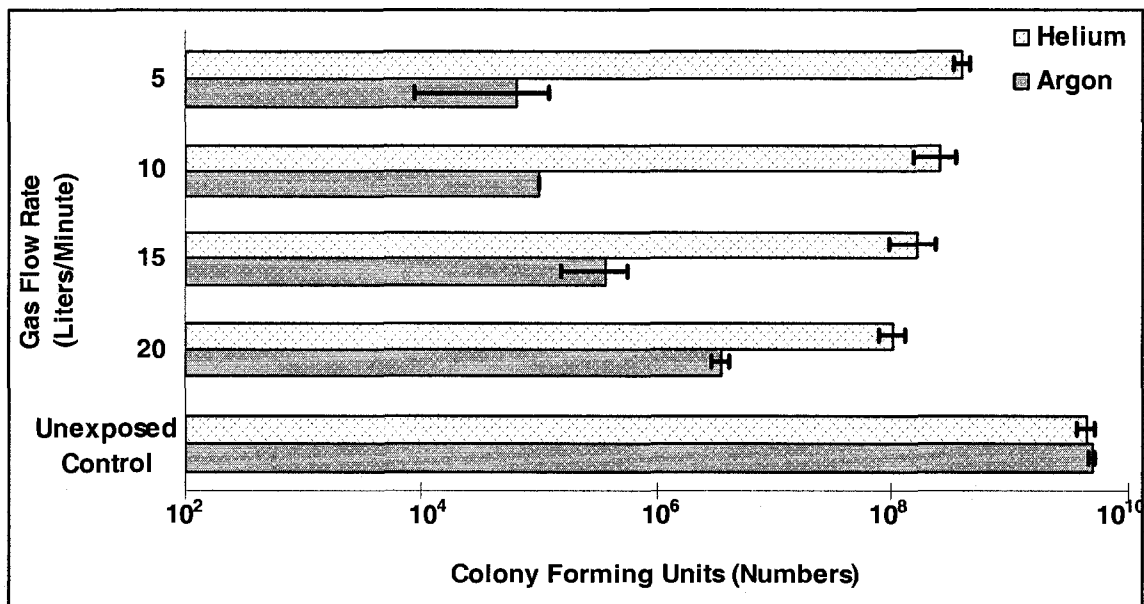


Figure 8.9: Survival of *E. coli*, when comparing the flow rates of helium and argon as the main feed-gas. Power delivered and gas flow rate for oxygen were 150 W and 6 sccm respectively.

8.4.7 Power Variation

As is evident in Figure 8.10, increasing the power yielded increased inactivation. This can be attributed to more dissociation of radicals and higher photon fluxes at higher power levels, as gas temperature measurements confirmed that there was only a minor effect on gas heating (data not presented).

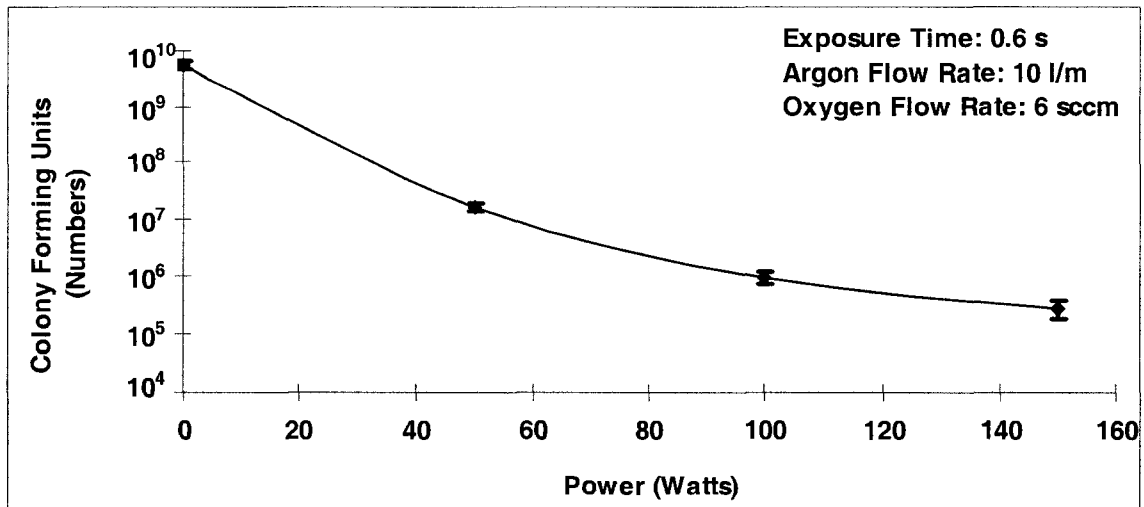


Figure 8.10: Survival plot of *E. coli*, with increased power.

8.5 Conclusion

Based on the results, some of the conclusions that can be drawn are as follows: UV plays a primary role in the inactivation process, while oxygen radicals play a secondary role. However, a synergistic effect was observed in the combination of UV and radicals that caused a higher rate of inactivation than possible using the two treatments in isolation. Gas temperature within the range observed in this study had a negligible effect on inactivation.

Chapter 9

Conclusions and Future Work

The results obtained by microarray data analysis seem to suggest that constituents of non-thermal atmospheric-pressure plasmas, UV light and oxygen radicals, act in a synergistic manner to induce various damage response genes in *E. coli*. The induction of the general repair mechanism, SOS response and last-resort error-prone repair mechanism, translesion synthesis, indicates that plasmas cause a substantial level of DNA damage and the incomplete induction of certain damage repair systems indicates that the bacteria are not successful at recovering from the incurred DNA damage.

The lack of induction of genes involved in heat shock response and also the observation of a minor effect on inactivation based on increase in temperature eliminates heat as a major player in bacterial inactivation.

Plasma conditions can vary a great deal depending on the device design and operating parameters. This can change the ratio of various constituent species of the plasma and hence can affect the genetic effect on bacteria resulting in different levels of inactivation. Therefore it is imperative to note that although we expect a similar genetic response of the bacteria to plasma species produced by different devices, there also might be some differences.

Many regulons within a cell are highly temporal in nature, therefore to further knowledge on the temporal response of bacteria to plasma species, studies would be needed with several time points after plasma exposure.

Although microarrays are very effective at surveying the whole genome for genes of interest, the results should be verified using other methods. RT-PCR (Reverse Transcription Polymerase Chain Reaction) is a method for exponential amplification of mRNA transcripts, after they have been reverse transcribed into cDNA [Bustin2002]. This method is especially suited for mRNA molecules present in low numbers and targets one to a few genes at a time. Specifically related to this dissertation, some genes part of the SOS regulon would be good candidates for RT-PCR analysis.

There are many advantages to using *E. coli* as a test organism to study the genetic response of bacteria to plasmas, however the bacterium is not known for its resilience against microcidal agents. Therefore differential gene expression on a genome wide scale should also be investigated in strains of some more resistant species such as *B. atrophaeus*.

Finally, various optimization experiments coupled with microarray analysis shed new light into the mechanism of plasma inactivation and the research conducted as part of this dissertation proves that non-thermal atmospheric-pressure plasma is a potentially promising tool for surface decontamination and sterilization in the future.

References

Abaibou1995: Abaibou H, Pommier J, Benoit S, Giordano G, Mandrand-Berthelot MA “Expression and characterization of the *Escherichia coli fdo* locus and a possible physiological role for aerobic formate dehydrogenase.” *J Bacteriol* 177 (24): 7141-7149.

Akischev1994: Akishev YS, Deryugin AA, Karal'Nik VB, Kochetov IV, Napartovich AP, Trushkin NI “Numerical simulation and experimental study of an atmospheric-pressure direct-current glow discharge” *Plasma Physics Reports* 20 (6): 511-524.

Al2005: Al Mamun AA, Humayun MZ “*Escherichia coli* DNA polymerase II can efficiently bypass 3,N(4)-ethenocytosine lesions in vitro and in vivo.” *Mutat Res* 593: 164-176

Altuvia1997: Altuvia S, Weinstein-Fischer D, Zhang A, Postow L, Storz G “A small, stable RNA induced by oxidative stress: role as a pleiotropic regulator and antimutator.” *Cell* 90 (1): 43-53.

Altuvia1998: Altuvia S, Zhang A, Argaman L, Tiwari A, Storz G “The *Escherichia coli* OxyS regulatory RNA represses *fhlA* translation by blocking ribosome binding.” *EMBO J* 17 (20): 6069-6075

Arslanbekov1998: Arslanbekov RR, Kudryavtsev AA, Tobin RC “On the hollow-cathode effect: conventional and modified geometry.” *Plasma Sources Sci Tech* 7: 310-322.

Babayan1998: Babayan SE, Jeong JY, Tu VJ, Park J, Selwyn GS, Hicks RF “Deposition of silicon dioxide films with an atmospheric-pressure plasma jet.” *Plasma Sources Sci Technol* 7: 286-288.

Bagg1981: Bagg A, Kenyon CJ, Walker GC “Inducibility of a gene product required for UV and chemical mutagenesis in *Escherichia coli*.” *Proc Natl Acad Sci USA* 78 (9): 5749-5753.

Barron1987: Barron A, Jung JU, Villarejo M “Purification and characterization of a glycine betaine binding protein from *Escherichia coli*.” *J Biol Chem* 262 (24): 11841-11846.

Becherel2001: Becherel OJ, Fuchs RP “Mechanism of DNA polymerase II-mediated frameshift mutagenesis.” *Proc Natl Acad Sci USA* 98 (15): 8566-8571.

Berardini1999: Berardini M, Foster PL, Loechler EL “DNA polymerase II (*polB*) is involved in a new DNA repair pathway for DNA interstrand cross-links in *Escherichia coli*.” *J Bacteriol* 181 (9): 2878-2882.

Berdichevs2002: Berdichevsky A, Izhar L, Livneh Z “Error-free recombinational repair predominates over mutagenic translesion replication in *E. coli*.” *Mol Cell* 10 (4): 917-924.

Blake1982: Blake R, O'Brien TA, Gennis RB, Hager LP "Role of the divalent metal cation in the pyruvate oxidase reaction." *J Biol Chem* 257 (16): 9605-9611.

Boyd2003: Boyd TJM, Sanderson JJ *The physics of plasmas 1st ed* pp. 1-10
Cambridge Cambridge University Press.

Brash1985: Brash DE, Haseltine WA "Photoreactivation of *Escherichia coli* reverses *umuC* induction by UV light." *J Bacteriol* 163 (2): 460-463.

Brokx2004: Brokx SJ, Ellison M, Locke T, Bottorff D, Frost L, Weiner JH
"Genome-wide analysis of lipoprotein expression in *Escherichia coli* MG1655." *J Bacteriol* 186 (10): 3254-3258.

Brown1969: Brown NC, Canellakis ZN, Lundin B, Reichard P, Thelander L
"Ribonucleoside diphosphate reductase. Purification of the two subunits, proteins B1 and B2." *Eur J Biochem* 9 (4): 561-573.

Brown1978: Brown SC "A short history of gaseous electronics." In *Gaseous electronics* ed. Hirsh MN, pp. 1-2 Oskam HJ New York Academy press.

Brown1999: Brown MH, Paulsen IT, Skurray RA "The multidrug efflux protein NorM is a prototype of a new family of transporters." *Mol Microbiol* 31 (1): 394-395.

Bustin2002: Bustin SA "Quantification of mRNA using real-time reverse transcription PCR (RT-PCR): trends and problems" *J Mol Endocrinology* 29: 23-39.

Butland2005: Butland G, Peregrin-Alvarez JM, Li J, Yang W, Yang X, Canadien V, Starostine A, Richards D, Beattie B, Krogan N, Davey M, Parkinson J, Greenblatt J,

Emili A “Interaction network containing conserved and essential protein complexes in *Escherichia coli*.” *Nature* 433 (7025): 531-537.

Chatterji2002: Chatterji M, Nagaraja V “GyrI: a counter-defensive strategy against proteinaceous inhibitors of DNA gyrase.” *EMBO Rep* 3 (3): 261-267.

Chen1974: Chen FF *Introduction to plasma physics* pp. 1-3 New York Plenum Press.

Claiborne1979: Claiborne A, Fridovich I “Purification of the o-dianisidine peroxidase from *Escherichia coli* B. Physicochemical characterization and analysis of its dual catalytic and peroxidatic activities.” *J Biol Chem* 254 (10): 4245-4252.

Cole1983: Cole ST “Characterisation of the promoter for the LexA regulated *sulA* gene of *Escherichia coli*.” *Mol Gen Genet* 189 (3): 400-404.

Cole1985: Cole ST, Condon C, Lemire BD, Weiner JH “Molecular biology, biochemistry and bioenergetics of fumarate reductase, a complex membrane-bound iron-sulfur flavoenzyme of *Escherichia coli*.” *Biochim Biophys Acta* 811 (4): 381-403.

Courcelle2003: Courcelle J, Hanawalt PC “RecA-dependent recovery of arrested DNA replication forks.” *Annu Rev Genet* 37: 611-646.

Daley2005: Daley DO, Rapp M, Granseth E, Melen K, Drew D, von Heijne G “Global topology analysis of the *Escherichia coli* inner membrane proteome.” *Science* 308 (5726): 1321-1323.

deBoer1992: de Boer PA, Crossley RE, Rothfield LI “Roles of MinC and MinD in the site-specific septation block mediated by the MinCDE system of *Escherichia coli*.” *J Bacteriol* 174 (1): 63-70.

DeLisa2001: DeLisa MP, Wu CF, Wang L, Valdes JJ, Bentley WE “DNA microarray-based identification of genes controlled by autoinducer 2-stimulated quorum sensing in *Escherichia coli*.” *J Bacteriol* 183 (18): 5239-5247.

EPA1999: United States Environmental Protection Agency Office of Water, Alternative Disinfectants and Oxidants Guidance Manual, EPA 815-R-99-014 (4607).

Escarcelle1994: Escarceller M, Hicks J, Gudmundsson G, Trump G, Touati D, Lovett S, Foster PL, McEntee K, Goodman MF “Involvement of *Escherichia coli* DNA polymerase II in response to oxidative damage and adaptive mutation.” *J Bacteriol* 176 (20): 6221-6228.

Ferrandez1998: Ferrandez A, Minambres B, Garcia B, Olivera ER, Luengo JM, Garcia JL, Diaz E “Catabolism of phenylacetic acid in *Escherichia coli*. Characterization of a new aerobic hybrid pathway.” *J Biol Chem* 273 (40): 25974-25986.

Ferrandez2000: Ferrandez A, Garcia JL, Diaz E “Transcriptional regulation of the divergent paa catabolic operons for phenylacetic acid degradation in *Escherichia coli*.” *J Biol Chem* 275 (16):12214-12222.

Fischer2005: Fischer M, Romisch W, Illarionov B, Eisenreich W, Bacher A “Structures and reaction mechanisms of riboflavin synthases of eubacterial and archaeal origin.” *Biochem Soc Trans* 33 (4): 780-784.

Foster1995: Foster PL, Gudmundsson G, Trimarchi JM, Cai H, Goodman MF “Proofreading-defective DNA polymerase II increases adaptive mutation in *Escherichia coli*.” *Proc Natl Acad Sci USA* 92 (17): 7951-7955.

Kamenetskii1972: Kamenetskii F, Albertovich D *Plasma the fourth state of matter* pp. 1-5 New York Plenum Press.

Fridman2005: Fridman A, Chirokov A, Gutsol A “Non-thermal atmospheric pressure discharges.” *J Phys D: Appl Phys* 38: R1-R24.

Friedberg1995: Friedberg EC, Walker GC, Siede W *DNA Repair and Mutagenesis* 407-462. Washington, DC ASM Press.

Gambling1953: Gambling WA, Edels H “The High-Pressure Glow Discharge in Air.” *British Journal of Applied Physics* 5: 36-39.

Gambling1956: Gambling WA “Cathodic glow to arc transition.” *Can J Phys* 34: 1466-1470.

Godoy2006: Godoy VG, Jarosz DF, Walker FL, Simmons LA, Walker GC “Y-family DNA polymerases respond to DNA damage-independent inhibition of replication fork progression.” *EMBO J* 25 (4): 868-879.

Gonzalez2006: Gonzalez CF, Proudfoot M, Brown G, Korniyenko Y, Mori H, Savchenko AV, Yakunin AF “Molecular basis of formaldehyde detoxification: Characterization of two s-formylglutathione hydrolases from *Escherichia coli*, FrmB and YeiG.” *J Biol Chem* 281 (20): 14514-14522

Griffith2004: Griffith KL, Shah IM, Wolf RE “Proteolytic degradation of *Escherichia coli* transcription activators SoxS and MarA as the mechanism for reversing the induction of the superoxide (SoxRS) and multiple antibiotic resistance (Mar) regulons.” *Mol Microbiol* 51 (6):1801-1816.

Grisolia1985: Grisolia V, Carlomagno MS, Nappo AG, Bruni CB “Cloning, structure, and expression of the *Escherichia coli* K-12 *hisC* gene.” *J Bacteriol* 164 (3): 1317-1323.

Gupta1999: Gupta PK, Roy RJ, Prasad M “DNA chips, microarrays and genomics.” *Curr Sc.* 77: 875-884.

Haemig2004: Haemig HA, Brooker RJ “Importance of conserved acidic residues in *mntH*, the Nramp homolog of *Escherichia coli*.” *J Membr Biol* 201 (2): 97-107.

Hama1994: Hama H, Kayahara T, Ogawa W, Tsuda M, Tsuchiya T “Enhancement of serine-sensitivity by a gene encoding rhodanese-like protein in *Escherichia coli*.” *J Biochem (Tokyo)* 115 (6): 1135-40.

Hardie2003: Hardie KR, Cooksley C, Green AD, Winzer K “Autoinducer 2 activity in *Escherichia coli* culture supernatants can be actively reduced despite maintenance of an active synthase, LuxS.” *Microbiology* 149 (Pt 3): 715-728.

Heberlein2002: Heberlein J “New approaches in thermal plasma technology.” *Pure and Appl Chem* 74: 327-335.

HennSax2002: Henn-Sax M, Thoma R, Schmidt S, Hennig M, Kirschner K, Sterner R “Two (betaalpha)(8)-barrel enzymes of histidine and tryptophan biosynthesis have similar reaction mechanisms and common strategies for protecting their labile substrates.” *Biochemistry* 41 (40): 12032-12042.

Herrmann2002: Herrmann HW, Selwyn GS, Henins I, Jaeyoung P, Jeffery M, Williams JM “Chemical Warfare Agent Decontamination Studies in the Plasma Decon Chamber.” *IEEE Trans on Plasma Sci* 30 (4): 1460-1470.

Higashitani1997: Higashitani A, Ishii Y, Kato Y, Koriuchi K “Functional dissection of a cell-division inhibitor, SulA, of *Escherichia coli* and its negative regulation by Lon.” *Mol Gen Genet* 254 (4): 351-357.

Hudson1993: Hudson AJ, Andrews SC, Hawkins C, Williams JM, Izuhara M, Meldrum FC, Mann S, Harrison PM, Guest JR “Overproduction, purification and characterization of the *Escherichia coli* ferritin.” *Eur J Biochem* 218 (3): 985-995.

Huisman1996: Huisman TT, Pilipcinec E, Remkes F, Maaskant J, de Graaf FK, Oudega B “Isolation and characterization of chromosomal mTn 10 insertion mutations affecting K88 fimbriae production in *Escherichia coli*.” *Microb Pathog* 20 (2): 101-108.

Hussein1998: Hussein MJ, Green JM, Nichols BP “Characterization of mutations that allow p-aminobenzoyl-glutamate utilization by *Escherichia coli*.” *J Bacteriol* 180 (23): 6260-6268.

Ishino1992: Ishino Y, Iwasaki H, Fukui H, Mineno J, Kato I, Shinagawa H
“Aphidicolin inhibits DNA polymerizing activity but not nucleolytic activity of
Escherichia coli DNA polymerase II.” *Biochimie* 74 (2): 131-136.

Kandror2002: Kandror O, DeLeon A, Goldberg AL “Trehalose synthesis is
induced upon exposure of *Escherichia coli* to cold and is essential for viability at low
temperatures.” *Proc Natl Acad Sci USA* 99 (15): 9727-9732.

Kanuri2005: Kanuri M, Nechev LV, Kiehna SE, Tamura PJ, Harris CM, Harris
TM, Lloyd RS “Evidence for *Escherichia coli* polymerase II mutagenic bypass of
intrastrand DNA crosslinks.” *DNA Repair (Amst)* 4 (12): 1374-1380.

Karp2007: Karp PD, Keseler IM, Shearer A, Latendresse M, Krummenacker M,
Paley SM, Paulsen I, Collado-Vides J, Gama-Castro S, Peralta-Gil M, Santos-Zavaleta A,
Penaloza-Spinola MI, Bonavides-Martinez C, Ingraham J “Multidimensional annotation
of the *Escherichia coli* K-12 genome” *Nucl Acids Res* 35: 7577-7590.

Kelly-Wintenberg1999: Kelly-Wintenberg K, Hodge A, Montie TC, Deleanu L,
Sherman D, Roth JR, Tsai P, Wadsworth L “Use of one atmosphere uniform glow
discharge plasma to kill a broad spectrum of microorganisms.” *Journal of Vacuum
Science & Technology A* 17 (4): 1539-1544

Kenyon1980: Kenyon CJ, Walker GC “DNA-damaging agents stimulate gene
expression at specific loci in *Escherichia coli*.” *Proc Natl Acad Sci USA* 77 (5): 2819-
2823.

Kim2001: Kim SR, Matsui K, Yamada M, Gruz P, Nohmi T “Roles of chromosomal and episomal *dinB* genes encoding DNA pol IV in targeted and untargeted mutagenesis in *Escherichia coli*.” *Mol Genet Genomics* 266 (2): 207-215.

Kirkici1995: Kirkici, H. Bruno D “Operating characteristics of a segmented hollow cathode over a wide pressure range.” *IEEE Trans Plasma Sci* 23 (3): 229-234.

Klem1993: Klem TJ, Davisson VJ “Imidazole glycerol phosphate synthase: the glutamine amidotransferase in histidine biosynthesis.” *Biochemistry* 32 (19): 5177-5186.

Koch1998: Koch WH, Woodgate R “The SOS Response.” In *DNA Damage And Repair, Volume 1: DNA Repair in Prokaryotes and Lower Eukaryotes*, ed. Nickoloff JA, Hoekstra MF pp. 107-125 Totowa, NJ: Humana Press, Inc.

Koinuma1992: Koinuma H, Ohkubo H, Hashimoto T, Inomata K, Shiraishi T, Miyanaga A, Hayashi S “Development and application of a microbeam plasma generator.” *Appl Phys Lett* 60: 816.

Kosa2004: Kosa JL, Zdraveski ZZ, Currier S, Marinus MG, Essigmann JM “RecN and RecG are required for *Escherichia coli* survival of Bleomycin-induced damage.” *Mutat Res* 554 (1-2): 149-157.

Kuban2004: Kuban W, Jonczyk P, Gawel D, Malanowska K, Schaaper RM, Fijalkowska IJ “Role of *Escherichia coli* DNA polymerase IV in in vivo replication fidelity.” *J Bacteriol* 186 (14): 4802-4807.

Kunhardt2000: Kunhardt EE “Generation of Large-Volume, Atmospheric-Pressure, Nonequilibrium Plasmas.” *IEEE Trans Plasma Sci* 28 (1): 189-200.

Kuzminov1999: Kuzminov A “Recombinational repair of DNA damage in *Escherichia coli* and bacteriophage lambda.” *Microbiol Mol Biol Rev* 63 (4): 751-813.

Lambalot1995: Lambalot RH, Walsh CT “Cloning, overproduction, and characterization of the *Escherichia coli* holo-acyl carrier protein synthase.” *J Biol Chem* 270 (42): 24658-24661.

Landry2000: Landry J, Sutton A, Tafrov ST, Heller RC, Stebbins J, Pillus L, Sternglanz R “The silencing protein SIR2 and its homologs are NAD-dependent protein deacetylases.” *Proc Natl Acad Sci USA* 97 (11): 5807-5811.

Laroussi1996: Laroussi M “Sterilization of contaminated matter with an atmospheric pressure plasma.” *IEEE Trans Plasma Sci* 24 (3): 1188-1991.

Laroussi2000: Laroussi M, Alexeff I, Kang W “Biological decontamination by nonthermal plasmas.” *IEEE Trans Plasma Sci* 28: 184-188.

Laroussi2005: Laroussi M, Lu X “Room-temperature atmospheric pressure plasma plume for biomedical applications.” *Appl Phys Lett* 87: 113902-113903.

Laurinavic2001: Laurinavichene TV, Tsygankov AA “H₂ consumption by *Escherichia coli* coupled via hydrogenase 1 or hydrogenase 2 to different terminal electron acceptors.” *FEMS Microbiol Lett* 202 (1): 121-124.

Lee1997: Lee PT, Hsu AY, Ha HT, Clarke CF “A C-methyltransferase involved in both ubiquinone and menaquinone biosynthesis: isolation and identification of the *Escherichia coli* *ubiE* gene.” *J Bacteriol* 179 (5): 1748-1754.

Leer1975: Leer JC, Hammer-Jespersen K “Multiple forms of phosphor-deoxyribomutase from *Escherichia coli*. Physical and chemical characterization.” *Biochemistry* 14 (3): 599-607.

Lewis1994: Lewis LK, Harlow GR, Gregg-Jolly LA, Mount DW “Identification of high affinity binding sites for LexA which define new DNA damage-inducible genes in *Escherichia coli*.” *J Mol Biol* 241 (4): 507-523.

Li2001a: Li C, Wong WH “Model-based analysis of oligonucleotide arrays: model validation, design issues and standard error application.” *Genome Biol Res* 2 (8): research032.

Li2001b: Li C, Wong WH “Model-based analysis of oligonucleotide arrays: expression index computation and outlier detection.” *Proc Natl Acad Sci USA* 98: 31-36.

Liang2000: Liang X, Thorpe C, Schulz H “2,4-Dienoyl-CoA reductase from *Escherichia coli* is a novel iron-sulfur flavoprotein that functions in fatty acid beta-oxidation.” *Arch Biochem Biophys* 380 (2): 373-379.

Lin1989: Lin JJ, Sancar A “A new mechanism for repairing oxidative damage to DNA: (A)BC excinuclease removes AP sites and thymine glycols from DNA.” *Biochemistry* 28 (20): 7979-7984.

Lishutz1999: Lipshutz RJ, Fodor SP, Gingeras TR, Lockhart DJ “High density synthetic oligonucleotide arrays.” *Nat. Genet* 21: 20–24.

Locher1998: Locher KP, Rees B, Koebnik R, Mitschler A, Moulinier L, Rosenbusch JP, Moras D “Transmembrane signaling across the ligand-gated FhuA receptor: crystal structures of free and ferrichrome-bound states reveal allosteric changes.” *Cell* 95 (6): 771-778.

Loewen1990: Loewen PC, Switala J, Smolenski M, Triggs-Raine BL “Molecular characterization of three mutations in *katG* affecting the activity of hydroperoxidase I of *Escherichia coli*.” *Biochem Cell Biol* 68 (7-8): 1037-1044.

Lomba1997: Lomba MR, Vasconcelos AT, Pacheco AB, de Almeida DF “Identification of *yebG* as a DNA damage-inducible *Escherichia coli* gene.” *FEMS Microbiol Lett* 156 (1):119-122.

Lusetti2004: Lusetti SL, Drees JC, Stohl EA, Seifert HS, Cox MM “The DinI and RecX proteins are competing modulators of RecA function.” *J Biol Chem* 279 (53): 55073-55079.

Madan2003: Madan Babu M, Teichmann SA “Evolution of transcription factors and the gene regulatory network in *Escherichia coli*.” *Nucleic Acids Res* 31 (4): 1234-1244.

MaorShosha2000: Maor-Shoshani A, Reuven NB, Tomer G, Livneh Z “Highly mutagenic replication by DNA polymerase V (UmuC) provides a mechanistic basis for SOS untargeted mutagenesis.” *Proc Natl Acad Sci USA* 97 (2): 565-570.

Masse2002: Masse E, Gottesman S “A small RNA regulates the expression of genes involved in iron metabolism in *Escherichia coli*.” *Proc Natl Acad Sci USA* 99 (7): 4620-4625.

Massines1998: Massines F, Rabehi A, Decomps P, Gadri RB, Ségur P, Mayoux C “Experimental and theoretical study of a glow discharge at atmospheric pressure controlled by dielectric barrier.” *J Appl Phys* 83(6): 2950-2957.

Masters1981: Masters PS, Hong JS “Genetics of the glutamine transport system in *Escherichia coli*.” *J Bacteriol* 147 (3): 805-819.

McKenzie2001: McKenzie GJ, Lee PL, Lombardo MJ, Hastings PJ, Rosenberg SM “SOS mutator DNA polymerase IV functions in adaptive mutation and not adaptive amplification.” *Mol Cell* 7 (3): 571-579.

McKenzie2003: McKenzie GJ, Magner DB, Lee PL, Rosenberg SM “The *dinB* operon and spontaneous mutation in *Escherichia coli*” *J Bacteriol* 185 (13): 3972-3977.

Meddows2004: Meddows TR, Savory AP, Lloyd RG “RecG helicase promotes DNA double-strand break repair.” *Mol Microbiol* 52 (1): 119-132.

Meddows2005: Meddows TR, Savory AP, Grove JI, Moore T, Lloyd RG “RecN protein and transcription factor DksA combine to promote faithful recombinational repair of DNA double-strand breaks.” *Mol Microbiol* 57 (1): 97-110.

Meyer1990: Meyer RR, Laine PS “The single-stranded DNA-binding protein of *Escherichia coli*.” *Microbiol Rev* 54 (4): 342-380.

Mogi1986: Mogi T, Yamamoto H, Nakao T, Yamato I, Anraku Y “Genetic and physical characterization of *putP*, the proline carrier gene of *Escherichia coli* K12.” *Mol Gen Genet* 202 (1): 35-41.

Moisan2001: Moisan M, Barbeau J, Moreau S, Pelletier J, Tabrizian M, Yahia L’H “Low-temperature sterilization using gas plasmas: a review of the experiments and an analysis of the inactivation mechanisms.” *Internat J of Pharm* 226: 1-21.

Muller1998: Muller K, Matzanke BF, Schunemann V, Trautwein AX, Hantke K “FhuF, an iron-regulated protein of *Escherichia coli* with a new type of [2Fe-2S] center.” *Eur J Biochem* 258 (3): 1001-1008.

Nakanishi1998: Nakanishi A, Oshida T, Matsushita T, Imajoh-Ohmi S, Ohnuki T “Identification of DNA gyrase inhibitor (GyrI) in *Escherichia coli*.” *J Biol Chem* 273 (4): 1933-1938.

Napolitano2000: Napolitano R, Janel-Bintz R, Wagner J, Fuchs RP “All three SOS-inducible DNA polymerases (Pol II, Pol IV and Pol V) are involved in induced mutagenesis.” *EMBO J* 19 (22): 6259-6265.

Nassau1996: Nassau PM, Martin SL, Brown RE, Weston A, Monsey D, McNeil MR, Duncan K “Galactofuranose biosynthesis in *Escherichia coli* K-12: identification and cloning of UDP-galactopyranose mutase.” *J Bacteriol* 178 (4): 1047-1052.

Neeley2007: Neeley WL, Delaney S, Alekseyev YO, Jarosz DF, Delaney JC, Walker GC, Essigmann JM “DNA polymerase V allows bypass of toxic guanine oxidation products in vivo.” *J Biol Chem* 282 (17): 12741-12748.

Neidhardt1996: Neidhardt FC, Curtiss III R, Ingraham JL, Lin ECC, Low Jr. KB, Magasanik B, Reznikoff WS, Riley M, Schaechter M, Umbarger HE “*Escherichia coli* and *Salmonella*, Cellular and Molecular Biology” 2nd ed. pp. 156-169 Washington, D.C. ASM Press.

Niehaus1991: Niehaus F, Hantke K, Uden G “Iron content and FNR-dependent gene regulation in *Escherichia coli*.” *FEMS Microbiol Lett* 68 (3): 319-323.

Nohmi1988: Nohmi T, Battista JR, Dodson LA, Walker GC (1988). “RecA-mediated cleavage activates UmuD for mutagenesis: mechanistic relationship between transcriptional derepression and posttranslational activation.” *Proc Natl Acad Sci USA* 85 (6): 1816-1820.

Nonet1987: Nonet ML, Marvel CC, Tolan DR “The *hisT-purF* region of the *Escherichia coli* K-12 chromosome. Identification of additional genes of the *hisT* and *purF* operons.” *J Biol Chem* 262 (25): 12209-12217.

Oh2001: Oh TJ, Jung IL, Kim IG “The *Escherichia coli* SOS gene *sbmC* is regulated by H-NS and RpoS during the SOS induction and stationary growth phase.” *Biochem Biophys Res Commun* 288 (4): 1052-1058.

Ohmori2001: Ohmori H, Friedberg EC, Fuchs RP, Goodman MF, Hanaoka F, Hinkle D, Kunkel TA, Lawrence CW, Livneh Z, Nohmi T, Prakash L, Prakash S, Todo T, Walker GC, Wang Z, Woodgate R “The Y-family of DNA polymerases.” *Mol Cell* 8 (1): 7-8.

Opperman1999: Opperman T, Murli S, Smith BT, Walker GC “A model for a *umuDC*-dependent prokaryotic DNA damage checkpoint.” *Proc Natl Acad Sci USA* 96 (16): 9218-9223.

Orren1989: Orren DK, Sancar A “The (A)BC excinuclease of *Escherichia coli* has only the UvrB and UvrC subunits in the incision complex.” *Proc Natl Acad Sci USA* 86 (14): 5237-5241.

Pages2003: Pages V, Koffel-Schwartz N, Fuchs RP “*recX*, a new SOS gene that is co-transcribed with the *recA* gene in *Escherichia coli*.” *DNA Repair (Amst)* 2 (3): 273-284.

Parsons1992: Parsons CA, Tsaneva I, Lloyd RG, West SC “Interaction of *Escherichia coli* RuvA and RuvB proteins with synthetic Holliday junctions.” *Proc Natl Acad Sci USA* 89 (12): 5452-5456.

PazElizur1996: Paz-Elizur T, Takeshita M, Goodman M, O'Donnell M, Livneh Z “Mechanism of translesion DNA synthesis by DNA polymerase II. Comparison to DNA polymerases I and III core.” *J Biol Chem* 271 (40): 24662-24669.

Pearce1992: Pearce SR, Mimmack ML, Gallagher MP, Gileadi U, Hyde SC, Higgins CF “Membrane topology of the integral membrane components, OppB and OppC, of the oligopeptide permease of *Salmonella typhimurium*.” *Mol Microbiol* 6 (1): 47-57.

Phadtare2006: Phadtare S, Tadigotla V, Shin WH, Sengupta A, Severinov K “Analysis of *Escherichia coli* Global Gene Expression Profiles in Response to Overexpression and Deletion of CspC and CspE.” *J Bacteriol* 188 (7): 2521-2527.

Pichoff1995: Pichoff S, Vollrath B, Touriol C, Bouche JP “Deletion analysis of gene *minE* which encodes the topological specificity factor of cell division in *Escherichia coli*.” *Mol Microbiol* 18 (2): 321-329.

Portalier1974: Portalier RC, Robert-Baudouy JM, Nemoz GM “Studies of mutations in the uronic isomerase and altronic oxidoreductase structural genes of *Escherichia coli* K 12.” *Mol Gen Genet* 128 (4): 301-319.

Qiu2005: Qiu X, Sundin GW, Wu L, Zhou J, Tiedje, JM “Comparative analysis of differentially expressed genes in *Shewanella oneidensis* MR-1 following exposure to UVC, UVB, and UVA radiation.” *J Bacteriol* 187 (10): 3556–3564.

Rahman2005: Rahman A “Atmospheric Pressure Microplasma Characterization” *Ph.D. dissertation, Dept of Elect and Comp Eng, Colorado State Univ., Fort Collins, CO.*

Rahul2005: Rahul R, Stan O, Rahman A, Littlefield E, Hoshimiya K, Yalin AP, Sharma A, Pruden A, Moore CA, Yu, Z, Collins, GJ “Optical and RF electrical characteristics of atmospheric pressure open-air hollow slot microplasmas and application to bacterial inactivation” *J Phys D: Appl Phys* 38: 1750–1759.

Raizer1997: Raizer YP *Gas Discharge Physics* (Chapter 8) New York: Springer.

Rangarajan2002: Rangarajan S, Woodgate R, Goodman MF (2002). "Replication restart in UV-irradiated *Escherichia coli* involving pols II, III, V, PriA, RecA and RecFOR proteins." *Mol Microbiol* 43 (3): 617-628.

Reed2003: Reed JL, Vo TD, Schilling CH, Palsson BO "An expanded genome-scale model of *Escherichia coli* K-12 (iJR904 GSM/GPR)." *Genome Biol* 4 (9): R54.

Reidl1991: Reidl J, Boos W "The *malX malY* operon of *Escherichia coli* encodes a novel enzyme II of the phosphotransferase system recognizing glucose and maltose and an enzyme abolishing the endogenous induction of the maltose system." *J Bacteriol* 173 (15): 4862-4876.

Ren2004: Ren D, Bedzyk LA, Thomas SM, Ye RW, Wood TK "Gene expression in *Escherichia coli* biofilms." *Appl Microbiol Biotechnol* 64 (4): 515-524.

Revington2005: Revington M, Semesi A, Yee A, Shaw GS "Solution structure of the *Escherichia coli* protein *ydhR*: A putative mono-oxygenase." *Protein Sci* 14: 3115-3120

Rezuchova2003: Rezuchova B, Miticka H, Homerova D, Roberts M, Kormanec J "New members of the *Escherichia coli* sigmaE regulon identified by a two-plasmid system." *FEMS Microbiol Lett* 225 (1): 1-7.

RobertBaud1982: Robert-Baudouy J, Jimeno-Abendano J, Stoeber F "D-Mannonate and D-altronate dehydratases of *Escherichia coli* K12." *Methods Enzymol* 90 Pt E: 288-294.

Rosenbluth1983: Rosenbluth MN, Sagdeev RZ, Galeev AA, Sudan RN *Basic Plasma Physics (1st ed)* pp. 3-6 New York North-Holland Publishing Company.

Roth2001: Roth JR, *Industrial Plasma Engineering Vol 1* pp. 117-158 London, Institute of Physics Publishing.

Sancar1988: Sancar A, Sancar GB “DNA repair enzymes.” *Annu Rev Biochem* 57: 29-67

Sargent1998: Sargent F, Ballantine SP, Rugman PA, Palmer T, Boxer DH (1998). “Reassignment of the gene encoding the *Escherichia coli* hydrogenase 2 small subunit--identification of a soluble precursor of the small subunit in a *hypB* mutant.” *Eur J Biochem* 255 (3): 746-754.

Sargentini1986: Sargentini NJ, Smith KC “Quantitation of the involvement of the *recA*, *recB*, *recC*, *recF*, *recJ*, *recN*, *lexA*, *radA*, *radB*, *uvrD*, and *umuC* genes in the repair of X-ray-induced DNA double-strand breaks in *Escherichia coli*.” *Radiat Res* 107 (1): 58-72.

Schneider1998: Schneider BL, Kiupakis AK, Reitzer LJ “Arginine catabolism and the arginine succinyltransferase pathway in *Escherichia coli*.” *J Bacteriol* 180 (16): 4278-4286.

Schutze1998: Schutze A, Jeong JY, Babayan SE, Park J, Selwyn GS, Hicks RF “The atmospheric-pressure plasma jet: A review and comparison to other plasma sources.” *IEEE Trans Plasma Sci* 26 (6): 1685-1694.

Selinger2000: Selinger DW, Cheung KJ, Mei R, Johansson EM, Richmond CS, Blattner FRD, Lockhart J, Church GM “RNA expression analysis using a 30 base pair resolution *Escherichia coli* genome array.” *Nat Biotechnol* 18: 1262–1268.

Selwyn2001: Selwyn, GS, Herrmann HW, Park J, Henins I “Materials processing using an atmospheric pressure, RF-generated plasma source.” *Contrib to Plasma Phys* 41 (6): 610-619.

Serina2004: Serina S, Nozza F, Nicastro G, Faggioni F, Mottl H, Deho G, Polissi A “Scanning the *Escherichia coli* chromosome by random transposon mutagenesis and multiple phenotypic screening.” *Res Microbiol* 155 (8): 692-701.

Shah1994: Shah R, Bennett RJ, West SC “Activation of RuvC Holliday junction resolvase in vitro.” *Nucleic Acids Res* 22 (13): 2490-2497.

Sharma2005: Sharma A, Pruden A, Yu Z, Collins GJ “Bacterial Inactivation in Open Air by the Afterglow Plume Emitted from a Grounded Hollow Slot Electrode.” *Environ Sci Technol* 39: 339-344.

Sharma2006: Sharma A, Pruden A, Stan O, Collins GJ “Bacterial Inactivation Using an RF-Powered Atmospheric Pressure Plasma.” *IEEE Trans Plasma Sci, Special Issue - Non-thermal Medical and Biological Applications of Ionized Gases & EM Fields*, 34 (4): 1290-1296.

Smith2003: Smith, HB, Charles C, Boswell RW “Breakdown behavior in radio-frequency argon discharges.” *Phys of Plasmas* 10 (3): 875-881.

Snyder2007: Snyder L, Champness W *Molecular Genetics of Bacteria-3rd ed* pp. 459-497 Washington, D.C. ASM Press.

Steelman1992: Steelman VM "Issues in sterilization and disinfection." *Urologic Nursing* 12: 123-127.

Stevenson1994: Stevenson G, Neal B, Liu D, Hobbs M, Packer NH, Batley M, Redmond JW, Lindquist L, Reeves P "Structure of the O antigen of *Escherichia coli* K-12 and the sequence of its *rfb* gene cluster." *J Bacteriol* 176 (13): 4144-4156.

Stoffels2002: Stoffels E, Flikweert AJ, Stoffels WW, Kroesen GMW "Plasma needle: a non-destructive atmospheric plasma source for fine surface treatment of (bio)materials" *Plasma Sources Sci Technol* 11: 383-388.

Stohl2003: Stohl EA, Brockman JP, Burkle KL, Morimatsu K, Kowalczykowski SC, Seifert HS "*Escherichia coli* RecX inhibits RecA recombinase and coprotease activities in vitro and in vivo." *J Biol Chem* 278 (4): 2278-2285.

Sulzenbach2004: Sulzenbacher G, Alvarez K, Van Den Heuvel RH, Versluis C, Spinelli S, Campanacci V, Valencia C, Cambillau C, Eklund H, Tegoni M "Crystal structure of *E. coli* alcohol dehydrogenase YqhD: evidence of a covalently modified NADP coenzyme." *J Mol Biol* 342 (2): 489-502.

Suzuki2005: Suzuki H, Koyanagi T, Izuka S, Onishi A, Kumagai H (2005). "The *yliA*, *-B*, *-C*, and *-D* Genes of *Escherichia coli* K-12 Encode a Novel Glutathione Importer with an ATP-Binding Cassette." *J Bacteriol* 187 (17): 5861-5867.

Tang2000: Tang M, Pham P, Shen X, Taylor JS, O'Donnell M, Woodgate R, Goodman MF “Roles of *E. coli* DNA polymerases IV and V in lesion-targeted and untargeted SOS mutagenesis.” *Nature* 404 (6781): 1014-1018.

Tessman1994: Tessman I, Kennedy MA (1994). “DNA polymerase II of *Escherichia coli* in the bypass of abasic sites in vivo.” *Genetics* 136 (2): 439-448.

Tjaden2002: Tjaden B, Saxena RM, Stolyar S, Haynor DR, Kolker E, Rosenow C “Transcriptome analysis of *Escherichia coli* using high-density oligonucleotide probe arrays.” *Nucleic Acids Res* 30: 3732–3738.

Tjaden2006: Tjaden B, Goodwin SS, Opdyke JA, Guillier M, Fu DX, Gottesman S, Storz G “Target prediction for small, noncoding RNAs in bacteria.” *Nucleic Acids Res* 34 (9): 2791-2802.

Tonk1929: Tonks L, Langmuir I “Oscillations in ionized gas.” *Phys Rev* 33: 195-210.

Touati1988: Touati D “Transcriptional and posttranscriptional regulation of manganese superoxide dismutase biosynthesis in *Escherichia coli*, studied with operon and protein fusions.” *J Bacteriol* 170 (6): 2511-2520.

Uehara2004: Uehara T, Park JT “The N-acetyl-D-glucosamine kinase of *Escherichia coli* and its role in murein recycling.” *J Bacteriol* 186 (21): 7273-7279.

Van2001a: Van Dyk TK, DeRose EJ, Gonye GE “LuxArray, a high-density, genomewide transcription analysis of *Escherichia coli* using bioluminescent reporter strains.” *J Bacteriol* 183 (19): 5496-505.

Van2001b: Van Dyk TK, Wei Y, Hanafey MK, Dolan M, Reeve MGJ, Rafalski A, Rothman-Denes LB, LaRossa RA “A genomic approach to gene fusion technology.” *Proc Natl Acad Sci USA* 98 (5): 2555-2560.

Voloshin2001: Voloshin ON, Ramirez BE, Bax A, Camerini-Otero RD “A model for the abrogation of the SOS response by an SOS protein: a negatively charged helix in DinI mimics DNA in its interaction with RecA.” *Genes Dev* 15 (4): 415-427.

Wagner1999: Wagner J, Gruz P, Kim SR, Yamada M, Matsui K, Fuchs RP, Nohmi T “The *dinB* gene encodes a novel *E. coli* DNA polymerase, DNA pol IV, involved in mutagenesis.” *Mol Cell* 4 (2): 281-286.

Wang1988: Wang TC, Smith KC “Different effects of *recJ* and *recN* mutations on the postreplication repair of UV-damaged DNA in *Escherichia coli* K-12.” *J Bacteriol* 170 (6): 2555-2559.

Wang2001: Wang Z “Translesion synthesis by the UmuC family of DNA polymerases.” *Mutat Res* 486 (2): 59-70.

Wang2002: Wang Z, Lazarov E, O'Donnell M, Goodman MF “Resolving a fidelity paradox: why *Escherichia coli* DNA polymerase II makes more base substitution errors in AT- compared with GC-rich DNA.” *J Biol Chem* 277 (6): 4446-4454.

Westwood1974: Westwood AW, Doelle HW “Glucose-6-phosphate and 6-phosphogluconate dehydrogenases and their control mechanisms in *Escherichia coli* K-12.” *Microbios* 9: 143-165.

Wing2006: Wing C, Errey JC, Mukhopadhyay B, Blanchard JS, Field RA (2006). “Expression and initial characterization of WbbI, a putative D-Galf:alpha-D-Glc beta-1,6-galactofuranosyltransferase from *Escherichia coli* K-12.” *Org Biomol Chem* 4 (21): 3945-3950.

Woodgate1991: Woodgate R, Ennis DG “Levels of chromosomally encoded Umu proteins and requirements for in vivo UmuD cleavage.” *Mol Gen Genet* 229 (1): 10-16.

Yalin2003: Yalin AP, Yu ZQ, Stan O, Hoshimiya K, Abdur R, Surla V, Collins GJ “Electrical and optical emission characteristics of radio-frequency-driven hollow slot microplasmas operating in open air.” *Appl Phys Lett* 83 (14): 2766-2768.

Yao1994: Yao Z, Valvano MA “Genetic analysis of the O-specific lipopolysaccharide biosynthesis region (*rfb*) of *Escherichia coli* K-12 W3110: identification of genes that confer group 6 specificity to *Shigella flexneri* serotypes Y and 4a.” *J Bacteriol* 176 (13): 4133-4143.

Yasuda1996: Yasuda T, Nagata T, Ohmori H “Multicopy suppressors of the cold-sensitive phenotype of the *pcsA68* (*dinD68*) mutation in *Escherichia coli*.” *J Bacteriol* 178 (13): 3854-3859.

Yasuda1998: Yasuda T, Morimatsu K, Horii T, Nagata T, Ohmori H “Inhibition of *Escherichia coli* RecA coprotease activities by DinI.” *EMBO J* 17 (11): 3207-3216.

Yasuda2001: Yasuda T, Morimatsu K, Kato R, Usukura J, Takahashi M, Ohmori H “Physical interactions between DinI and RecA nucleoprotein filament for the regulation of SOS mutagenesis.” *EMBO J* 20 (5): 1192-1202.

Yoshimasu2003: Yoshimasu M, Aihara H, Ito Y, Rajesh S, Ishibe S, Mikawa T, Yokoyama S, Shibata T (2003). “An NMR study on the interaction of *Escherichia coli* DinI with RecA-ssDNA complexes.” *Nucleic Acids Res* 31(6):1735-43.

Yu1993: Yu X, Egelman EH “The LexA repressor binds deep within the deep helical groove of the activated RecA filament.” *J Mol Biol* 231: 29-40.

Yu2003: Yu, ZQ, Hoshimiya K, Williams JD, Polvinen SF, Collins, GJ “Radio-frequency-driven near atmospheric pressure microplasma in a hollow slot electrode configuration.” *Appl Phys Lett* 83 (5): 854-856.

Yura2000: Yura T, Kanemori M, Morita MT “The Heat Shock Response: Regulation and Function.” In *Bacterial Stress Responses* ed. Storz G, Hengge-Aronis R pp. 3-10. Washington, D.C. ASM Press.

Zhang2002: Zhang A, Wassarman KM, Ortega J, Steven AC, Storz G “The Sm-like Hfq protein increases OxyS RNA interaction with target mRNAs.” *Mol Cell* 9 (1): 11-22.

Zheng2001: Zheng M, Wang X, Templeton LJ, Smulski DR, Larossa RA, Storz G “DNA microarray-mediated transcriptional profiling of the *Escherichia coli* response to hydrogen peroxide.” *J Bacteriol* 183 (15): 4562–4570.

Appendix A

Normalization Plots and CEL Images

The simultaneous analysis of multiple arrays can suffer from biases affecting the overall image intensity of an array. These biases are introduced if the images have been generated at different times and places. Normalization is a process of adjusting the overall chip brightness of the arrays to a similar level before comparing the expression level of genes between arrays.

Invariant Set Method

The method used in dChip to normalize arrays is based on the principle of an *invariant set* that works for a group of arrays, on the basis of identification of a common baseline array (having median overall brightness) and adjustment of the overall chip brightness of all the other arrays relative to the baseline array.

Specifically, the normalizing relation is a curve drawn on the scatter-plot of two arrays with the baseline array on y-axis and the array to be normalized on x-axis. The normalization is based on probes that belong to non-differentially expressed genes. It is not easy to determine which genes are non-differentially expressed, however the intensity ranks of non-differentially expressed genes are expected to be similar (where intensity

ranks on the two arrays are calculated separately). An iterative process is used to obtain a set of points (invariant set) representing presumably non-differentially expressed genes.

In detail, the iterative procedure starts with all PM probes on an array numbering in the thousands. A point is chosen in the new set if its *proportion rank difference* (PRD) in the two arrays divided by the number of all the PM probes is small enough. The threshold of being small is dependent on a point's average rank difference in the two arrays

For,

Large average rank difference in the two arrays: $PRD < 0.007$

Small average rank difference in the two arrays: $PRD < 0.003$

This strategy yields more points at lower intensity range. The above procedure is applied iteratively to the new sets until the number of points in a new set does not decrease anymore. A piecewise linear running median line is calculated and used as the normalization curve.

In the following normalization plots and normalized CEL (Cell Intensity) images "Treatment-1" array was used as the median intensity array.

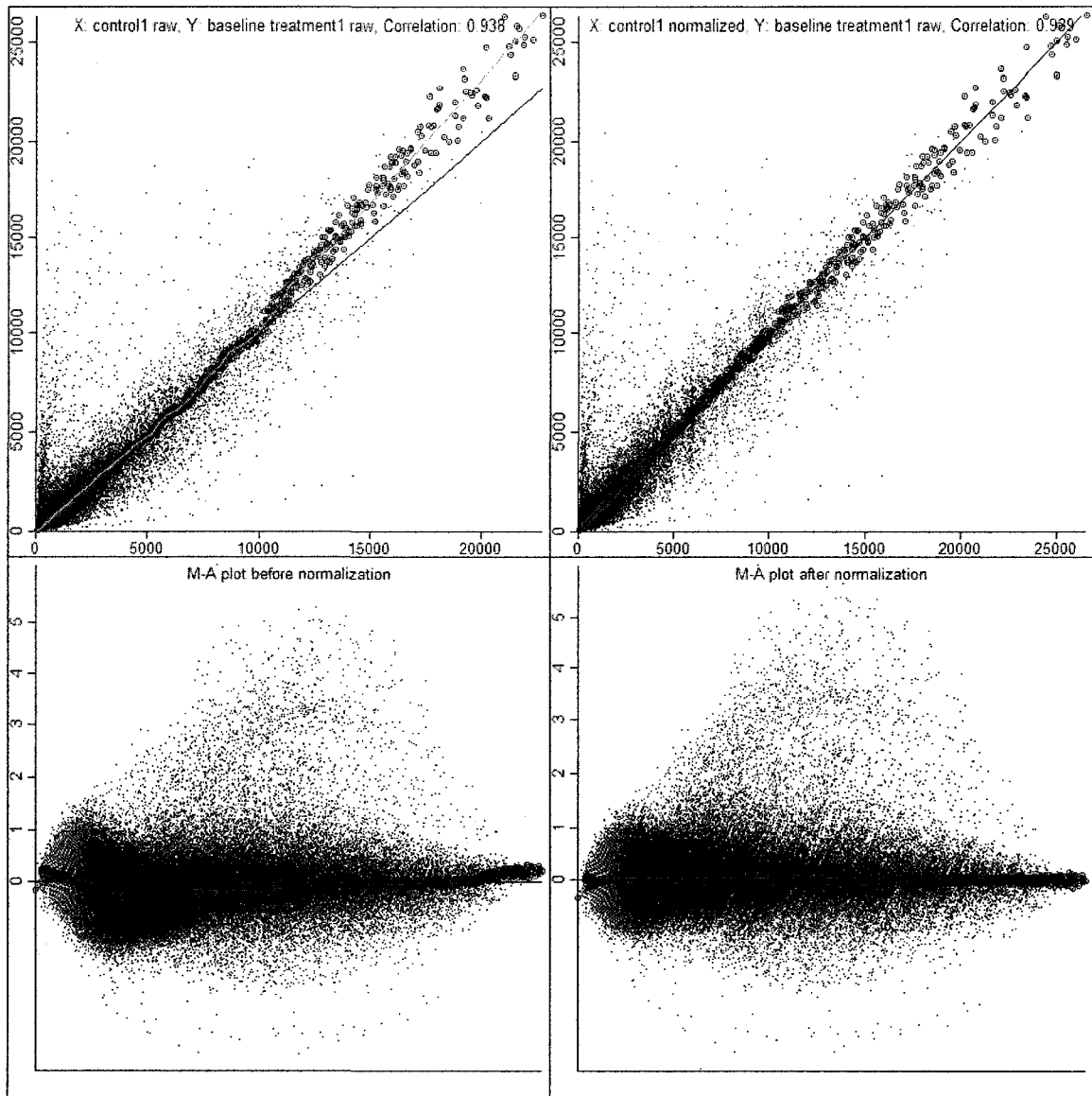


Figure A.1 “Control-1” array normalized with respect to “Treatment-1” array.

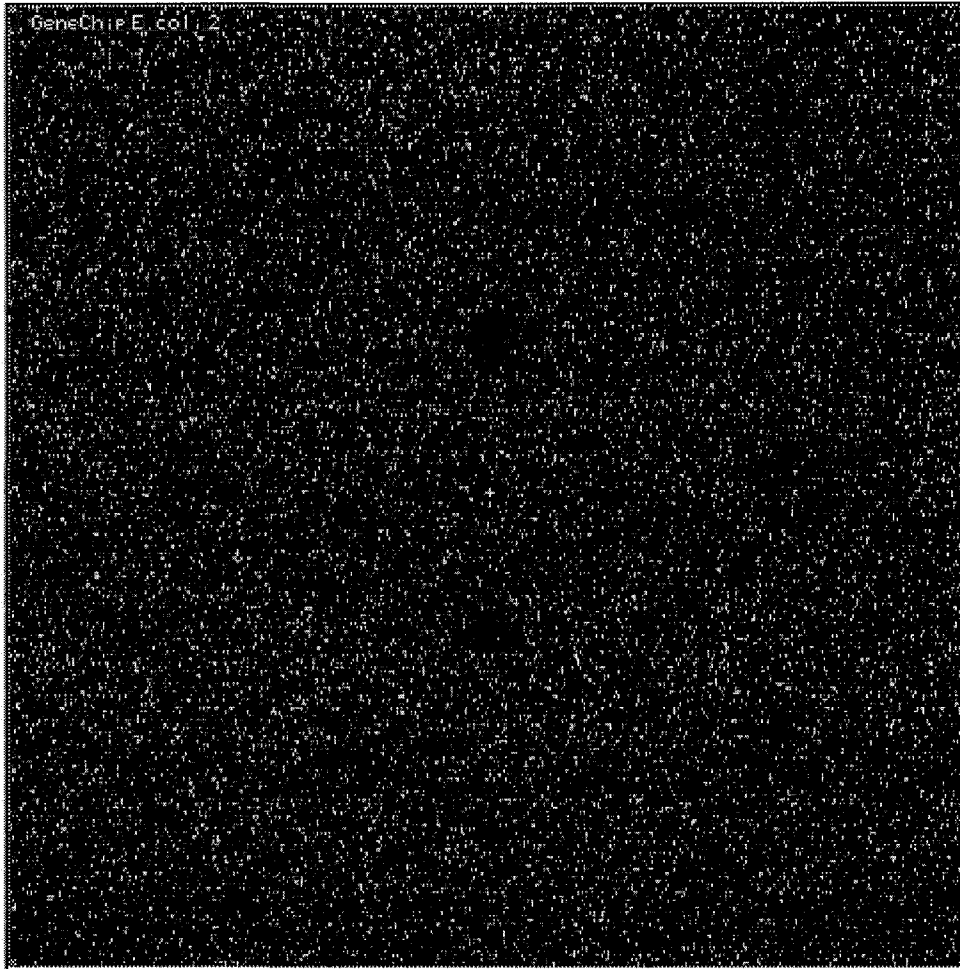


Figure A.2 CEL Image of “Control-1” array after normalization.

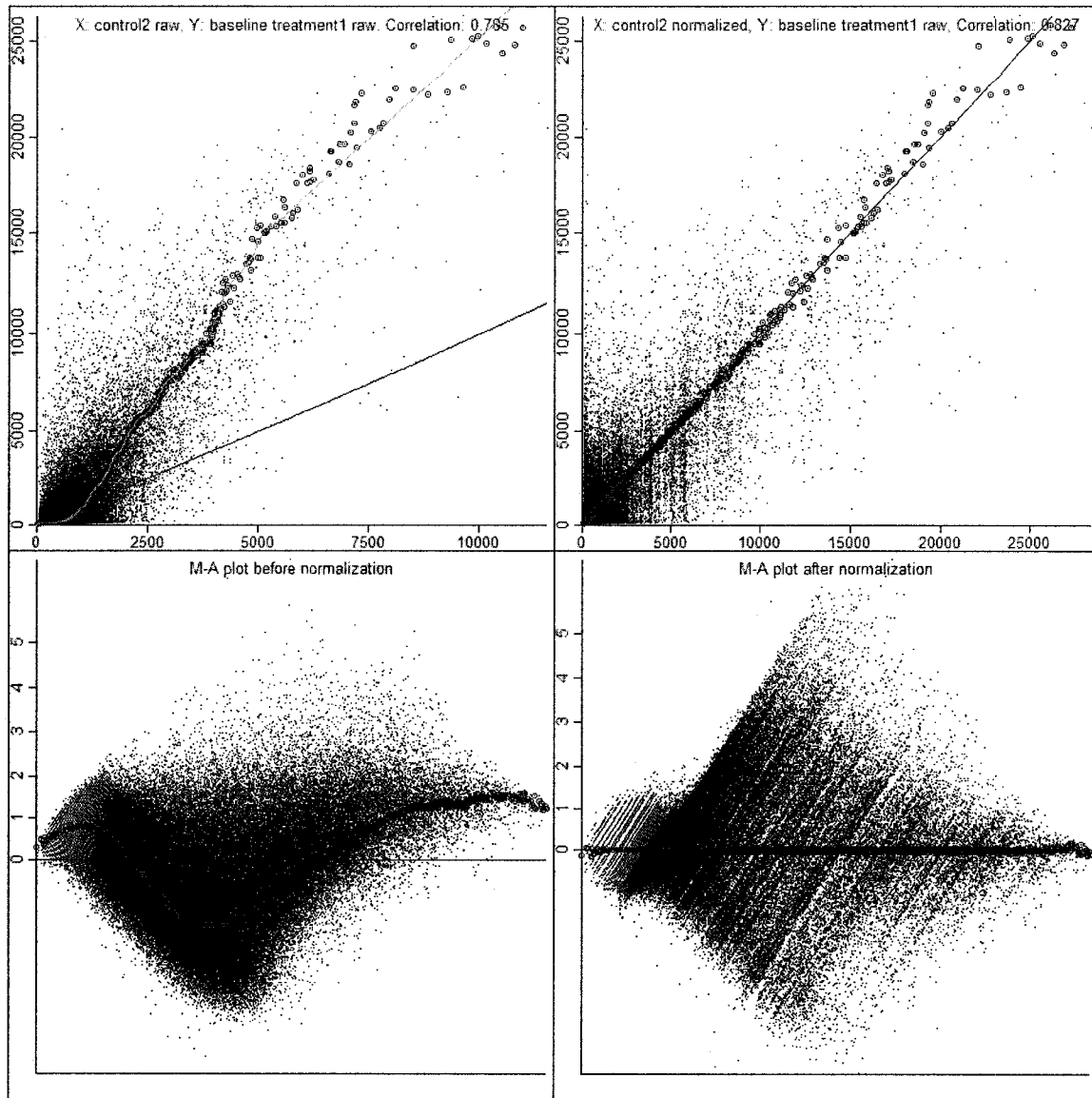


Figure A.3 “Control-2” array normalized with respect to “Treatment-1” array.

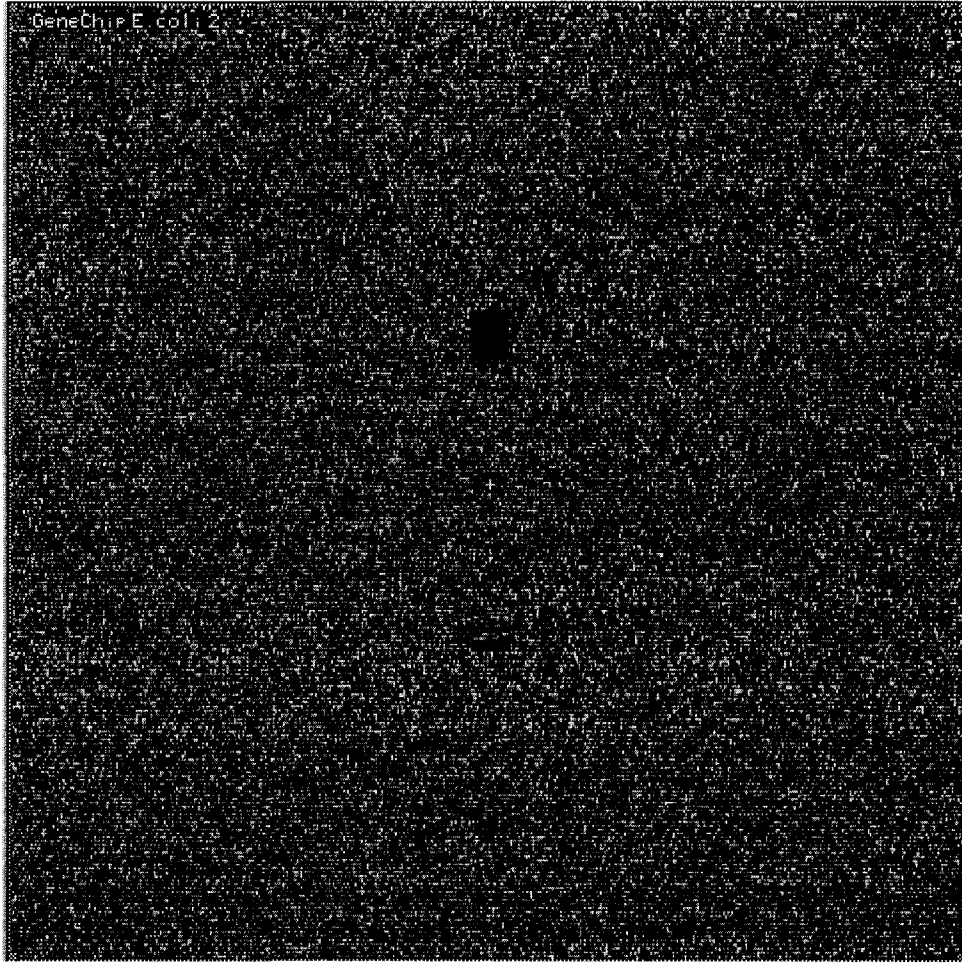


Figure A.4 CEL Image of “Control-2” array after normalization.

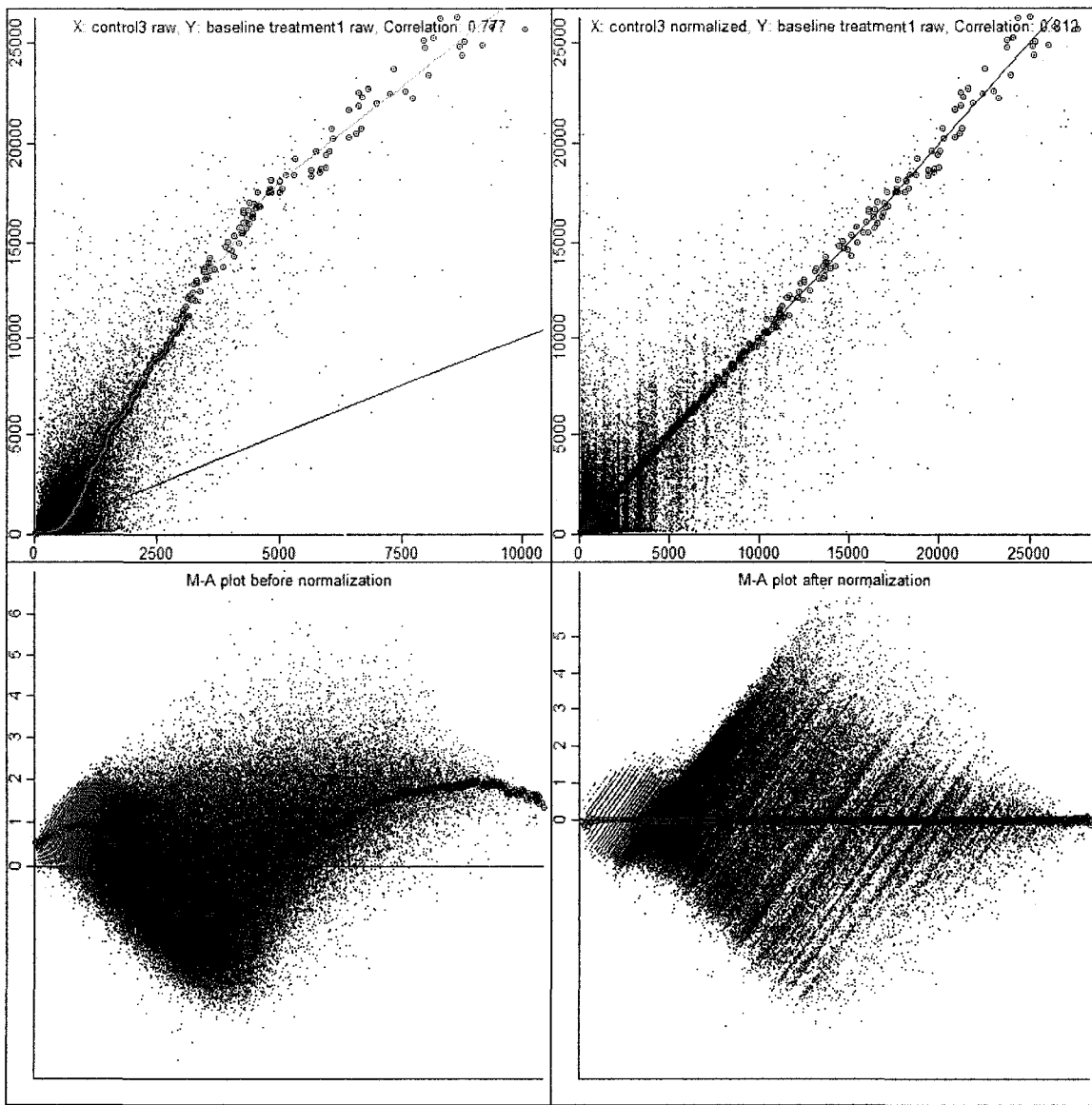


Figure A.5 “Control-3” array normalized with respect to “Treatment-1” array.

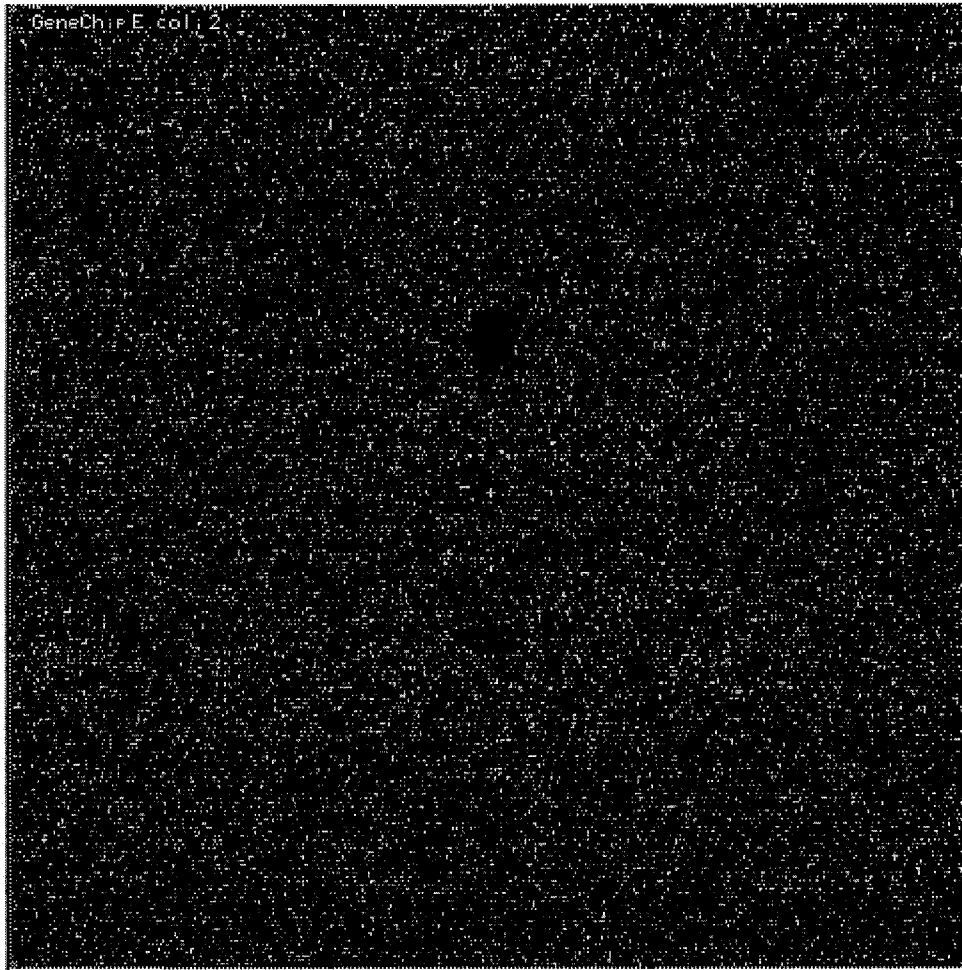


Figure A.6 CEL Image of “Control-3” array after normalization.

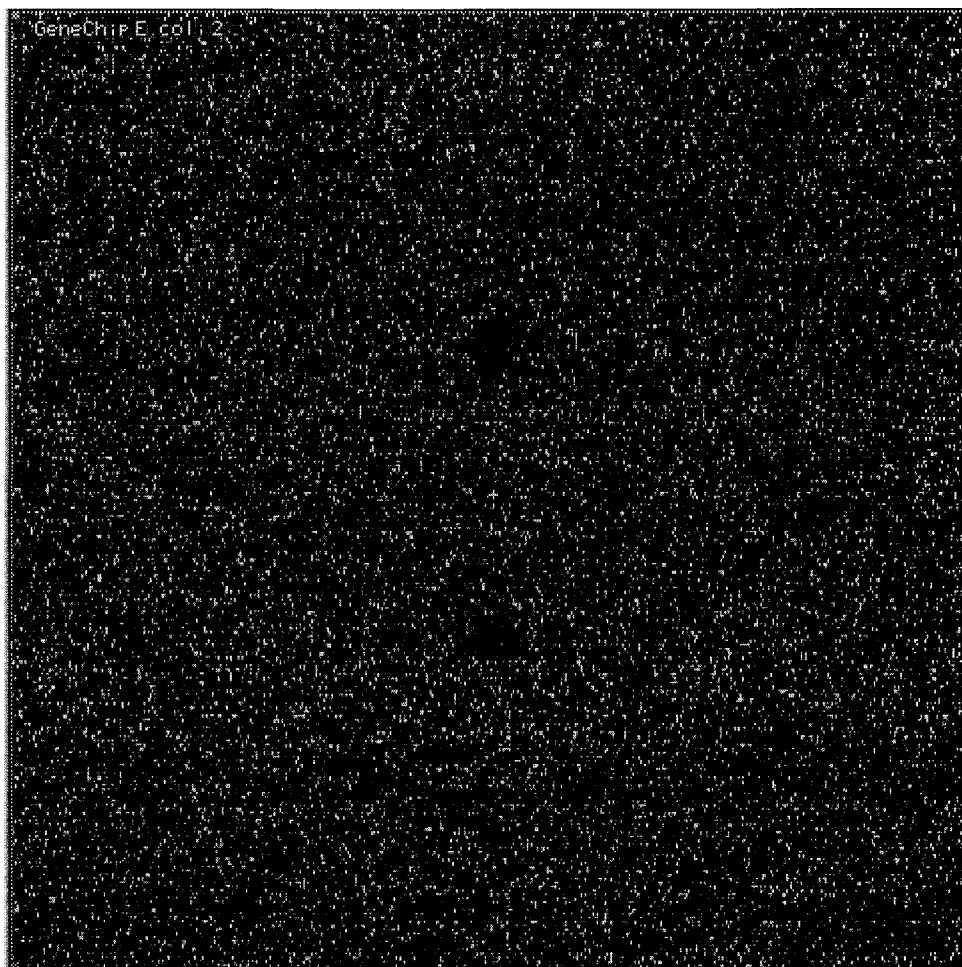


Figure A.7 CEL Image of “Treatment-1” array after normalization.

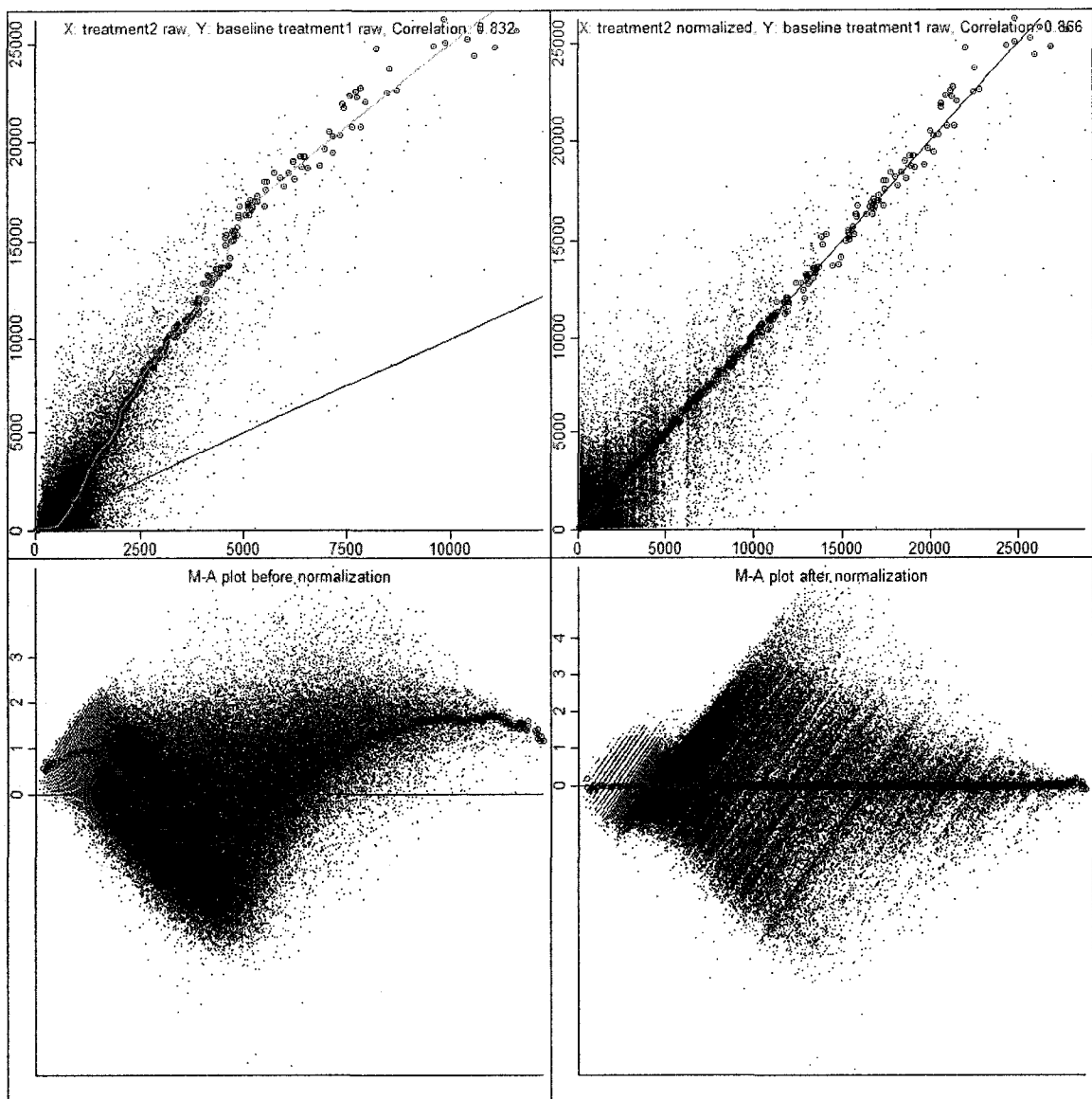


Figure A.8 "Treatment-2" array normalized with respect to "Treatment-1" array.

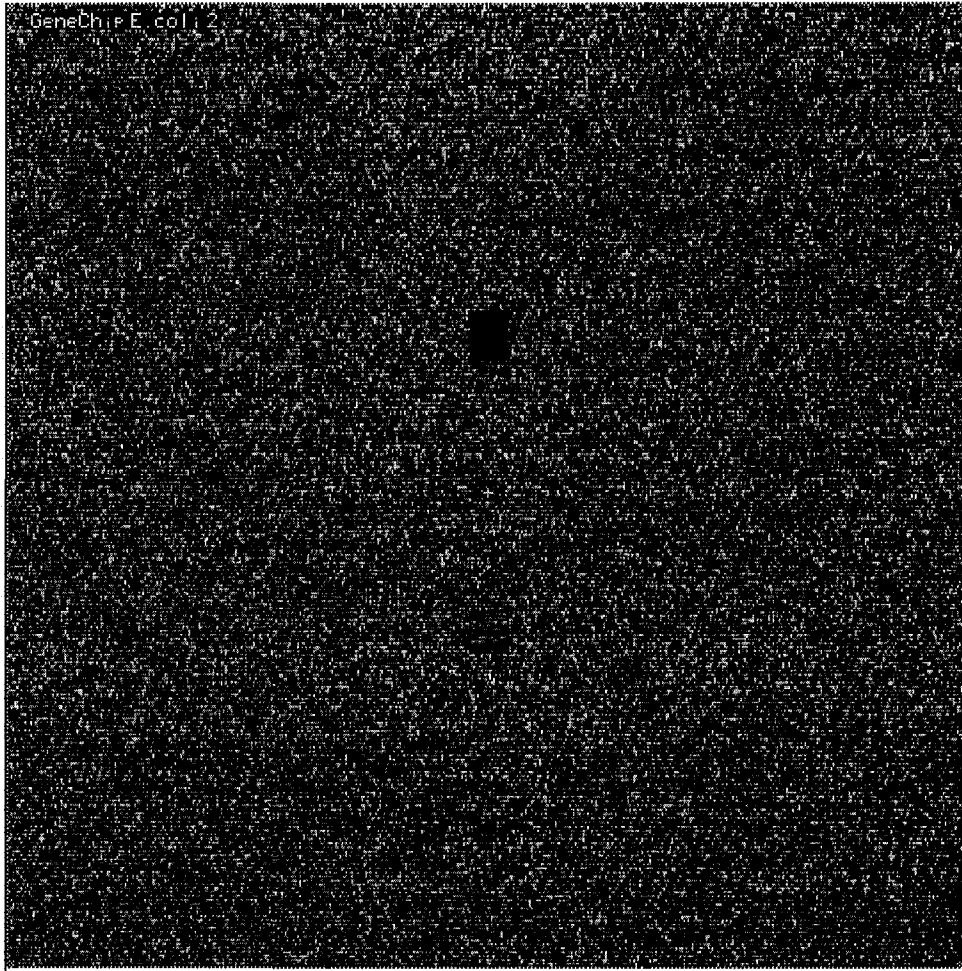


Figure A.9 CEL Image of “Treatment-2” array after normalization.

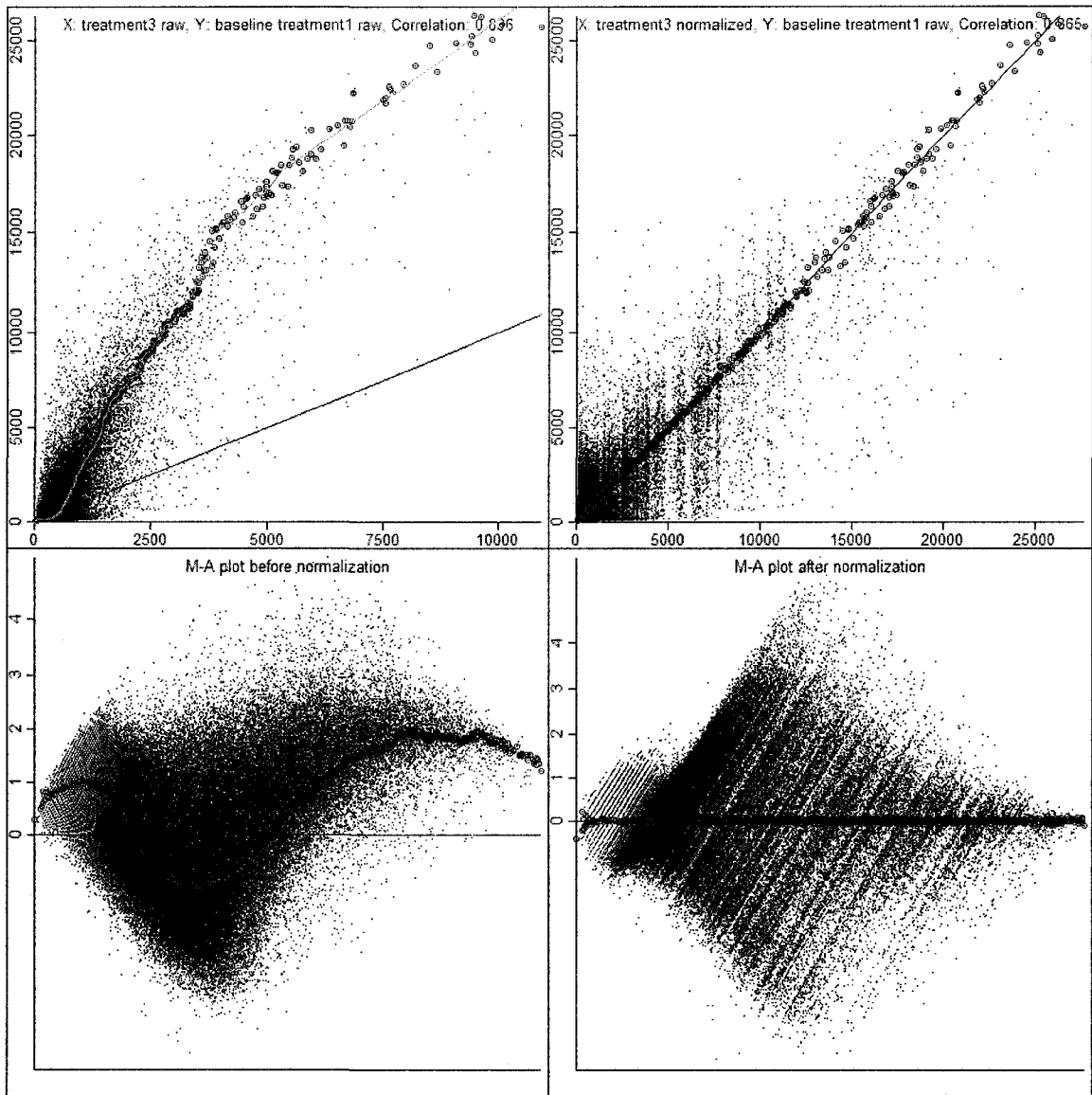


Figure A.10 “Treatment-3” array normalized with respect to “Treatment-1” array.

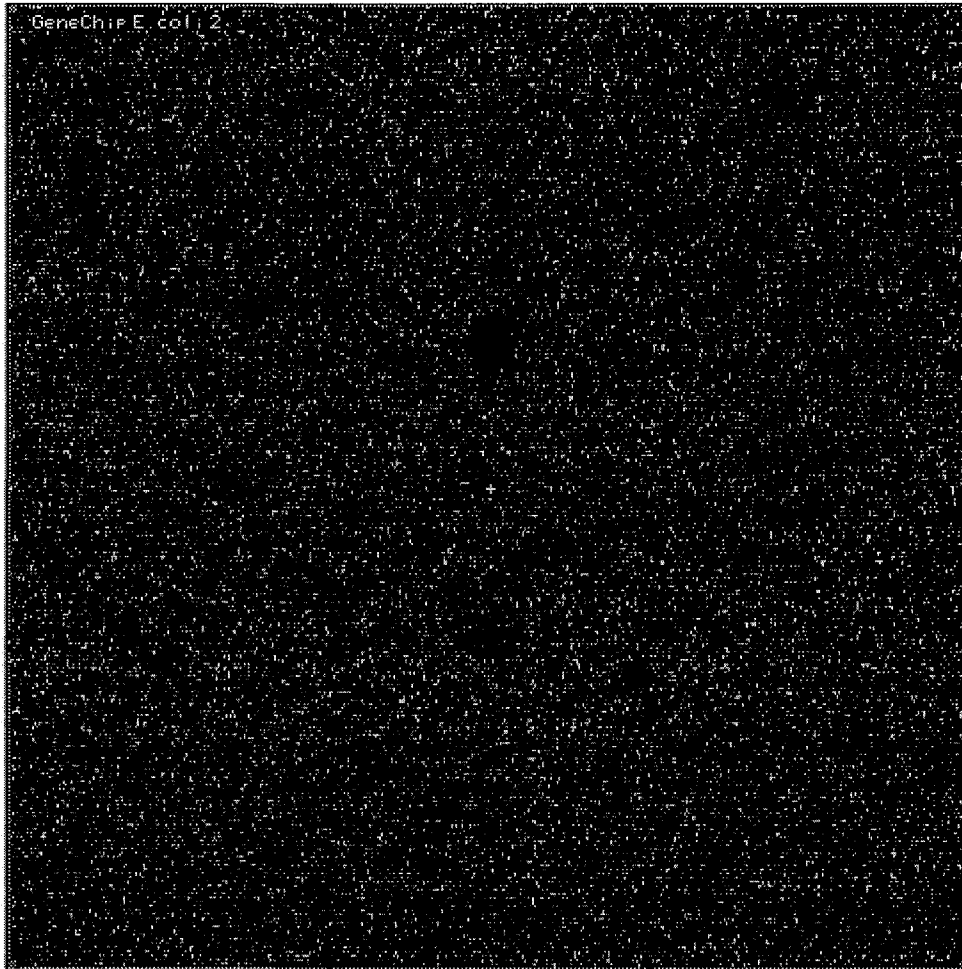


Figure A.11 CEL Image of “Treatment-3” array after normalization.

Appendix B

RNA Isolation and Microarray Sample

Preparation

– RNA Isolation Protocol - RNeasy Mini kit (Qiagen, Valencia, CA)

1. The bacterial cells were harvested by centrifugation at 5000 x g for 5 min at 4 °C. The supernatant was decanted and all remaining media was removed by aspiration. The remaining steps of the RNA isolation protocol were conducted at room temperature.
2. The bacterial pellet was loosened by flicking at the bottom of the tube and the bacteria were re-suspended thoroughly in 100 µl lysozyme-containing TE buffer using a vortex machine and subsequently the suspension was incubated at room temperature for 5 min. The concentration of lysozyme in TE buffer was set at 1 mg/ml.
3. 350 µl of Buffer RLT was added to the sample and a vortex machine was used to mix the sample thoroughly. It was ensured that Buffer RLT had β-ME (Beta-Mercaptoethanol) at the following concentration 10 µl β-ME /1 ml Buffer RLT.
4. 250 µl ethanol was added to the lysate and mixed thoroughly using a pipette.

5. The entire sample (700 μ l) was applied to an RNeasy mini column placed in a 2 ml collection tube and centrifugation was performed at $> 8000 \times g$ for 15 s. Following centrifugation, the flow-through was discarded
6. Buffer RW1 was added to the RNeasy column and centrifugation was performed at $> 8000 \times g$ for 15 s. Following centrifugation, the flow-through and collection tube were discarded.
7. The RNeasy column was transferred to a new collection tube, filled with 500 μ l Buffer RPE and centrifugation was performed at $> 8000 \times g$ for 15 s. Following centrifugation, the flow-through was discarded.
8. The previous step was repeated again except the centrifugation this time was for 2 min to dry the silica-gel membrane.
9. RNA was eluted by transferring the RNeasy column to a new collection tube, adding 40 μ l RNase-free water directly onto the RNeasy silica-gel membrane and centrifuging at $> 8000 \times g$ for 60 s.

The quality and quantity of the eluted RNA were determined by measuring absorbance at 260 nm and 280 nm by photospectrometry (Nanodrop, Wilmington, DE). It was ensured that there was at least 10 μ g RNA yield to be used as starting material for microarray processing. A_{260}/A_{280} ratio was maintained between 1.8 and 2.1. RNA was stored at -80°C for downstream microarray processing.

– **Prokaryotic Sample Preparation Protocol (Affymetrix, CA)**

The extracted RNA from the previous step was used for analysis using high density oligonucleotide microarrays (Affymetrix Inc, CA). The basic steps in the microarray processing are listed below

- Target preparation
 - cDNA synthesis
 - cDNA purification
 - cDNA fragmentation
 - Terminal Labeling
- Target Hybridization
- Probe array wash and stain
- Probe Scan
- Data Analysis

Here are the above steps listed in detail

– **Target preparation> cDNA synthesis**

The first step in target preparation was cDNA synthesis. This consisted of two steps. First, the following mixture was made for primer annealing.

Components	Volume	Final Concentration
Total RNA	10 µg	0.33 µg/µl
75 ng/µl Random hexamer primers	10 µl	25 ng/µl
Diluted poly-A RNA controls	2 µl	1:32
Total volume	30 µl	

The above RNA-primer mixture was incubated at the following temperature

- 70 °C for 10 min
- 25 °C for 10 min
- Chilled to 4°C

The above RNA-primer mixture was used for cDNA synthesis as follows

Components	Volume	Final Concentration
RNA-Primer hybridization mix (from previous step)	30 μ l	
5X 1 st Strand Buffer	12 μ l	1X
100 mM DTT	6 μ l	10 mM
10 mM dNTPs	3 μ l	0.5 mM
SUPERase•In (20 U/ μ l)	1.5 μ l	0.5 U/ μ l
SuperScript II (200 U/ μ l)	7.5 μ l	25 U/ μ l
Total Volume	60 μl	

The above reaction was incubated at the following temperatures:

- 25 °C for 10 min
- 37 °C for 60 min
- 42 °C for 60 min
- SuperScript II inactivated at 70°C for 10 min
- Chilled to 4 °C

To remove any remaining RNA, 20 μ l of 1N NaOH was added and the mixture was incubated at 65 °C for 30 min followed by addition of 20 μ l of 1N HCl to neutralize the mixture.

— **cDNA Purification**

MinElute PCR purification kit (Qiagen, Valencia, CA) was used to clean up the cDNA synthesis product using the following protocol-

1. 5 volumes of Buffer PB were added to the previously synthesized cDNA.

2. A MinElute column was placed in a 2 ml collection tube, the sample was applied to the column and centrifugation was performed for 1 min.
3. The flow-through was discarded and the column was placed back in the collection tube
4. 750 μ l Buffer PE was applied to wash the column and centrifugation was performed for 1 min. Additional centrifugation for 1 min was performed after discarding the flow-through for removal of residual ethanol present in Buffer PE.
5. The MinElute column was placed in a clean 1.5 ml collection tube and 11 μ l Buffer EB (10 mM Tris·Cl, pH 8.5) was added to the column for elution
6. The eluted cDNA's quantity was estimated by 260 nm absorbance. It was ensured that all samples had at least 3 μ g cDNA yield.

– **Target preparation> cDNA fragmentation**

The following reaction mix was prepared for cDNA fragmentation

Components	Volume	Final Concentration
10X One-Phor-All Buffer	2 μ l	1X
cDNA	10 μ l	-
DNase I	0.6U / μ g of cDNA	0.5 U/ μ l
Nuclease free water	Up to 20 μ l	-
Total Volume	20 μl	

- The above reaction mix was incubated at 37 °C for 10 min
- DNase I was inactivated at 98 °C for 10 min
- The fragmented cDNA was applied directly to the terminal labeling reaction

— Target Preparation>Terminal Labeling

The following reaction mix was prepared for terminal labeling

Components	Volume
5X Reaction Buffer	10 μ l
GeneChip DNA Labeling Reagent, 7.5 mM	2 μ l
Terminal Deoxynucleotidyl Transferase	2 μ l
Fragmentation cDNA Product Up to	20 μ l
Water	16 μ l
Total Volume	50 μl

— The reaction mix obtained above was incubated at 37 °C for 60 min

— The reaction was stopped by adding 2 μ l of 0.5M EDTA

— Thus the target was ready to be hybridized onto the probe arrays

Target Hybridization

Hybridization Cocktail for each array had the following components

Components	Volume	Final Concentration
2X Hybridization Buffer	40 μ l	1X
3 nM B2 Control Oligo	1.3 μ l	50 pM
10 mg/ml Herring Sperm DNA	0.8 μ l	0.1 mg/ml
50 mg/ml BSA	0.8 μ l	0.5 mg/ml
100% DMSO	6.2 μ l	7.8%
Fragmented and Labeled cDNA	25 μ l	0.5 – 7.0 μ g
Molecular Biology Grade Water	5.9 μ l	
Total Volume	80 μl	

The hybridization cocktail was added to the probe array after the array had been brought to room temperature and then hybridized in a hybridization oven at 45 °C for 16 hours at 60 rpm.

— **Probe Array Wash and Stain**

After hybridization the hybridization cocktail was removed from the probe array and replaced with Wash Buffer A which has the following recipe

— **Wash Buffer A (Non-Stringent Wash Buffer): Recipe**

(6X SSPE, 0.01% Tween-20)

For 1,000 ml:

300 ml of 20X SSPE

1.0 ml of 10% Tween-20

699 ml of water

Filtered through a 0.2 µm filter

The probe array cartridges were then placed in the fluidics station and the fluidics script Mini_prok2v1 was used for washing and staining.

Here are the details of the Mini_prok2v1 fluidics script-

Post Hyb Wash #1: 10 cycles of 2 mixes/cycle with Wash Buffer A at 30 °C

Post Hyb Wash #2: 4 cycles of 15 mixes/cycle with Wash Buffer B at 50 °C

1st Stain: 5 min in Streptavidin Solution Mix at 35 °C

Post Stain Wash: 10 cycles of 4 mixes/cycle with Wash Buffer A at 30 °C

2nd Stain: 300 seconds in Antibody Solution Mix at 35 °C

3rd Stain: 300 seconds in SAPE Solution Mix at 35 °C

Final Wash: 15 cycles of 4 mixes/cycle with Wash Buffer A at 35°C
(holding temperature 25 °C)

Recipes of wash buffer B, Streptavidin solution mix, antibody solution mix and SAPE solution mix used in the above protocol are given below

– **Wash Buffer B: Stringent Wash Buffer**

(100 mM MES, 0.1M [Na+], 0.01% Tween-20)

For 1,000 ml:

83.3 ml of 12 X MES Stock

5.2 ml of 5M NaCl

1.0 ml of 10% Tween-20

910.5 ml of water

Filtered through a 0.2 µm filter

– **Streptavidin Solution Mix**

Components	Volume	Final Concentration
2X Stain Buffer	300.0 µl	1X
50 mg/ml BSA	24.0 µl	2 mg/ml
1 mg/ml Streptavidin	6.0 µl	10 µg/ml
Nuclease-free H ₂ O	270.0 µl	-
Total Volume	600 µl	

– **Antibody Solution Mix**

Components	Volume	Final Concentration
2X MES Stain Buffer	300.0 μ l	1X
50 mg/ml BSA	24.0 μ l	2 mg/ml
10 mg/ml Normal Goat IgG	6.0 μ l	0.1 mg/ml
0.5 mg/ml Anti-streptavidin antibody, biotinylated	6.0 μ l	5 μ g/ml
Nuclease-free H ₂ O	264.0 μ l	-
Total Volume	600 μl	

– **SAPE Solution Mix**

Components	Volume	Final Concentration
2X MES Stain Buffer	300.0 μ l	1X
50 mg/ml BSA	24.0 μ l	2 mg/ml
1 mg/ml Streptavidin Phycoerythrin	6.0 μ l	10 μ g/ml
Nuclease-free H ₂ O	270.0 μ l	-
Total Volume	600 μl	

After the arrays had been washed and stained they were scanned using a GeneChip[®] 3000 scanner (Affymetrix Inc., CA) and gene expression data was obtained for all the arrays.